CONTROL OF WIND INTEGRATED POWER GRID USING VOLTAGE CONTROLLABILITY AND VULNERABILITY DETECTION

by

Rabindra Maharjan

A dissertation submitted to the faculty of
The University of North Carolina at Charlotte
in partial fulfillment of the requirements
for the degree of Doctor of Philosophy in
Electrical Engineering

Charlotte

2016

Approved by:

_____
Dr. Sukumar Kamalasadan

_____
Dr. Yogendra P. Kakad

_____
Dr. Valentina Cecchi

_____
Dr. Brett Q. Tempest

ABSTRACT

RABINDRA MAHARJAN. Control of wind integrated power grid using voltage controllability and vulnerability detection. (Under the direction of DR. SUKUMAR KAMALASADAN)

Modern power grids are the largest and most complex engineered systems. Integration of distributed resources like wind farms and economic constraints push power grids to operate close to their limits. Due to this, power system is subject to various stability threats. Voltage stability is one of the most prominent issues that constraints modern power grid. It is directly linked to the reactive power balance in an area. Generators are the prominent source of reactive power. Besides generators, various other reactive power sources like capacitor and reactor banks are used throughout the grid for reactive power support. In a modern power grid with high penetration of renewable energy, reactive support from sources such as wind farms and PV farms are becoming mandatory. Similar to the excitation controller system in conventional synchronous machine, terminal voltage and reactive power generation is regulated by converter controller system in the renewable sources. These controllers regulate reactive power within their reactive power capability limit for voltage control based on the reference voltage set points.

In the North America, generally, operators switch on/off additional capacitor/reactor banks instead of changing set points of generator excitation controllers to adjust the mismatch of reactive power generation and consumption in an area. Lack of access of generator controls to system operators and local nature of reactive power flow are the common arguments provided for this practice. Access of system operators to the generator controls can be improved in the North America as a large number of utility operators in North America owns both transmission and generation system. Hence, the system operators can provide a priority to generators for reactive power and voltage control before switching additional reactive power sources. This will be

easier and economically beneficial as generators will be used to its full capacity instead of additional sources.

With the advancement of communication technology and measurement units, the generator excitation controller and converter controllers is not only limited to terminal voltage control but used for system wide voltage control as well. Similar to hierarchical levels of frequency control, a hierarchical voltage control architecture with primary, secondary and tertiary voltage control has been proposed in some European countries. The primary voltage control is the voltage control in local sense while the secondary level voltage control is based on areas or zones. Similar to this methodology, a voltage control area concept has been introduced to support reactive power requirements within the areas or zones of power grid where the generators are given priority before switching additional reactive power sources. This is much more meaningful and important when more renewable energy resources are introduced to the grid as these sources will be distributed throughout a grid.

This dissertation proposes a method for online identification of VCA based on reactive power sensitivities. Then for voltage control action the bus prone to voltage instability is identified. Voltage stability index (VSI) utilizing maximum loadability margin is proposed to monitor and detect vulnerable buses. Area for voltage control action is decided by identifying an area belonging to the vulnerable bus detected using VSI. Further, a secondary voltage control scheme based on the participation factor of generators in the VCA is proposed for the voltage control of the grid. The effectiveness of proposed technique is demonstrated using IEEE 39 test system and modified IEEE 39 wind power test system.

DEDICATION

This dissertation is dedicated to my parents for their unconditional love and support.

ACKNOWLEDGEMENTS

Many people have contributed to the research work reported in this dissertation in various ways and their efforts are most sincerely appreciated.

I would like to express my profound gratitude to Dr. Sukumar Kamalasadan, my advisor and the chair of the advisory committee for his continuous guidance, unfailing support, and constant encouragement throughout the duration of my study.

Next, I would like to thank committee members Dr. Yogendra Kakad and Dr. Valentina Cecchi for their valuable suggestions and support. I am grateful to Dr. Brett Q. Tempest for accepting to be in my dissertation committee.

I am thankful to all my fellow students in Power Energy and Intelligent Systems Laboratory (PEISL) and ECE department for wonderful academic and research environment. My sincere gratitude to Dr. Kamalasadan, Electrical and Computer Engineering Department, Energy Production and Infrastructure Center(EPIC) and the Graduate School of UNC Charlotte for financial support in the form of Graduate Assistantship and Graduate Assistant Support Plan (GASP).

I am grateful to my parents, Ram and Ratna Devi Maharjan and my sisters, Rabina and Rojina for their eternal love, support, and encouragements throughout these years. Lastly, I would like to express my deepest gratitude to my wife Alika, for supporting and encouraging me during my pursuit of this goal.

TABLE OF CONTENTS

LIST OF TABLES

LIST OF FIGURES

LIST OF ABBREVIATIONS

AVR	Automatic Voltage Regulator
DFIG	Doubly Fed Induction Generator
FERC	Federal Energy Regulatory Commission
IEEE	Institute of Electrical and Electronics Engineers
ISO	Independent System Operator
NERC	North American Electric Reliability Corporation
PMU	Phasor Measurement Unit
pu	Per Unit
SVC	Secondary Voltage Control
VCA	Voltage Control Area
VSC	Voltage Source Converter
VSI	Voltage Stabilty Index
WECC	Western Electricity Coordinating Council

LIST OF SYMBOLS

V_k	voltage at bus k
Z_k^L	load impedance of bus k
P_k	real power of bus k
Q_k	reactive power of bus k
δ_m	voltage angle at bus k
Z_{kk}	k^{th} diagonal element of network impedance matrix
Z_{th}	thevenin equivalent impedance of network
V_{th}	thevenin equivalent voltage of network
Z_{km}	impedance betwee buses k and m
Y_{km}	admittance between bus k and bus m
θ_{km}	admittance angle at bus k and bus m
Y_{kk}	k^{th} diagonal element of network admittance matrix
J_g	jacobian vector
J	load flow jacobian
S_{qg}	reactive power sensitivity of generator to load bus
W_k	pooled within cluster sum of squares
d	squared euclidean distance
D	euclidean distance
C_j	centroid of cluster j

CHAPTER 1: INTRODUCTION

This dissertation is focused on the control of wind integrated power grid to prevent it from voltage instability and voltage collapse. The voltage control is employed by monitoring vulnerability of voltage level towards voltage collapse and employing identification of control area to identify voltage controllability of generator for online voltage and reactive power control. The voltage controllability is defined by the reach of reactive power reserve of generator which is defined by voltage control area. A secondary voltage control of power grid based on voltage controllability and monitoring of vulnerability of a bus is proposed in this dissertation.

This chapter is organized as follows. Section 1.1 provides a background and motivation for this work. The dissertations' problem statement is presented in Section 1.2. Section 1.4 provides overview and methodology of the research. In Section 1.4, a summary of research contributions is given. Finally, an overview of the thesis organization is presented in Section 1.5.

1.1 Motivation

The power grid is a network of electrical components to generate, transmit and distribute electrical power from a generation point to an industrial or domestic end-user. Modern power grids are some of the largest and most complex engineered systems. Integration of distributed resources, growing consumer demand, and strong economic incentives for grid operators are pushing the grid to operate close to their physical limits [1, 2]. When these physical limits are approached or breached, power systems can experience a form of network-wide failure termed voltage collapse. Voltage collapse is initiated from the local phenomenon of progressive decrease of voltage in buses which

is known as voltage instability. Voltage collapse is one of the major reason leading to a system blackout. A blackout is a condition where a major portion or all of an electrical network is de-energized resulting in a loss of electric supply to a portion or all of that networks customer demand. The following is a list of blackouts and near blackouts related to voltage collapse [3].

1. Blackout of June 25, 1998 in Eastern U.S. and Canada The blackout was initiated by disconnection of one of the five 230kV lines from Beck power plant going north to Toronto. The blackout affected 30 million people in Canada and USA, including New York City and lasted 13 hours. [4, 5]

2. Blackout of June 25, 1998 in Upper Midwest The blackout was initiated by a lightning storm in Minnesota and affected 152,000 people in Minnesota, Montana, North Dakota, South Dakota, and Wisconsin in the United States; and Ontario, Manitoba, and Saskatchewan in Canada. Outages lasted upto 19 hours. [5]

3. Blackout of July 6 and 19, 1999 in Northeast U.S. A nonoutage disturbances were caused by above-expected load in the PJM system. A near blackout situation with prolonged voltage reductions to 0.95 p.u. A voltage collapse was barely averted through the use of emergency procedures. [5]

4. Blackout of August 14, 2003, in the Eastern U.S. and Canada

   The blackout was initiated by subsequent tree contacts of sagging conductors on the Stuart Atlanta, Harding Chamberlin, Hanna Juniper, and Star South Canton 345-kV transmission lines. The blackout affected up to 50 million people and caused shutdowns of more than 250 power plants with the total generation capacity loss reaching 61,800 MW. The estimated economic damage was 4.5-10 billion. [6]

5. Blackout of July 12, 2004 in Southern Greece and Athens

   The blackout was caused by the loss of Unit 2 (300 MW) at the Lavrio power station in the Athens area. [7]

6. Blackout of May 24-25,2005 Blackout in Moscow region, Russia

   The blackout was caused by a combination of factors including severe equipment damages at the Chagino substation, short-circuits due to sagging of overheated conductors on the 110 and 220 kV lines, reactive power shortage and voltage decline in the southern part of the Moscow Power System, and others. The Moscow blackout left at least 4 million people without electricity supply for more than 24 hours. [8]

7. Blackout of July 31, 2012 in northern, eastern, and north-eastern India The blackout was caused by major grid disturbance in the northern, eastern and north-eastern electricity grids. Approximately 48 GW of load across 21 States and 1 Union Territory were affected. Over 600 million people (nearly half of Indias population), were left without power. [9]

Analysis of these blackouts indicated need of a tool for monitoring system security margins including voltage vulnerability under the normal and contingency conditions [3]. A system enters a state of voltage instability when a disturbance, increase in load demand, or change in system condition causes a progressive and uncontrollable decline in voltage. The main factor causing voltage instability is the inability of the power system to meet the demand for reactive power. Voltage stability is the ability of a power system to maintain acceptable voltages at all buses in the system under normal operating conditions and after being subjected to a disturbance. It is known that voltage magnitudes alone are poor indicators of voltage stability or security. Voltages can be near normal with generators, synchronous condensers, and SVCs near current limiting levels, thus resulting in a possible voltage collapse. Therefore, it is useful

to assess voltage stability of power systems by means of voltage stability index, a scalar magnitude that can be monitored as the system parameters change. The index based instability measure captures a unique system behavior in terms of a number and interprets them to give the notion of distance to instability. Operators can use the index to know closeness of the system to voltage collapse in an intuitive manner and react accordingly. Voltage instability is linked to the inability of the generation-transmission system to provide the power requested by loads [10]. Therefore, a family of methods aimed at detecting maximum load power conditions has been presented in literatures as impedance matching condition for detection of voltage instability [11–14]. The basic assumption is that the whole power system seen from one load can be replaced by a thevenin equivalent. The problem of voltage collapse may be simply explained by an inability of the power system to supply the reactive power or by an excessive absorption of reactive power by the system itself. It is to be understood as a reactive problem and it is strongly affected by the load behavior (i.e. constant Q for varying voltages) [15]. Therefore, a index based on impedance matching and detection of maximum load power conditions to predict voltage instability as well as proximity to voltage collapse is presented in this dissertation. The proposed method is based on a fast method of thevenin equivalent calculation, thus it can be applied for online application [16]. The voltage stability index of system gives the measure of vulnerability of system.

Voltage problem is always accompanied with reactive power problem and dealt singly as voltage and reactive power problem due to the fact that the voltage phenomena is primarily driven by reactive power a much less intuitive concept than active power. Reactive power represents the ebb and flow of energy in the electromagnetic fields of system components. This energy is stored and released during each a.c. cycle, allowing system components to function normally and to facilitate the transfer of useful active power with minimal transmission losses [1, 10]. Understanding and

controlling reactive power is, therefore, essential for the efficient and safe operation of the grid. Unlike active power, reactive power is local and hence voltage problem is also localized but cascading effect of voltage instability leads to voltage collapse. Hence, it is important to tackle local voltage and reactive power problem to prevent voltage collapse It is a well-known fact that for most system contingencies, the effect of outages on the system is of a local nature, which means the major effects of a perturbation are limited to a certain neighborhood close to the original perturbation [17]. For voltage security, if the area of a close neighborhood with reactive power deficiencies can be identified, then reactive power and voltage control can be implemented by establishing reactive power reserve. The areas of close neighborhood in power system prone to voltage instability under particular operating condition are referred as voltage control area (VCA). VCA is a group of buses which are connected to the rest of the system by a weak voltage boundary. Reactive power reserve is a group of generators which are the primary sources of reactive power in a VCA. The control areas have been traditionally identified using Jacobian matrix [18, 19] and recently electrical distance has been used to identify control areas but these are too restricted for offline applications [17, 20]. A control area of a system depends on the configuration of a power grid. Contingencies like, loss of line or loss of generators and other affects the configuration of the system and therefore, control areas are affected. Identification of control area should reflect changes in the system configuration and control area should be adaptive [21]. To fulfill the need to find online identification of voltage control area, a method based on machine learning and reactive power sensitivities is presented which can effectively divide the system into various VCAs for the voltage and reactive power control.

For reactive power improvement, capacitor banks are extensively used to hold up voltage levels at substations and along transmission lines even in closer proximity to generators due to the lack of proper communications and voltage monitoring.

Even though these capacitor banks keep the system within operational constraints, it conceals the low stability margin of the network, leading to increased voltage collapse risks [22]. With the advancement of communication technology and measurement units like phasor measurement units, automatic voltage control (AVC) which are traditionally used to control voltage of the generator terminal can be used for system wide voltage control. Similar to frequency control, hierarchical levels of voltage control has been proposed in different countries. They are broadly classified as primary, secondary and tertiary voltage control. The primary voltage control corresponds to the fast actions performed by the automatic voltage regulators (AVR) of the machines in a local sense. Secondary voltage control is a slower level of control in which capacitor/reactor banks, LTCs and sometimes AVRs within a control area perform the control actions in a regional sense. Tertiary voltage control is the level at which the optimal voltage profile of the network is calculated in a multiregional sense. The tertiary level provides the set points for the controllers in the other two levels [23–25]. The secondary control scheme is implemented in European countries with the concept of pilot bus [26–28]. A pilot bus is the representative of buses of control area with voltage profile reflecting the pattern of other buses in the area. There are various techniques to select pilot bus like the one with the greatest short circuit capacity [20, 29] or with optimization problem to minimize voltage deviation after random disturbance [30]. Once the pilot bus was selected, all the control actions were aimed at regulating the voltage at this bus. Thus, the AVR's set-points were changed as needed to meet the set-point voltage at the pilot buses. The pilot bus selection was important due to the lack of measurement of all the buses and inability to handle large amounts of data coming from different buses. Monitoring of individual buses has been feasible with the large installations of synchrophasors across the power systems around the world and advanced technique enabling control centers to handle large amount of data. The accuracy of detection of voltage instability is increased

when all the buses are monitored. In North America and other countries, operator switches shunt capacitor or reactor banks and adjusts transformer taps for voltage control action. But better communication technology enables to relay the voltage instability index of buses and take control action in AVRs of generators for the voltage control as a secondary voltage scheme instead of switching of additional reactive power compensator.

The possibility of fossil fuel shortage in the near future and due to growing environmental concerns, renewable energy has gained major attention in recent years. Among the various renewable energy sources, wind power has the most favorable technical and economic prospects [31]. In recent years wind penetration level in both transmission and distribution networks has been increasing. According to American Wind Energy Association (AWEA) total installed wind power capacity is 68 GW [32]. Department of Energy (DOE) laid a vision of 20% wind by 2030 [33]. According to NERC the actual growth in wind installed capacity has increased dramatically and the total installed capacity in recent years has exceeded the pace required to reach 20% that is 300 GW of the wind by 2030. Given the increase in wind generation and the highly variable nature of the resource, the impact of increased penetration in power grid need to be studied and proper management of wind power sources must be insured for reliable and secure power system operation. It was acceptable to trip the wind turbine in the event of a large disturbance resulting in significant voltage dip. But with the evolution variable speed wind turbine technology and high penetration of wind power into transmission network, FERC order 661-A mandated wind turbine to remain online during severe voltage disturbance for a period time with a defined voltage profile [34]. Voltage regulation in power systems is directly related to the control of reactive power. The recent grid codes demand wind farms not only to operate continuously during voltage and frequency fluctuation but also provide reactive power control capabilities, often in response to the power system voltage,

much as conventional power plants [35]. In this dissertation,a participation of a wind generator as a reactive reserve generator in the proposed secondary voltage control has been presented.

1.2 Problem Statement

Wind integrated power system are more complex due to operation in stressed condition with weak transmission and heavily loaded condition. Due to this, the problem of voltage instability and voltage collapse is a major issue of wind integrated power system. Voltage instability may be caused by various system aspects and most of which can be directly or indirectly linked to the inability of the generators or other reactive power sources to provide the adequate amount of reactive power to maintain the voltage to permissible steady level. Variable speed wind generation is capable of reactive power generation but the nature of generation is different than the conventional generator. Due to the higher penetration of wind generators , grid operators mandate wind generators to act as a conventional synchronous machine with reactive power capability. Traditionally, operators switch on shunt capacitor or reactor banks and adjust transformers for voltage control action under-utilizing the reactive power capability of conventional as well as wind generators. This is mainly due to inadequate communication technology to relay grid information to a generator and lack of proper control of set-point for AVRs. With the advancement in communication technology and data processing capability, voltage instability information of buses can be relayed to control center and ultimately to generation operators for control action. As reactive power cannot of transmitted to a farther distance, the voltage and reactive power is a local phenomenon. The local nature of voltage and reactive power problem can be better realized by isolating the grid into different coherent groups which has similar characteristics for reactive power and voltage problem. Due to this, proper control action of generators acting as reactive power reserves using secondary voltage control scheme can decrease the requirement of additional reactive

power sources to ensure voltage stability in every bus. Voltage stability of a system can be maintained by identifying buses prone to instability and adequately supplying reactive power by secondary voltage control action using the control generators in the voltage control area. An effort has been made in this dissertation to develop a voltage instability monitoring index and voltage control areas to effectively apply voltage and reactive power control to prevent the wind integrated system from voltage collapse and subsequently system blackouts.

1.3 Research Overview and Methodology

In this dissertation,a control technique for wind integrated power grid to prevent voltage instability and voltage collapse is developed using voltage controllability and vulnerability detection. Voltage vulnerability detection is a crucial topic of investigation for a security of the grid. An improved voltage stability index capable of predicting proximity to voltage collapse represented by a scalar number is developed. The index is based on the concept of maximum loading capability and through the help of fast method of Thevenin equivalent calculation can be utilized for online monitoring of bus voltage. The index is used as control criteria for application of secondary voltage control of the system. The effectiveness of the proposed voltage stability index is demonstrated by simulations on a two bus test system, IEEE 39 bus test system, IEEE 118 bus test system and 32 bus radial test system in Matlab [36]. The concept of local nature of voltage and reactive power problem is used to divide the system into different voltage control areas. The voltage vulnerability and reactive power allocation in the power system depend on the balance of reactive power among generators and loads, thus the system is partitioned based on reactive power sensitivities and clustering technique. The sensitivity matrix can be simply calculated with a jacobian matrix of generator reactive power to state vector and load flow jacobian. VCAs are identified for various test systems like IEEE 39 bus system and IEEE 68 bus system and compared with traditional VCA identification techniques. Further,

machine learning techniques are used for online clustering of reactive power sensitivities for partitioning of power grid into VCAs. The effectiveness of the method is verified on IEEE 39 bus system and IEEE 68 bus system. A wind integrated power system is developed in commercial power system software Siemens PSS\E [37] for voltage control simulation. VSI as voltage instability detection criteria and VCA identification using reactive power sensitivities algorithm script are run in Python to automate PSS\E [37]. The effectiveness of secondary voltage control, VSI, and online clustering is shown in both power grid with and without wind generator. Comparison of voltage control of the system with and without wind generator is demonstrated.

1.4 Research Contribution

Following are identified research contributions which together provide a means for control of wind integrated power grid.

- A simple voltage stability index based on maximum power loading is developed. The index is a scalar measure which predicts the proximity of bus to the voltage collapse. Since the index can be calculated using system measurements and employs fast Thevenin calculation method, it can be effective voltage stability monitoring index with various applications.

- A novel identification method of voltage control area based on reactive power sensitivities is proposed. The method can be applied for the online application as it employs a direct approach for sensitivity calculation and machine learning technique for clustering. The online application of the method is a important contribution over a conventional offline methods.

- Formulation of secondary voltage control scheme based on voltage controllability and vulnerability detection for a smooth operation of a power grid and prevention from voltage collapse leading to blackouts. The effectiveness of wind generator for the proposed secondary voltage control of a power grid has been

demonstrated to prove that it can participate in a regional voltage and reactive power control as well.

1.5 Disseratation Organization

The dissertation is organized as follows:

- Chapter 1: This chapter discusses the motivation of the research and provides research overview and methodology. It summarizes the contributions of the research work.

- Chapter 2: This chapter presents the concept of voltage stability and literature review on voltage analysis techniques. Also, literatures on wind power and reactive power control is presented.

- Chapter 3: The proposed voltage stability index to detect voltage vulnerability is presented in this chapter.

- Chapter 4: This chapter presents proposed reactive sensitivity based identification of voltage control areas of power system. Application of the proposed technique in test system is presented and comparison with other methods are shown.

- Chapter 5: This chapter presents online clustering of sensitivities for identification of voltage control areas. Application in various test systems is presented.

- Chapter 6: This chapter presents voltage control of wind integrated power grid using proposed voltage vulnerability criteria and proposed method of identification of voltage control areas

- Chapter 7: This chapter is conclusion and discussion of future works.

CHAPTER 2: VOLTAGE STABILITY AND WIND POWER

2.1 Introduction

Power system stability is defined as the ability of an electric power system to regain a state of operating equilibrium after being subjected to a physical disturbance, with most system variables bounded so that practically the entire system remains intact [38]. The integration of distributed resources and operation of power system in highly stressed condition to meet growing consumer demands and economic incentives have increased the risks of voltage instability. Wind farm, one of the widely used renewable distributed resource has evolved from being fixed speed power generator to variable speed power generator with reactive power capability. This chapter briefly introduces voltage stability concepts along with its causes and control mechanism. Also, wind power control architecture is presented along with its voltage control mechanism.

This chapter is organized as follows. Section 2.2 introduces voltage stability of power systems. Various voltage stability analysis techniques are reviewed in section 2.3. Section 2.4 briefly reviews online voltage stability techniques. Voltage stability in wind integrated power grid is presented in section 2.5. Section 2.6 presents reactive power and voltage control in wind generator. Section 2.7 presents the overview of control of DFIG followed by conclusion in section 2.8.

2.2 Voltage Stability

Voltage stability is defined as the ability of a power system to maintain steady voltages at all the buses in the system after being subjected to a disturbance from a given initial operating condition. It depends on the ability to maintain/restore

equilibrium between load demand and load supply from the power system. The instability that may result occurs in the form of a progressive fall or rise of voltages of some buses. A possible outcome of voltage instability is a loss of load in an area, or tripping of transmission lines and other elements by their protective systems leading to cascading outages [10, 38, 39].

Voltage collapse is typically associated with the reactive power demands of loads not being met because of limitations on the production and transmission of reactive power. Although many other variables are typically involved, some physical insight into the nature of voltage collapse may be gained by examining the production, transmission, and consumption of reactive power. Generators, transmission line, and loads are among the most important components [40]. Following are the major factors causing voltage instability problems.

- Generator reactive power

  The generator is the main source for reactive power (Q) which is limited by field current limit (If) and armature current limit (Ia). The operation region for reactive power generation constrained by these limits is shown as a curve popularly knows as capability curve of a generator. When reactive power is constrained by If, the reactive power becomes voltage dependent. The maximum load power is severely reduced when the field current of the local generator becomes limited. Generator limits may also cause limit-induced bifurcation when voltage collapse occur right after the generator limits are reached.

- Transmission network capability

  The transmission network is the important constraints for voltage stability. Maximum deliverable power is limited by the transmission network determined by thermal and stability considerations as well as possible line outages that reduce transmission capacity.

- System loads

  The major factor which influences system instability is system load. Static load models are constant power, constant current, constant impedance while Dynamic models are represented by differential equations. Induction machine is typical dynamic load model. Another important load aspect is the load tap changing (LTC) transformer which is one of the key mechanisms in load restoration. Reactive power demands of loads increase with motor stalling, load increases or changes in load composition such as an increased proportion of compressor load.

Synchronous condensers or static var compensator are also sources of reactive power and the limits on theses also affects the voltage stability. Most of these changes have a significant effect on reactive power production, consumption, and transmission. Switching of shunt capacitors, blocking of tap-changing transformers, re-dispatch of generation, rescheduling of generator and pilot bus voltages, secondary voltage regulation, load shedding, and temporary reactive power overload of generators are some of the control actions used as countermeasures against voltage collapse.

2.2.1 Classification of Voltage Stability

The classification of power system stability according to [38] is shown in Fig. 2.1. From the point of view of techniques used to analyze the voltage stability, it is categorized into small-disturbance and large-disturbance voltage stability. Small disturbance stability deals with the situation when the system is subjected to a small perturbation, and large-disturbance stability deals with larger disturbances such as loss of generation, loss of line etc. The classification along with causes, measuring factors and determination technique is shown in Table 2.1.

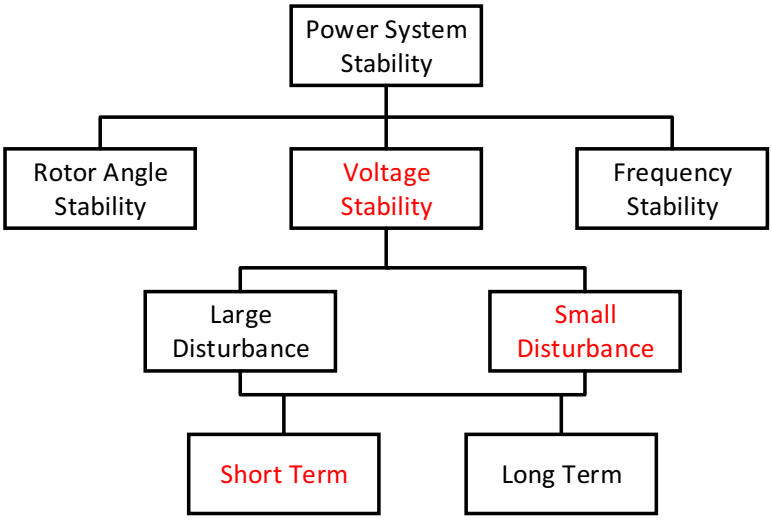

Figure 2.1: Classifcation of power system stability

Table 2.1: Classification of voltage stability based on disturbance

Stability	**Causes**	**Measuring factors**	**Determination**
Small-disturbance	Small perturbations as incremental change in system load	Characteristics of load, continuous controls, & discrete controls	Linearizion of power system with appropriate assumption.
Large-disturbance	System faults, loss of generation, or circuit contingencies	System & load characteristics, interactions of both continuous and discrete controls & protections	Examination of nonlinear response of the power system .

Voltage stability problem is classified into short-term and long-term based on the time span of disturbance in a power system. This kind of voltage collapse is usually associated with the fast response of voltage controllers, such as generator automatic voltage regulator (AVRs). Proper tuning of the system voltage controllers can normally avoid short-term voltage instability problems. The classification with time

span, components involved and analysis techniques is shown in Table 2.2. A voltage stability problem in the long-term time frame is mainly due to the large electrical distance between the generator and the load, and thus depends on the detailed topology of the power system. In general, short-term voltage instability and long-term voltage instability are all caused by the inability of the system to supply the required load demand.

Table 2.2: Classification of voltage stability based on time

Stability	**Components**	**Time**	**Analysis**
Short-term	Fast acting load components as induction motors, electronically controlled loads and HVDC converters	Order of several seconds	Solution of appropriate system differential equations.
Long-term	Slower acting equipments as tap-changing equipments, thermostatically controlled loads and generator current limits	Several minutes	Static analysis to estimate stability margins, identify factors influencing stability.

2.3 Voltage Stability Analysis Techniques

Time-domain simulations, in which appropriate modeling is included, captures the events and their chronology leading to instability. However, such simulations are time-consuming and do not readily provide sensitivity information and the degree of stability. There are two main approaches of voltage stability analysis in nonlinear power systems: dynamic and static. Although they are classified as two different analyses, the two approaches should be used in a complementary manner depending on the study interest.

The dynamic analysis implies the use of a model characterized by non-linear dif-

ferential and algebraic equations which include generators dynamics or tap changing transformers. The overall system equations may be expressed in the following general from [41]:

$$\dot{a} = f(x, V) \tag{2.1}$$

And a set of algebraic equations:

$$I(x, V) = Y_N V \tag{2.2}$$

With a set of known initial conditions (x_0, V_0), where x is the state vector of the system, V the bus voltage vector, I the current injection vector and Y_N the network node admittance matrix. The equations (2.1)- (2.2), can be solved in time-domain by using any of the numerical integration methods and network power-flow analysis methods. This approach requires a lot of computations as well as calculation time and does not provide information regarding the sensitivity or degree of instability but is useful for detailed study of specific voltage collapse situation, coordination of protection and control and testing of remedial measures.

The static approach captures snapshots of system conditions at various time frames along the time-domain trajectory. At each of these time frames, time derivatives of the state variables $(\dot{x})$ in (2.1) are assumed to be zero and the state variables take on values appropriate to the specific time frame. Consequently, the overall system equations reduce to purely algebraic equations allowing the use of static analysis technique. System dynamics influencing voltage stability are usually slow so many aspects of the problem can be effectively analyzed by using the static method. If appropriately used can provide much insight into the nature of the problem and different key contributing factors [42]. In static approach one of the common method to determine stability is computing the $V-P$ and $Q-V$ curves at selected buses. The P-V curves are the most used method of predicting voltage security. They are used

to determine the loading margin of a power system. The margin between the voltage collapse point and the current operating point is used as voltage stability criterion. [43] presents the practical application of an approach based on $V - Q$ sensitivity and [42] presents modal analysis approach.

2.3.1 Voltage Stability Studies via Sensitivity Analysis

In voltage stability analysis besides finding the voltage stability results, it is equally important to identify parameters which influence the system performance and stability. A common approach in doing sensitivity analysis is to define a stability index and then study how the different parameters affect this index and eventually stability. By sensitivity technique, useful information about the relationships between state, control, and dependent variables can be established.

2.3.2 Voltage Stability Studies via Index

In voltage stability analysis, it is useful to assess voltage stability of power systems by means of voltage stability index, a scalar magnitude that can be monitored as system parameters change. Operators can use the index to know how close the system is to voltage collapse in an intuitive manner and react accordingly. Various voltage stability indexes are presented in the literature. These can be broadly classified into following categories.

1. Voltage stability index base on Jacobian matrix

   Jacobian matrix based VSIs can calculate the voltage collapse point or maximum loadability limit and determine the voltage stability margin. This has a high computation time hence, is not suitable for online assessment. In [44], a second order performance index or index 'i' is presented which overcome the weakness of first order index such as the minimum singular value index. The voltage stability index proposed in [45] is based on the tangent vector, which gives information on how system variables are affected by changing the load.

The V/V_0 index in [46] is a simple index to compute. The ratio V/V_0 at each node yields a voltage stability map of the system, allowing for immediate detection of weak and effective countermeasure spots.

2. Voltage stability index based on system variables

   System variables based VSIs, which uses the elements of the admittance matrix and some system variables such as bus voltages or power flow through lines, require less computation and, therefore, are adequate for online monitoring. The disadvantage of this index is that they cannot accurately estimate the margin, so they can just present critical lines and buses. These indexes have been classified into two groups as in [47]: bus voltage computation index and line stability index.

   - Bus voltage computation index

     Bus voltage computation index is also known as nodal voltage stability index. Voltage stability index called L index based on the solution of the power flow equations was presented in [15]. Reference [48] presented VSI that varies almost linearly with load and requires only some local information such as bus voltage magnitude and load current magnitude.

   - Line stability index

     Most of the line stability indexes are formulated based on the power transmission concept in a single line. L_{mn} index proposed an overall system stability index base on the concept of power flow through a single line [49]. Line Stability Factor (LQP) index is based on a concept of power flow through a single line [50]. The fast voltage stability index (FVSI) proposed by [51] is formulated based on a power transmission line. Voltage Collapse Point Indicators (VCPI) index proposed by [52] investigates the stability of each line of the system and they are based o the concept of

maximum power transferred through a line.

2.4 Online Stability Assessment

The continuous inclusion of renewable generation resources, evolution in technology and changes in market mechanisms has increased the uncertainty level of power system operations. Quick and effective measures against rapidly generating systems are essential to enhance the system efficiency and maintain reliability. Therefore methodology of real time control will play a crucial role in maintaining these goals [53]. An essential component at maintaining the stable operation of power systems is online voltage stability management to predict and control the voltage stability of operating power system on a real time basis [54]. Online voltage stability monitoring is the process of obtaining voltage stability information for a given operating scenario. The prediction should be fast and accurate such that control signals can be sent to appropriate locations quickly and effectively. Various methods are mentioned in literature for online voltage stability assessment and monitoring. Most of the literature can be categorized into two categories according to the approaches as follows

- Stability information directly from phasor measurement for operating conditions. Simple and requires few computations, based on Thevenin equivalent of a system [11].

- Offline observations are used to build a statistical model of the power system and the model takes measurements consisting of current state as the input and returns the voltage stability information as the output. Generally, the model measurements are done by one of the artificial intelligence technique such as expert systems, decision trees, and neural networks while voltage stability information is provided as output in the form of voltage stability index or margin.

The foremost literature on online voltage stability is [55],in which forecasting aided state estimator (FASE) provides real-time information for voltage security monitoring.

In FASE a state forecasting step is added to a traditional static power system state estimation algorithm. The online voltage instability can be studied based on the method of the assessment. As per different assessment, it is divided into various sections as voltage stability based on index and voltage stability assessment using artificial intelligence techniques. Various techniques of voltage stability based on the index will be presented below.

2.4.1 Voltage Stability Index

The index based instability measure captures the unique system behavior in terms of a number and interprets them to give the notion of distance to instability. For online voltage assessment all of the indices presented in section 2.3.2 might not be suitable due to computation time and complexity. An index can be used as a reference value to run a control routine. The indexes for online voltage monitoring are categorized based on their approach and some of them are given below.

2.4.1.1 Index from Direct Phasor Measurements

The development of phasor measurement technology together with other advances in computational facilities, networking infrastructure, and communications has opened new perspectives for wide-area monitoring and control [56]. The phasor measurement based approach for estimation of voltage stability index can be extended to general systems [57, 58]. Phasor measurement based voltage instability monitoring can be classified into two broad categories: methods based on local measurements and methods based on the observability of the whole region. The first, need few or no information exchange between the monitoring locations, while the second one requires time-synchronized measurements. [59–61] has presented methods based on local measurement using Thevenin equivalent method. Reference [62] uses the availability of reactive power reserves without any discussion of the relationship with the Thevenin equivalent. [63, 64] also presents the voltage stability assessment using local phasor

measurement. The voltage stability index method based on the observability of the whole region is presented in [65, 66]. The VSI presented in [67] is based on time-synchronized measurements available in Wide Area Monitoring System (WAMS) and the VSI determines the voltage stability margins of all system load buses.

2.4.1.2 Index from Load Flow Jacobian

The use of singularity of the power flow jacobian matrix as an indicator of steady state stability was first pointed out by [68], where the sign of the determinant of the load flow Jacobian was used to determine the system stability. The eigenvalue decomposition technique for voltage stability index determination was discussed in [42]. Index based on minimum singular value of Newton-Raphson power flow Jacobian matrix was presented [69]. Effectiveness of various voltage stability indexes are compared in [70] and further three more indexes based on readily available Jacobian matrix elements from load flow are presented.

2.4.1.3 Other Techniques

Similar to L-index, another important voltage instability index was presented whose feasible value ranges from 0 to 1 with values closer to 1 suggesting the system is closer to instability [71]. The limit criterion is such that both, load flow jacobian singularity and the maximum power transfer theorem hold true. A method to relate the VAR reserve level with voltage stability margin by monitoring certain key generators which have a prominent role in determining the level of voltage stability through their reactive reserves was proposed in [54]. While [53] has used reactive power reserve sensitivities approach, [72] presents voltage collapse index based on closely located power flow solution pairs and [73] presents voltage collapse index based on sensitivity analysis. [74] proposes real-time reactive security monitoring by monitoring the contingent VAR margins of all the zones within a given system. Zones are a group of one or more tightly coupled generator buses, together with the union of the sets of load

buses that they mutually support. The idea behind the method is that the voltage stability problem has a local origin and that it is directly related to the availability of reactive power sources. References [19, 75, 76] proposes the determination of proximity to voltage collapse by monitoring the reactive reserves which are obtained by determining voltage control area.

2.5 Voltage Stability of Wind Integrated Power Grid

The possibility of fossil fuel shortage in the near future and due to the growing environmental concerns, renewable energy has gained major attention in recent years. Among the various renewable energy sources, wind power has the most favorable technical and economic prospects [31]. Given the increase in wind generation and the highly variable nature of the resource, the stability of power systems will be impacted significantly. The most common wind turbine technology installed in systems today is the doubly-fed induction generator (DFIG) machine. The older fixed speed squirrel cage induction generator (FSIG) machines are still in service, but it is uncommon for them to be utilized in new wind farm installations. Both machines contribute asynchronous power to the system, and as such, a large penetration of wind generation will impact the stability of the system, particularly the voltage stability of the system. The main advantage of the DFIG turbine is the ability to provide reactive power control without installing additional capacitive support. The DFIG can be operated in one of two control modes; firstly, fixed power factor (PF) control, where the turbine controls reactive power production in order to achieve a specified power factor; secondly, terminal voltage control, where the reactive power is controlled to meet a target voltage. The analysis methods and techniques for determining power system stability are well established for systems that consist mainly of large synchronous generating units. Traditional techniques are limited in capturing this variable behavior and new study techniques and methodologies will be required to properly quantify the stability of a power system. In particular, the variable nature of wind necessitates new

techniques to assess its impact. [77–80] have presented methods to incorporate wind generator nature for voltage stability analysis. A voltage stability assessment tool that incorporates wind variability is developed in [77]. The traditional methodology of drawing PV curves to assess static voltage stability margin is modified to address the intermittent nature of wind energy giving a three dimensional voltage secure region of operation for a range of variable wind. By combining power flow, economic dispatch, unit commitment and historical time-series data that capture the variability of the wind, into a single large-scale simulation. [78] presents a methodology that is suitable for analyzing a large power system and assessing its voltage stability as well as system response to other conditions under large penetrations of wind generation. It also shows that utilizing the control features of the DFIG wind turbine improves the voltage stability margin.

2.5.1 Impact of Wind Power in Voltage Stability

Traditional fixed speed wind power was used in distribution and sub-transmission network and served a small area of the load. These wind power were supported with additional reactive power sources to maintain voltage level. It was acceptable to trip the wind turbine in the event of a large disturbance resulting in significant voltage dip. But with the evolution of variable speed wind turbine technology and high penetration of wind power into transmission network, FERC order 661-A mandated wind turbine to remain online during severe voltage disturbance for a period of time with a defined voltage profile. As wind power sources are connected to the grid during voltage disturbances, the study of impacts of wind generation is crucial to alleviate voltage stability problem.

2.6 Reactive Power and Voltage Control in Wind Generator

A power grid contains a vast number of loads fed from many generating units, this complicates the problem of maintaining voltage within the required limit. The reac-

tive power requirement of the transmission system varies with the variation of load. Reactive power cannot be transmitted over a long distance so a proper selection and coordination of equipment for controlling reactive power and voltage are necessary. In a power grid, synchronous generator is a dispatchable generator which can generate or absorb reactive power depending on excitation. In a wind integrated power grid, wind generation is responsible for substituting the synchronous generator which is possible in case of type 3 and 4 variable wind turbines with reactive power capability. Variable speed wind generators are equipped with voltage source converters (VSC) which can be controlled by independent control of active and reactive power. These generators are capable of generating as well as absorbing reactive power. Like synchronous generator the reactive power generation in wind generators are limited by various machine parameters and limit of reactive power generation can be shown in reactive power capability curve. Reactive power capability curve governs the amount of reactive power generation in wind farms and the transmission of the reactive power is restricted to a short distance. Due to these, additional intermediate reactive power sources are required to maintain the voltage within the limit in all buses. Intermediate reactive power sources are additional cost so a coordinated optimum control of the reactive power of wind generators and these additional sources should be ensured to keep the operating cost to a minimum. The intermediate additional reactive power sources can be static or dynamic based on the network topology and requirements of a system.

2.7 Overview of Control of DFIG

The operation of DFIG in a wider range of wind speed is achieved with higher efficiency with a combination of electrical control of DFIG accompanied by control of wind turbine which is obtained by maximum power point tracking (MPPT) and Pitch control. The electrical control of DFIG is achieved by the control of voltage source converters. The objective of grid side converter is to maintain the dc link

voltage constant while the rotor side converter controls the voltage and power of the machine. The DFIG wind turbine rotor side converter has the capability to adjust the rotor currents to obtain the desired real and reactive power outputs on the stator side. The decoupled control of active and reactive power through RSC provides the ability to wind turbine to capture maximum energy from the wind and at the same time provide reactive power support to the grid.

2.7.1 Grid Side Converter Control

The main objective of grid side converter (GSC) control is to maintain the dc-link voltage constant regardless of magnitude and direction of rotor power. Also, the objective of grid side converter control is to control the reactive power exchange with the grid. Here, vector control scheme with a reference frame oriented along the grid voltage vector position enables the current regulated PWM converter to regulate DC-link voltage and reactive power by d and q axis current component [81]. Schematic of Grid side controller is shown in Figure 2.2

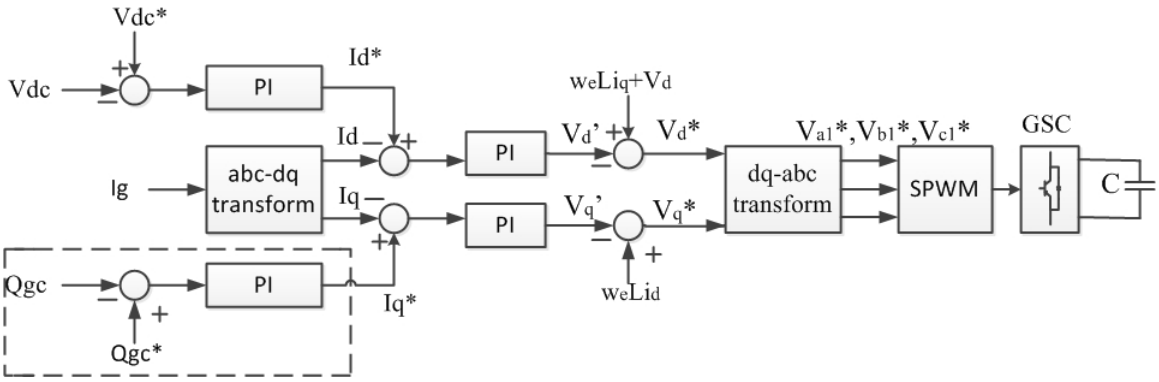

Figure 2.2: Schematic of GSC controller.

2.7.2 Rotor Side Converter Control

Rotor side converter control or induction machine control is carried to obtain independent control of active and reactive power. A vector control technique is used to decouple rotor current into $dq-$ axis which controls the active and reactive power separately. The electromagnetic torque of DFIG is controlled such that the rotor always

operates at the optimal speed given by maximum power tracking characteristics. In a DFIG both the active power and the reactive power at the stator can be controlled independently through the control of rotor-injected currents. This can be used to provide voltage regulation or reactive power support to the grid within the ratings of the system. The q-axis rotor current is controlled to control the reactive power.

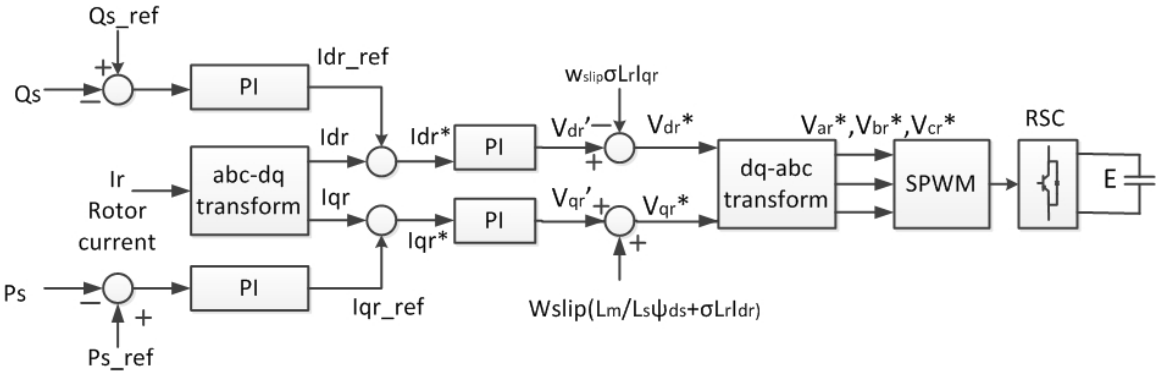

Figure 2.3: Schematic of RSC controller.

The torque or active power reference for the DFIG control is mainly obtained from the turbine control. The electromagnetic torque of DFIG is controlled such that the rotor always operates at the optimal speed given by maximum power tracking characteristics. The reactive power reference is obtained from a voltage regulation loop that regulates the voltage at the point of interconnection to the grid or from a set power factor command or from a direct system-level command for reactive power support as shown in Figure 2.4. The reactive power set point is dependent on the control mode of the DFIG. The two commonly used control modes are:

- Power factor control
- Voltage control

The stator real and reactive powers are controlled in the power factor control mode to maintain a constant power factor at the point of interconnection. The reactive power is controlled in the voltage control mode to maintain the voltage magnitude at

a specified value in the voltage control mode. The stator side converter is normally set at unity power factor. The error in reactive power is used to control the q-axis rotor current.

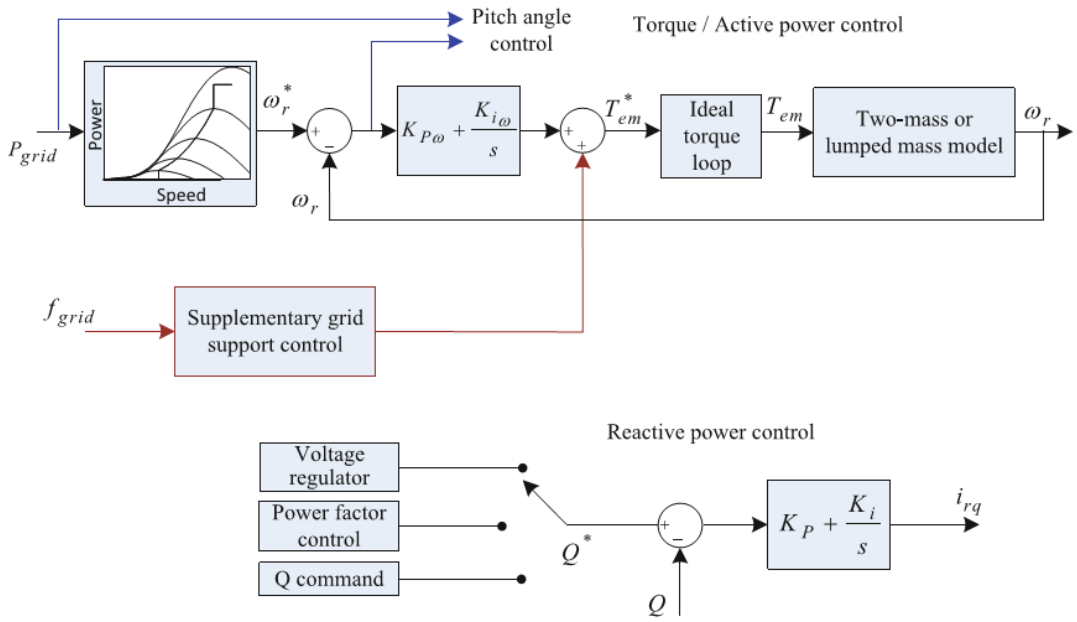

Figure 2.4: Schematic of RSC controller [82].

2.8 Conclusion

Any node in a power system is subjected to the voltage instability due to a disturbance. Voltage vulnerability of a node or system can be determined based on the severity and location of the disturbance. Voltage vulnerability of a bus or a system can be captured in the form of a voltage stability index. Wind power is capable of providing both active and reactive power with converter control. In next chapter, a voltage stability index for determining proximity to voltage instability based on the maximum loadability will be presented.

CHAPTER 3: PROPOSED VOLTAGE STABILITY INDEX

3.1 Introduction

This chapter describes the proposed voltage stability index which is used to predict the vulnerability of a grid. The index is calculated using the maximum loading capability of a bus combined with the Thevenin equivalent method for the aggregated representation. In voltage stability analysis, it is useful to assess voltage stability of power systems by means of voltage stability index. The index is a scalar magnitude that can be monitored as the system parameter changes. The index based instability measure captures a unique system behavior in terms of a number and interprets them to give the notion of distance to the instability. Operators can use these indexes to know how close the system is to voltage collapse in an intuitive manner and react accordingly. Although stability studies, in general, requires a dynamic model of the power system, in this chapter analysis of voltage behavior has been approached using static techniques, which has been widely used on the voltage stability analysis [83].

The voltage stability index (VSI) is derived based on the maximum loading capability and the Thevenin equivalent theory. The method based on maximum loading capability has been presented in [84, 85]. But those VSIs are restricted to distribution feeders only. This chapter presents the extension of the method for the application in a transmission system. To apply the index for a transmission system a fast method to reduce the system into two node system as in [16] is applied. The line characteristics of transmission and distribution radial systems are different. So, a different approach is used to get two bus equivalent of radial system. The VSI can be used to predict proximity to voltage collapse using either powerflow result or PMU data. The slope of the index indicated the speed to the collapse point. The performance of proposed

index is investigated to prove the claims made here and will be demonstrated in following sections.

This chapter is organized as follows. Section 3.2 presents the brief overview of maximum loadability. Section 3.3 present fast method for the Thevenin equivalent calculation. Proposed voltage stability index is presented in section 3.4. The test results of proposed index in various IEEE test system is presented in section 3.5. Conclusions are provided in section 3.6.

3.2 Maximum Loadability

Power system in a simple electric circuit form can be represented as a two bus network with a ideal voltage source E supplying a load S through line impedance $Z_{km}\angle\beta$, as shown in Fig. 3.1.

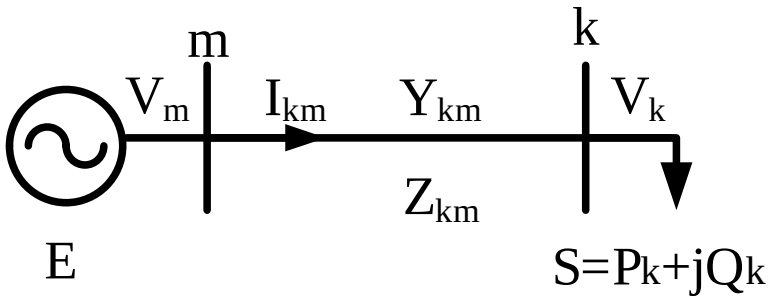

Figure 3.1: Two bus network

The load impedance of the two bus network can be obtained as

$$Z_k^L = \frac{|V_k|^2}{P_k - jQ_k} \tag{3.1}$$

where V_k is load node voltage. Let us denote load impedance as:

$$Z_k^L = Z_k^L\angle\phi \tag{3.2}$$

For above load, consider constant load power factor $cos\phi$ to obtain maximum power transfer or the maximum loading by increasing the value of the load. Increase in the

value of load causes more current to circulate in the circuit , leading to a voltage drop which is proportional to current. The current I is:

$$\begin{aligned} I &= \frac{V_m}{\sqrt[2]{[(Z_{km}\cos\beta + Z_k^L\cos\phi)^2 + (Z_{km}\sin\beta + Z_k^L\sin\phi)^2]}} \\ &= \frac{V_m}{Z_{km}\sqrt[2]{[1 + (Z_k^L/Z_{km})^2 + 2(Z_k^L/Z_{km})\cos(\beta-\phi)]}} \end{aligned} \tag{3.3}$$

Voltage at the terminal of load is :

$$\begin{aligned} V_k &= Z_k^L * I \\ &= Z_k^L * \frac{V_m}{Z_{km}\sqrt[2]{[1 + (Z_k^L/Z_{km})^2 + 2(Z_k^L/Z_{km})\cos(\beta-\phi)]}} \end{aligned} \tag{3.4}$$

Now, active power at the terminal of load is

$$P_k = V_k * I * cos\phi \tag{3.5}$$

$$= \frac{V_m^2/Z_{km}}{[1 + (Z_k^L/Z_{km})^2 + 2(Z_k^L/Z_{km})\cos(\beta-\phi)]} * \frac{Z_k^L}{Z_{km}} cos\phi \tag{3.6}$$

To get maximum power transferred:

$$\frac{\partial P_k}{\partial Z_k^L} = 0 \tag{3.7}$$

After few steps of calculation we get,

$$\frac{V_m^2(Z_{km} - Z_k^L)(Z_{km} + Z_k^L)cos\phi}{(Z_{km}^2 + 2Z_{km}Z_k^L\cos\beta + (Z_k^L)^2)^2} = 0 \tag{3.8}$$

$$V_m^2(Z_{km} - Z_k^L)(Z_{km} + Z_k^L)cos\phi = 0 \tag{3.9}$$

which gives,

$$Z_k^L = Z_{km} \tag{3.10}$$

for the maximum power transfer in the circuit for constant power factor load.

One of the common reasons for voltage instability is that the system is operating at the increased loading point beyond the maximum loading point. The maximum loadability limit is the point from where loading of the system can be no further increased and causes voltage collapse. Loading margin is defined as the distance from a known operating point to the voltage collapse. Estimating the maximum load ability limit or maximum loadability index of power systems is one approach to find voltage stability. Normal load flow can be employed to obtain loading curve which is known as PV curve. But drawback of using load flow method is that the Jacobian of a Newton Raphson power flow becomes singular at the steady state voltage stability limit which is the loadability limit as well. This problem can be eliminated by using Continuous power flow (CPF) technique to find PV curve which provides loadablity limit point as well [86]. CPF technique employs a predictor-corrector method to find a solution path of a set of power flow equation that have been reformulated to include a load parameter. Figure 3.2 is PV curve for bus 18 of NE 39 bus system for various load factors.

3.3 Thevenin Equivalent

Thevenin equivalent system represents complex electrical system with equivalent two nodes connected by Thevenin impedance and source represented by Thevenin voltage. It can be calculated using various methods by using basic electrical engineering rules. To find the Thevenin equivalent across the load bus k, loads of all buses except bus k are replaced by constant impedances and the generators are replaced by negligible reactance. Schematic diagram of Thevenin equivalent of a power system is shown in Fig. 3.3.

For the purpose of voltage stability analysis, various methods to reduce power systems into Thevenin equivalent are available in literatures. Chebbo et al. [87] used

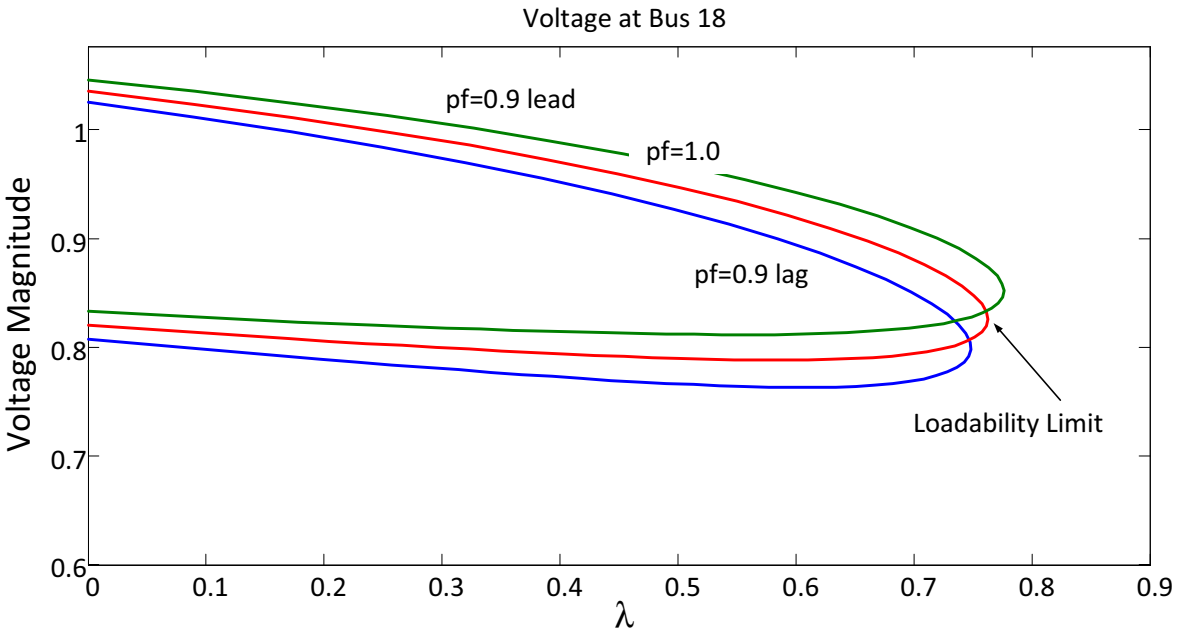

Figure 3.2: PV curves showing maximum loadablity

load flow solutions to calculate Thevenin equivalent model which include the effects of nonlinearity of loads and generators with some repetitive computation. A direct method to calculate Thevenin equivalent using single load flow solutions is presented in [16]. Calculation of Thevenin equivalent using local measurements are presented in [11] using curve fitting technique and [13] using Tellegen's theorem. A fast method of Thevenin equivalent calculation based on network impedance matrix is used to find Thevenin equivalent circuit for the application in proposed VSI [16].

The load impedance of bus k for a two node network or Thevenin equivalent of power system as shown in Fig.3.3 can be written restated as

$$Z_k^L = \frac{|V_k|^2}{P_k - jQ_k} \tag{3.11}$$

Fig. 3.4 is the schematic diagram of generator model in power system with constant terminal voltage and series reactance X_g of internal voltage source equal to zero . Here buses 1 to m are the generator buses and buses $m+1$ to n are the load buses.

In the figure, Z_{kk} shown in the Fig. 3.4 is k_{th} diagonal element of network impedance

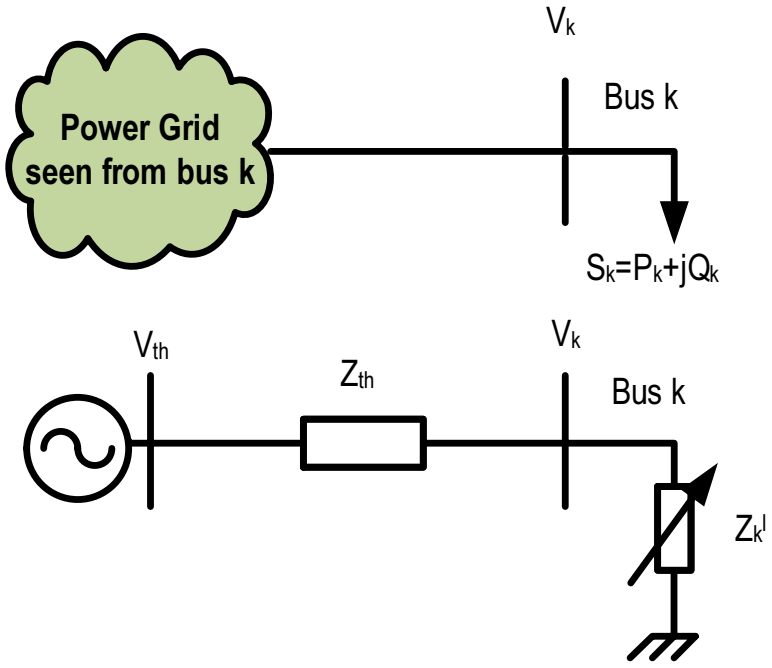

Figure 3.3: Thevenin equivalent of power system

(Z) matrix when all loads are considered and Z_{th} is impedance of bus k when load k is ignored. Z_{th} is the Thevenin impedance of the system for bus k. If Z_{kk} is the kth diagonal element of the Z matrix when all loads are considered, from Fig. 3.4 we get,

$$Z_{kk} = Z_k^L // Z_{th} = \frac{Z_k^L Z_{th}}{Z_k^L - Z_{th}} \tag{3.12}$$

and the thevenin impedance is given as:

$$Z_{th} = \left(\frac{1}{Z_{kk}} - \frac{1}{Z_k^L} \right)^{-1} \tag{3.13}$$

Fig. 3.5 shows the schematic diagram for calculation of Thevenin equivalent of bus k. If V_k is the voltage of the bus k found from the power flow solution, Thevenin voltage is calculated as in (3.14).

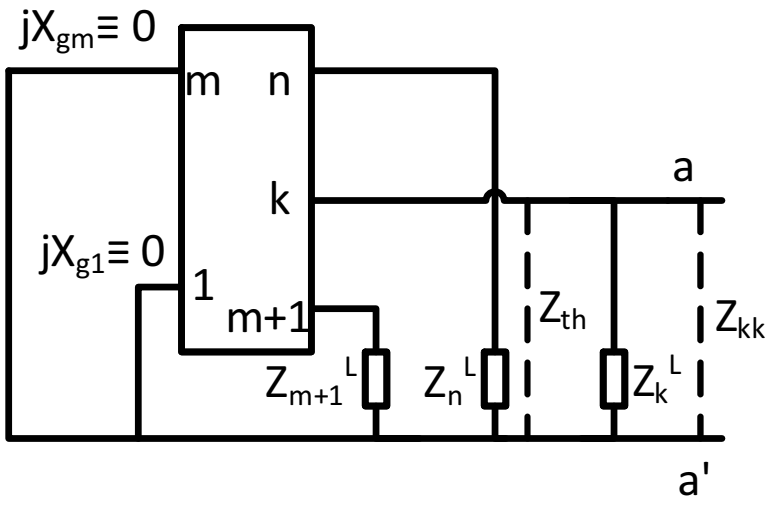

Figure 3.4: Generator model and Thevenin impedance of load bus

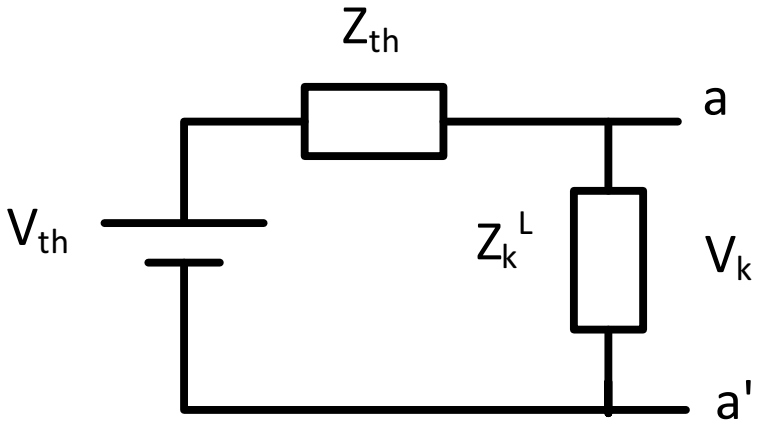

Figure 3.5: Calculation of Thevenin equivalent of bus k

and Thevenin voltage is given as:

$$V_{th} = \left(1 - \frac{Z_{th}}{Z_k^L}\right) V_k \tag{3.14}$$

Hence, Equations 3.13 and 3.14 are the thevenin impedance and thevenin voltage of thevenin equivalent across the load S of bus k of complex power system which can be represented as two node network as shown in Fig. 3.3 above.

3.4 Proposed Voltage Stability Index

A voltage stability index for determining proximity to the voltage collapse based on maximum loading capability is proposed in this section. The maximum loading capability of a load bus is calculated by using the concept of equivalent two bus as described in section 3.2. The voltage stability index proposed here should be able to predict proximity to voltage collapse and provide important information for security of the system. First let us consider a two node power system as shown in Fig. 3.1. In the following section we will derive VSI at bus k using the Thevenin equivalent system representation derived in section 3.3.

The active and reactive power at a bus in a power system network can be represented as:

$$\begin{aligned} P_k &= \sum_{m=1}^{n} |V_k||V_m||Y_{km}|Cos(\delta_m - \delta_k + \theta_{km}) \\ Q_k &= -\sum_{m=1}^{n} |V_k||V_m||Y_{km}|Sin(\delta_m - \delta_k + \theta_{km}) \end{aligned} \tag{3.15}$$

The power equations for two bus network as shown in Fig. 3.1 can be obtained from (3.15) as following.

$$P_k = V_k^2 Y_{kk} Cos\theta_{kk} + V_k V_m Y_{km} Cos(\delta_m - \delta_k + \theta_{km}) \tag{3.16}$$

$$P_k - V_k^2 Y_{kk} Cos\theta_{kk} = V_k V_m Y_{km} Cos(\delta_m - \delta_k + \theta_{km}) \tag{3.17}$$

Similarly, reactive power equations will be as following.

$$Q_k = -V_k^2 Y_{kk} Sin\theta_{kk} - V_k V_m Y_{km} Sin(\delta_m - \delta_k + \theta_{km}) \tag{3.18}$$

$$V_k^2 Y_{kk} Sin\theta_{kk} + Q_k = -V_k V_m Y_{km} Sin(\delta_m - \delta_k + \theta_{km}) \tag{3.19}$$

Squaring (3.17) gives,

$$P_k^2 + V_k^4 Y_{kk}^2 Cos^2(\theta_{kk}) - 2V_k^2 Y_{kk} Cos\theta P_k = (V_k V_m Y_{km})^2 Cos^2\Big(\delta_m - \delta_k + \theta_{km}\Big) \tag{3.20}$$

Squaring (3.19) gives,

$$V_k^4 Y_{kk}^2 Sin^2\theta_{kk} + Q_k^2 + 2V_k^2 Y_{kk} Sin\theta Q_k = (V_k V_m Y_{km})^2 Sin^2(\delta_m - \delta_k + \theta_{km}) \quad (3.21)$$

Adding (3.20) and (3.21) ,

$$V_k^4 Y_{kk}^2 + P_k^2 + Q_k^2 - 2V_k^2 Y_{kk}(P_k Cos\theta - Q_k Sin\theta) = (V_k V_m Y_{km})^2 \quad (3.22)$$

Rearranging,

$$V_k^4 Y_{kk}^2 - V_k^2((V_m Y_{km})^2 + 2Y_{kk}(P_k Cos\theta - Q_k Sin\theta) + (P_k^2 + Q_k^2) = 0 \quad (3.23)$$

$$(V_k^2)^2 Y_{kk}^2 - V_k^2((V_m Y_{km})^2 + 2Y_{kk}(P_k Cos(\theta) - Q_k Sin(\theta)) + (P_k^2 + Q_k^2) = 0 \quad (3.24)$$

Solution for voltage V_k at bus k, is expressed as

$$V_k^2 = \frac{-b \pm \sqrt{(b^2 - 4ac)}}{2a} \quad (3.25)$$

where,

$$\begin{aligned} a &= Y_{kk}^2 \\ b &= -(V_m^2 Y_{km}^2 + 2Y_{kk}(P_k Cos(\theta) - Q_k Sin(\theta)) \\ c &= (P_k^2 + Q_k^2) \end{aligned} \quad (3.26)$$

To get real solution of V_k^2, $(b^2 - 4ac) \geq 0$ should be true

Replacing a, b and c in $(b^2 - 4ac) \geq 0$

$$[-(V_m^2 Y_{km}^2 + 2Y_{kk}(P_k Cos(\theta) - Q_k Sin(\theta))]^2 - 4Y_{kk}^2(P_k^2 + Q_k^2) \geq 0 \quad (3.27)$$

Maximum loadability is reached when $(P_k + jQ_k)$ is increased to the point where (3.25) is equal to zero and from the voltage stability point of view maximum power transfer represents the closeness to voltage instability [88]. Assuming constant load

factor, $P_k + jQ_k$ is replaced by $VSI * (P_k + jQ_k)$ where VSI is voltage stability index which represent the closeness to voltage collapse. VSI is equal to 1 when the line is reaching its maximum power transfer limit. Once the VSI is less than 1 the maximum power transfer limit is violated and voltage becomes unstable. The slope of VSI will show the closeness to the voltage collapse.

$$[V_m^2 Y_{km}^2 + 2Y_{kk}(P_k Cos(\theta) VSI - Q_k Sin(\theta) VSI)]^2 - 4Y_{kk}^2 VSI^2 (P_k^2 + Q_k^2) = 0 \quad (3.28)$$

$$V_m^4 Y_{km}^4 + 4V_m^2 Y_{km}^2 Y_{kk} VSI(P_k Cos\theta - Q_k Sin\theta) + 4Y_{kk}^2 VSI^2 (P_k Cos\theta - Q_k Sin\theta)^2 - 4Y_{kk}^2 VSI^2 (P_k^2 + Q_k^2) = 0 \quad (3.29)$$

$$VSI^2 Y_{kk}^2 [(P_k Cos(\theta) - Q_k Sin(\theta))^2 - (P_k^2 - Q_k^2)] + VSI 4V_m^2 Y_{km}^2 Y_{kk}(P_k Cos(\theta) - Q_k Sin(\theta)) + V_m^4 Y_{km}^4 = 0 \quad (3.30)$$

where,

$$VSI = \frac{-b \pm \sqrt{(b^2 - 4ac)}}{2a} \quad (3.31)$$

$$\begin{aligned} a &= 4Y_{kk}^2 [(P_k Cos(\theta) - Q_k Sin(\theta))^2 - (P_k^2 + Q_k^2) \\ b &= 4V_m^2 Y_{km}^2 Y_{kk}(P_k Cos(\theta) - Q_k Sin(\theta)) \\ c &= V_m^4 Y_{km}^4 \end{aligned} \quad (3.32)$$

Equation (3.31) is the proposed voltage stability index (VSI) for the system which predicts proximity to the voltage collapse. Based on the earlier discussions for a larger power network we can replace the source voltage Vm with the Thevenin voltage Vth. Also, the Ykm can be represented as inverse of Zth and Ykk as inverse of Zkk. The flowchart for calculation of VSI is shown in Fig. 3.6.

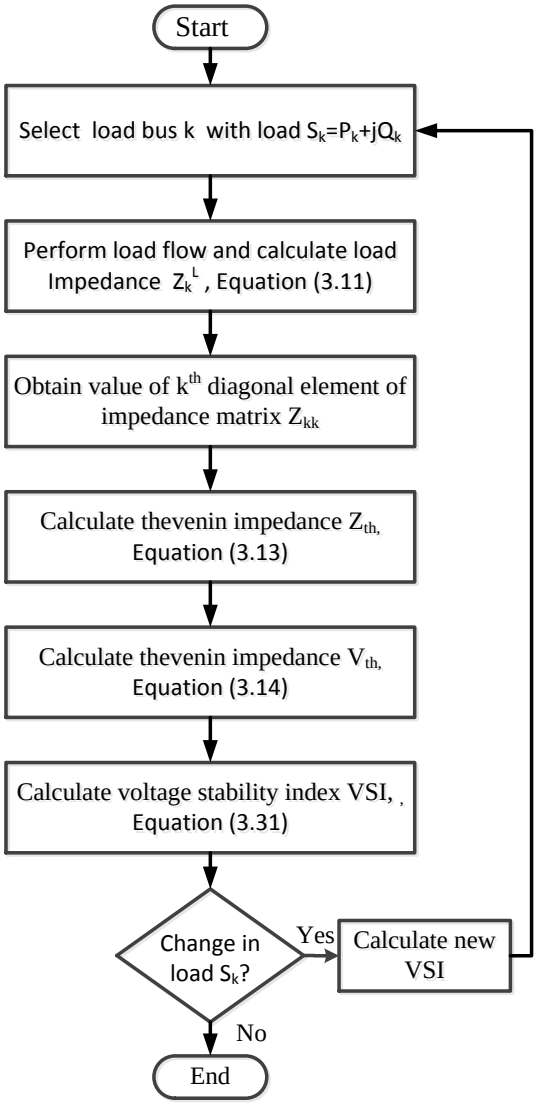

Figure 3.6: Flowchart for calculation of VSI

3.5 Test Cases

Voltage stability index is analysed in following test systems viz. two bus system, New England 10 machine 39 bus system [89] and IEEE 118 test case. The VSI will be compared with L-index [15] and VCPI [71].

3.5.1 Two-Bus Test System

The two-bus test system consists of the generator that supplies local load bus k over the branch Z_{line}. The assumed voltage for generator terminal m is V_m=(1.0+j0.0)pu, Z_{line}=(0.028+j0.096)pu and S_k=(150+j50) MVA. Plots of impedances and VSI are shown for loading change and reactive power change only in Figures 3.7-3.10. For two bus system Thevenin's impedance is equal to line impedance and had constant value of 0.1 pu as shown in Figures 3.7 and 3.9.

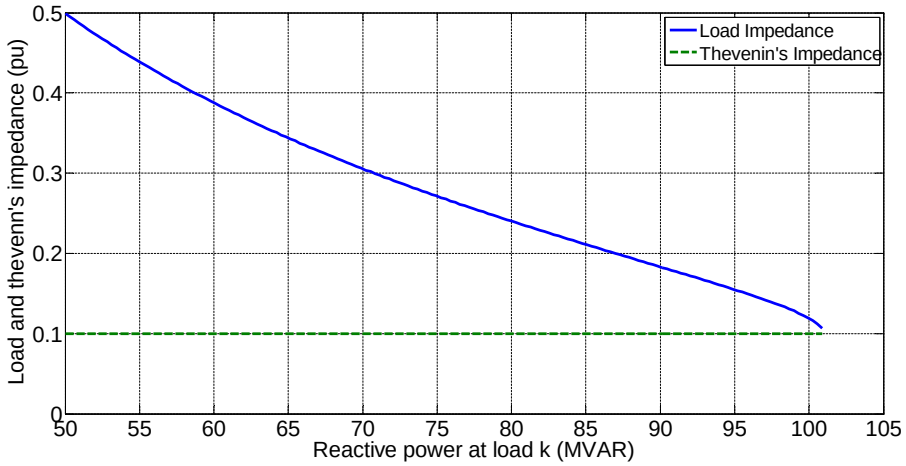

Figure 3.7: Load and thevenin's impedance vs constant power factor load change

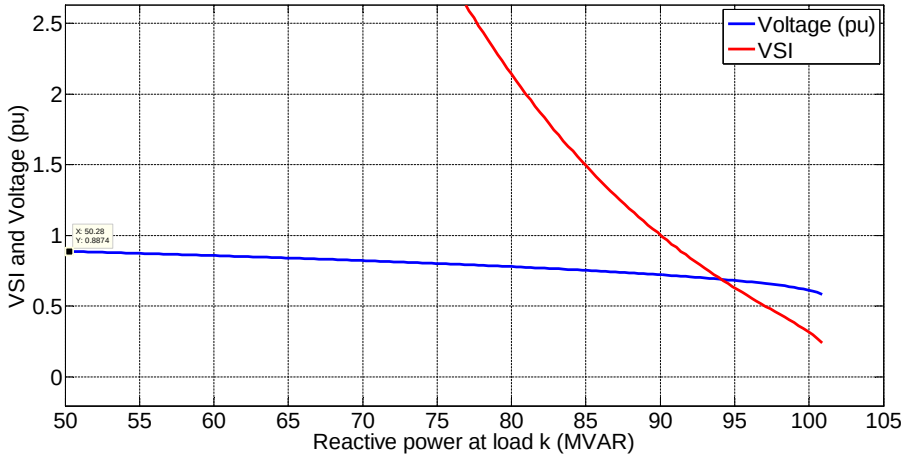

Figure 3.8: VSI and load voltage vs constant power factor load change

Under normal loading in both cases, the load impedance is much greater than the Thevenin's impedance. At the maximum loading, the load impedance is equal to Thevenin's impedance as in the case of maximum power transfer. At the point of maximum loading which is also the collapse point voltage in two cases are 0.58 pu and 0.55 pu and VSI are 0.24 and 0.02 from Figures 3.8 and 3.10 respectively. Considering only the collapse point indicated by very small VSI values close to zero in the voltage stability analysis will be a optimistic approach. When VSI=1, voltages in both cases are around 10% less than the nominal voltage. Voltages are 0.72 pu and 0.78 pu for Figures 3.8 and 3.10 respectively. So the VSI not only indicates the proximity to voltage collapse when its values are less but shows the voltage instability when VSI is less than value 1.

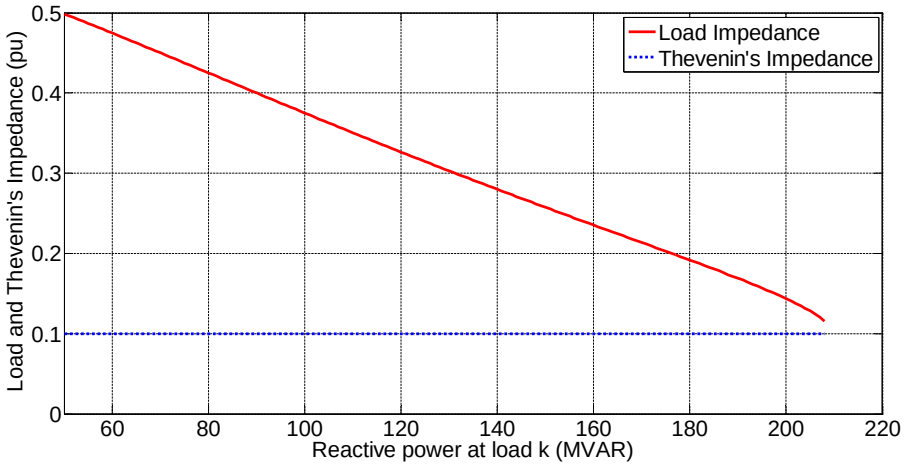

Figure 3.9: Load and Thevenin's impedance of two bus test system

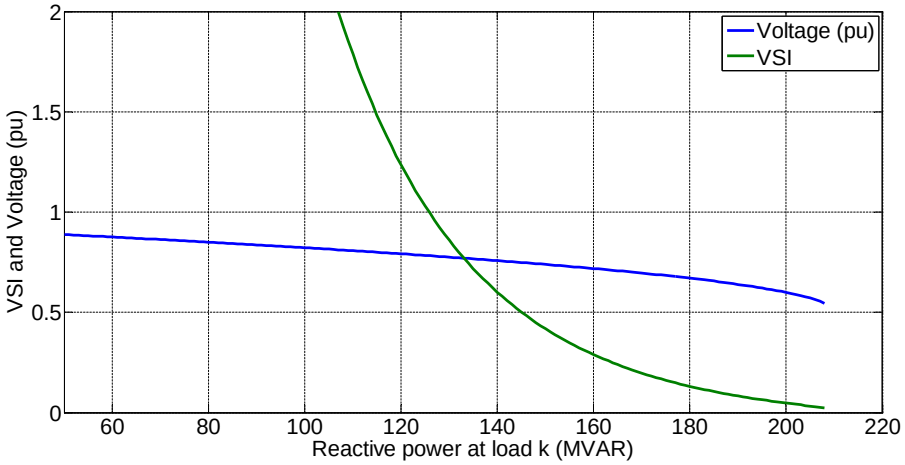

Figure 3.10: VSI and load voltage of two bus test system

3.5.2 New England 39 Bus Test System

New England 39 bus system is a 10 machine 39 bus system commonly referred as IEEE 39 bus system as well is shown in Fig. 4.4

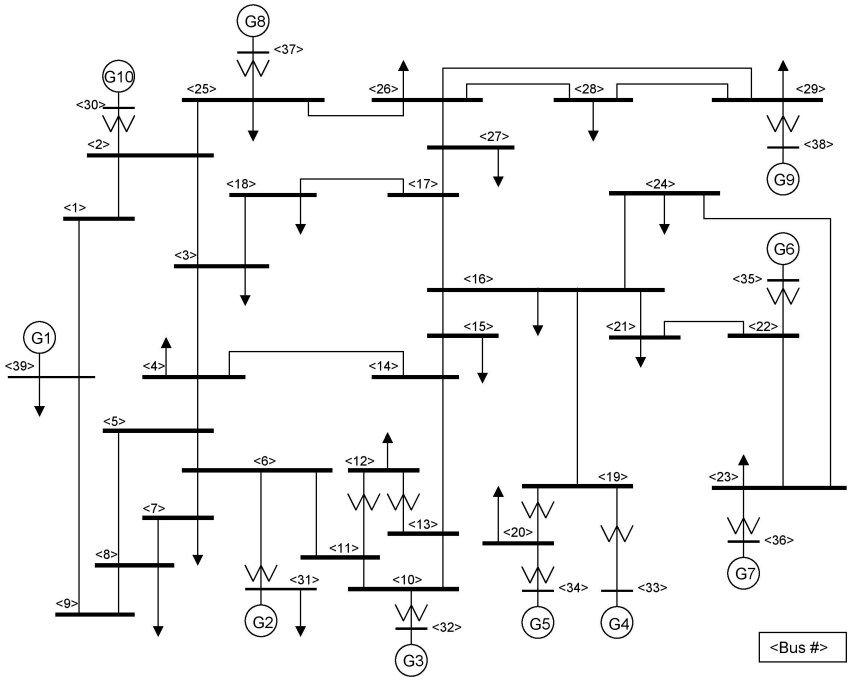

Figure 3.11: New England 39 bus 10 machine system.

VSI is calculated by changing reactive power of the load. The L index, VCPI and

VSI for various buses are shown in Figures 3.12, 3.13 and 3.14 respectively.

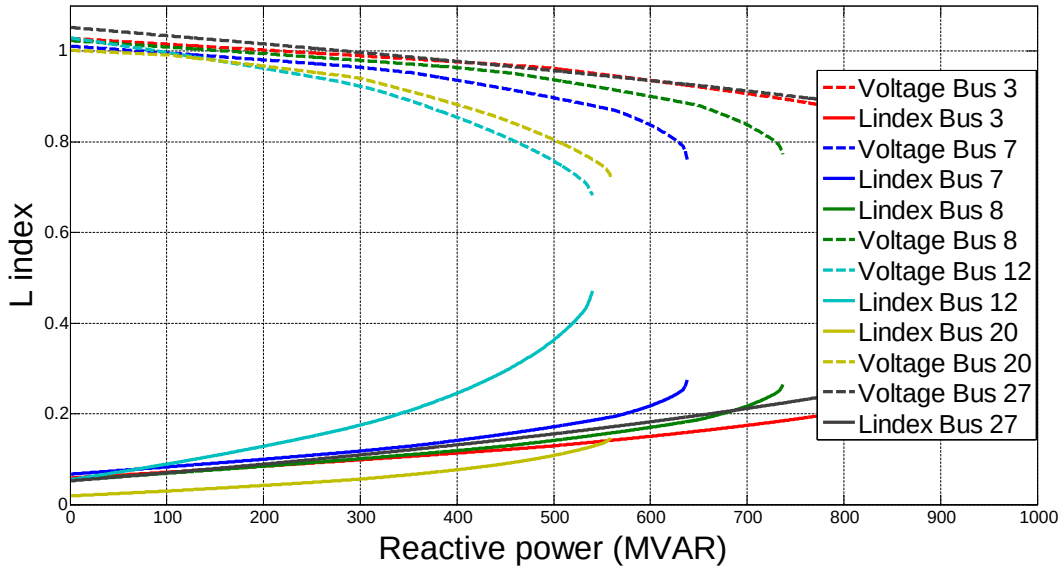

Figure 3.12: L-index for 39 bus system

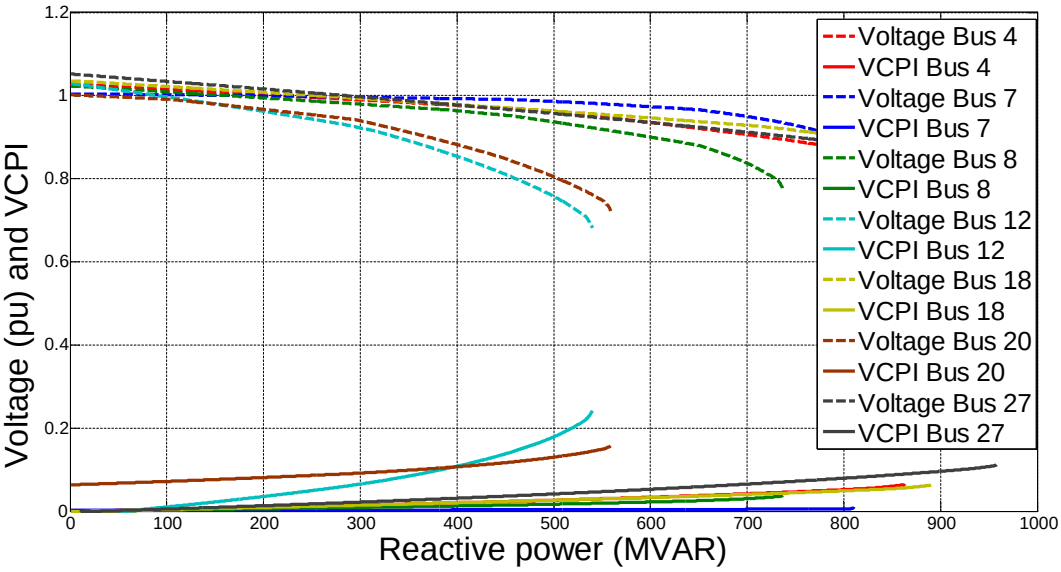

Figure 3.13: VCPI for 39 bus system

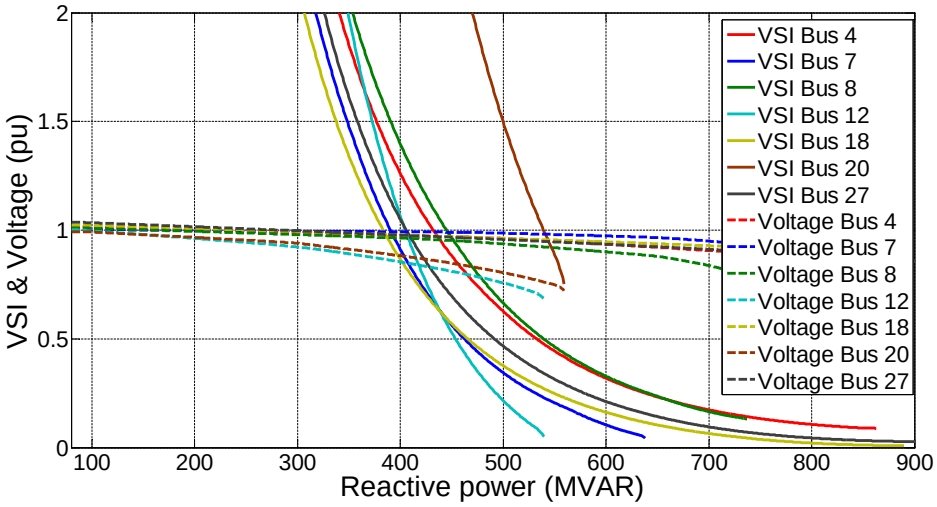

Figure 3.14: VSI for 39 bus system

Fig. 3.15 shows the comparison of L index and VCPI with the proposed VSI for bus 12 with reactive power change at load of bus 12. Here, VSI has value 1 when, reactive power of bus 12 is 405 MVAR. At this point, voltage of the bus is 0.85 pu and L index and VCPI are 0.25 and 0.11 respectively. At 0.8 pu voltage VSI value is 0.45 when reactive power is 461 MVAR. When reactive power is more than 540 MVAR, there is no solution. At the last solution point of 540 MVAR, voltage and VSI are 0.68 and 0.05 respectively. Similarly, L index and VCPI are 0.4712 and 0.23 respectively. The slope of VSI for the section when VSI is 1 to voltage 0.8 pu is 0.00986. The slope of VSI for remaining segment is 0.004988. Hence, when VSI is 1, the bus voltage is below permissible range and the bus enters into voltage instability stage. Further increase in reactive power load causes voltage drop and the VSI decreases as well indicating voltage collapse point.

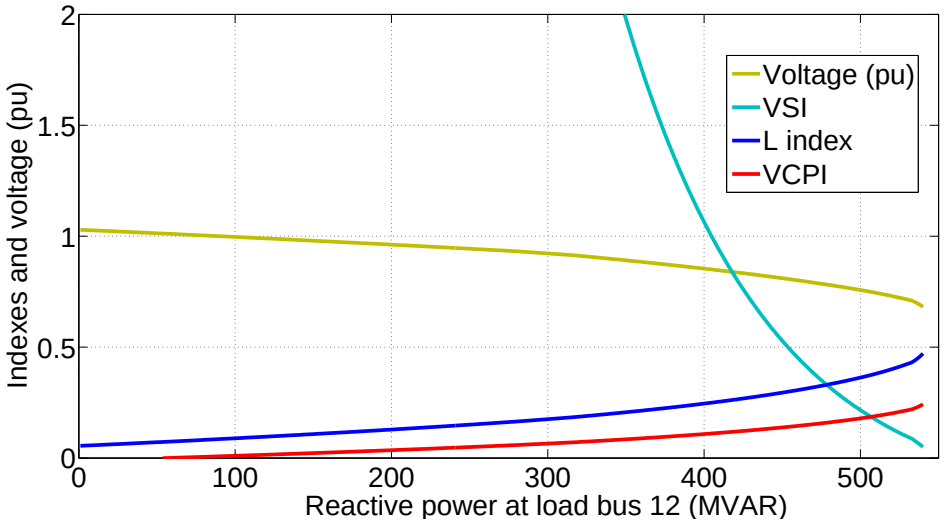

Figure 3.15: Comparison of indexes for bus 12 of 39 bus system

3.5.2.1 IEEE 118 Bus Test System

The IEEE 118 Bus Test Case represents a portion of the American Electric Power System (in the Midwestern US) as of December, 1962 The system contains 19 generators, 35 synchronous condensers, 177 lines, 9 transformers and 91 loads. The schematic diagram of IEEE 118 bus system is shown in Fig. 3.16.

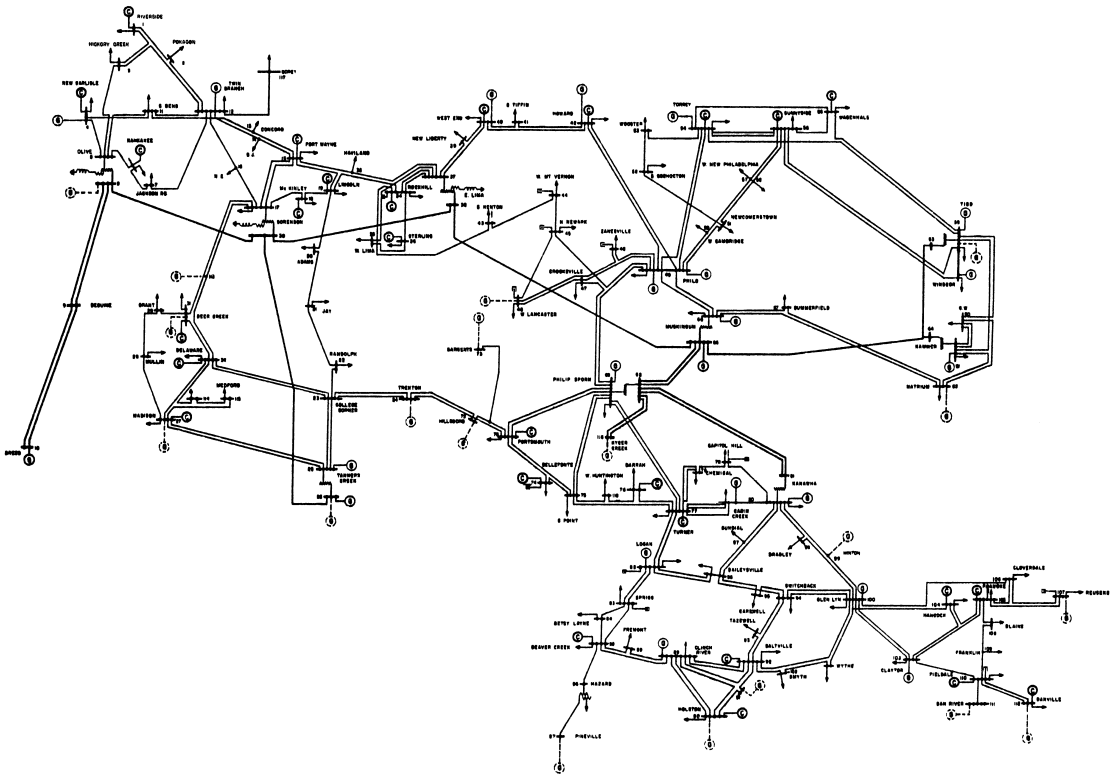

Figure 3.16: IEEE 118 bus system

Fig. 3.17 shows the VSI compared with VCPI. VSI is less than 1 when the reactive power is 212 MVAR predicting proximity to voltage collapse. Further increase in the reactive power, there is sharp decline in the VSI value. VSI is 0.2 when voltage of the bus is 0.85 and reactive power is 400 MVAR. At this load VCPI is 0.1. VSI and VCPI at reactive power of 540 MVAR and voltage of 0.8 pu is 0.08 and 0.17 respectively. The sharp change in value of VSI compare to VCPI shows the higher sensitivity of VSI towards indication of voltage collapse.

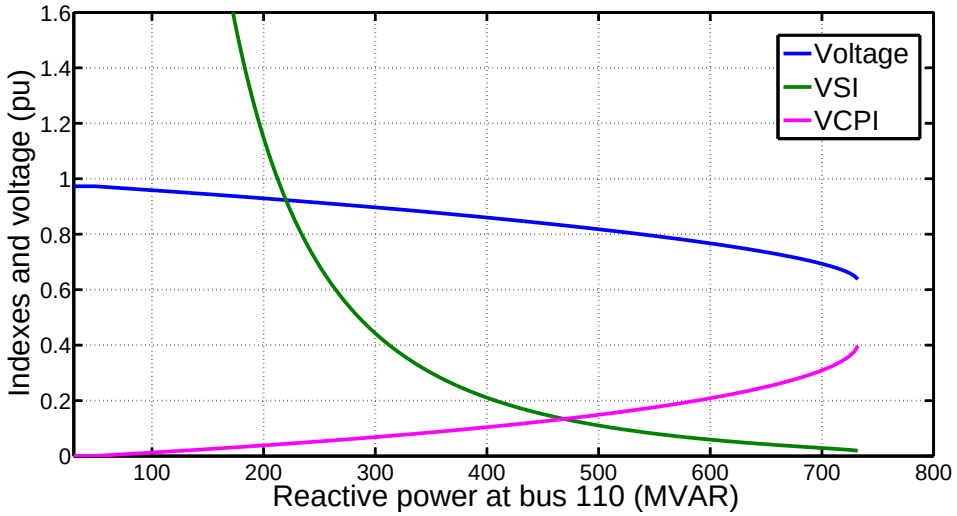

Figure 3.17: VSI and VCPI against reactive power at bus 110

Fig. 3.18 shows the voltages in surrounding buses when reactive power is changed in bus 110 and Fig. 3.19 shows the voltage stability index in those buses. Even though there is sharp voltage decrease in buses like 105 and 109, the corresponding VSI for these buses are well above 1 which indicates that these buses are not in the proximity of voltage collapse. This shows that monitoring voltage alone might not give the sufficient information to predict voltage collapse. In this case, an index which incorporates relevant system parameters besides voltage provides more accurate prediction of voltage collapse.

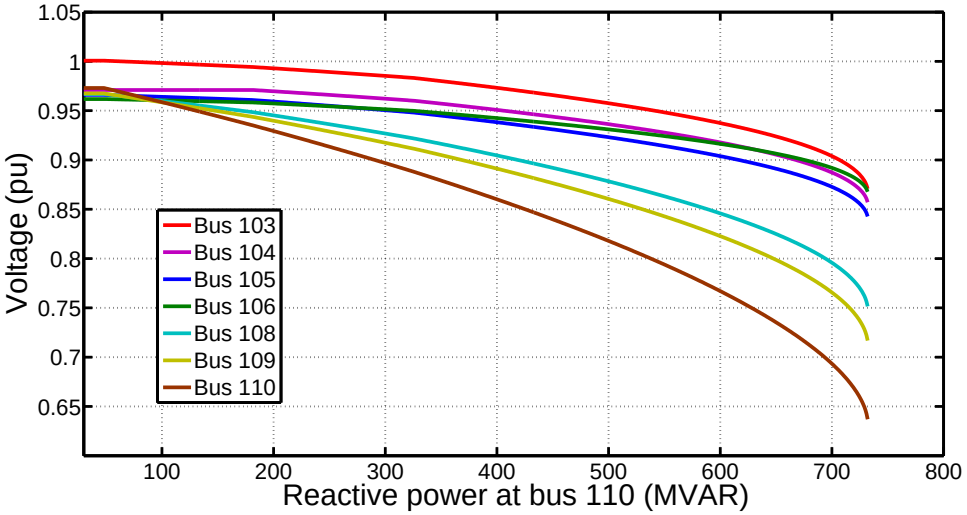

Figure 3.18: Voltage against reactive power change at bus 110

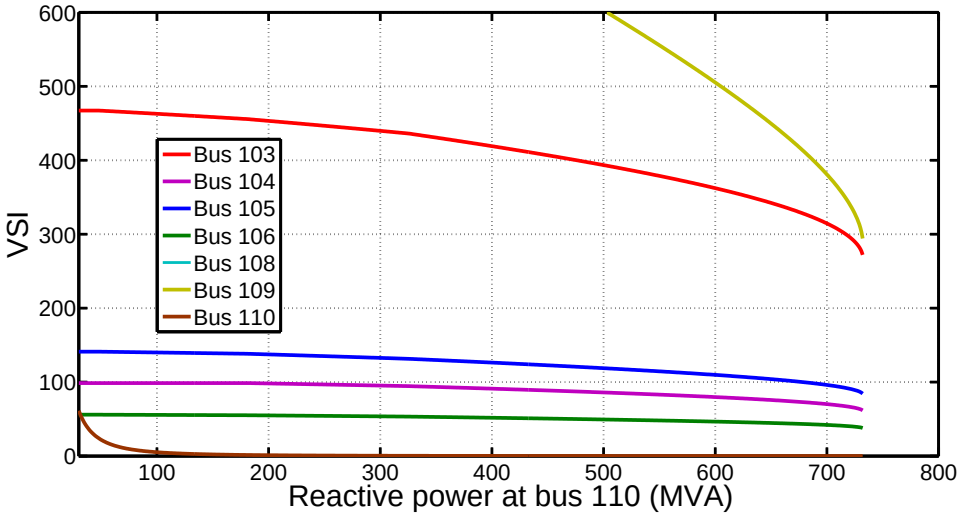

Figure 3.19: VSI against reactive power at bus 110

Fig. 3.20 is the comparison of proposed VSI with VCPI for buses 83 to 88 in IEEE 118 bus system.

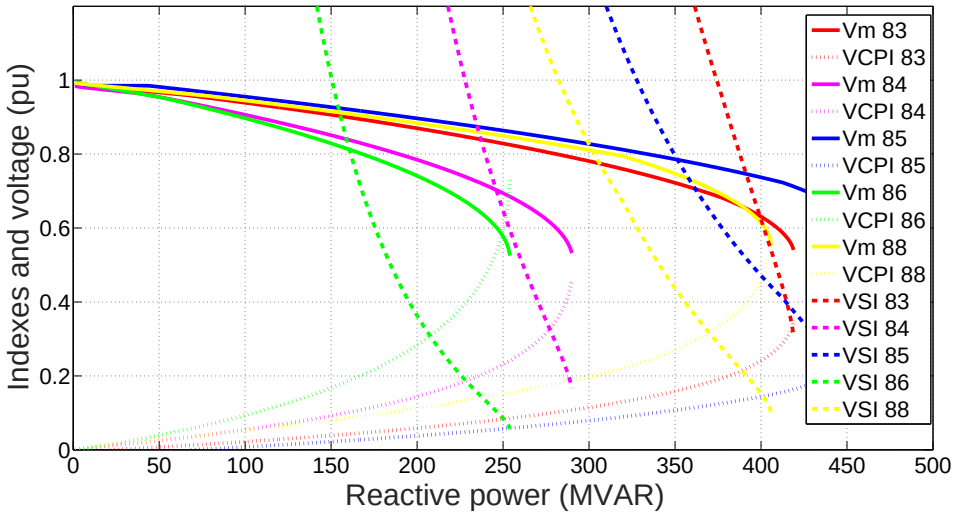

Figure 3.20: Comparison of VSI and VCPI for buses 83 to 88

Bus 86 is most vulnerable bus among the buses shown in Fig. 3.20 in 118 bus system. According to proximity to voltage instability the buses can be ranked as 86, 84, 88, 85 and 83. The VCPI gives the similar ranking except bus 85 is least vulnerable bus instead of bus 83.

3.5.3 Radial Test System

The voltage stability index derived in section 3.4 can be used to find VSI of radial system with slight modification. Radial system has higher R/X values while transmission system higher X/R values.The method presented to find two bus system in section 3.4 cannot be applied to radial system since radial system has sparse jacobian matrix. The method is applied to radial system with slight modification as in [90]. The modified method to find thevenin's equivalent of radial system is as following.

1. Run the load flow of the radial system and find the load voltage V_k and constant load $S_k = P_k + jQ_k$ of the bus k. Then calculate load current I_k as

$$I_k = \frac{P_k - jQ_k}{V_k^*} \tag{3.33}$$

2. run the load flow program without the load at the node k i.e.P_k =0; Q_k =0), obtaining the no-load voltage V_{th} of the Thevenin equivalent circuit

3. Finally, thevenin impedance of the radial system is evaluated as

$$Z_{th} = \frac{V_{th} - V_k}{I_k} \tag{3.34}$$

To apply proposed VSI into a radial system, firstly the radial system is reduced to two bus network as explained above and finally VSI is determined. The proposed method is applied in 32 bus radial test system shown in Fig.3.21. VSI calculated for bus 13 and bus 18 are shown in Fig. 3.22. Bus 13 and bus 18 are nodes of the same radial branch with almost equal load level in the test system and bus 18 is the weakest bus. For reactive power change in corresponding node load, VSI for bus 18 is 1 before VSI for bus 13 indicating bus 18 is prone to voltage instability.

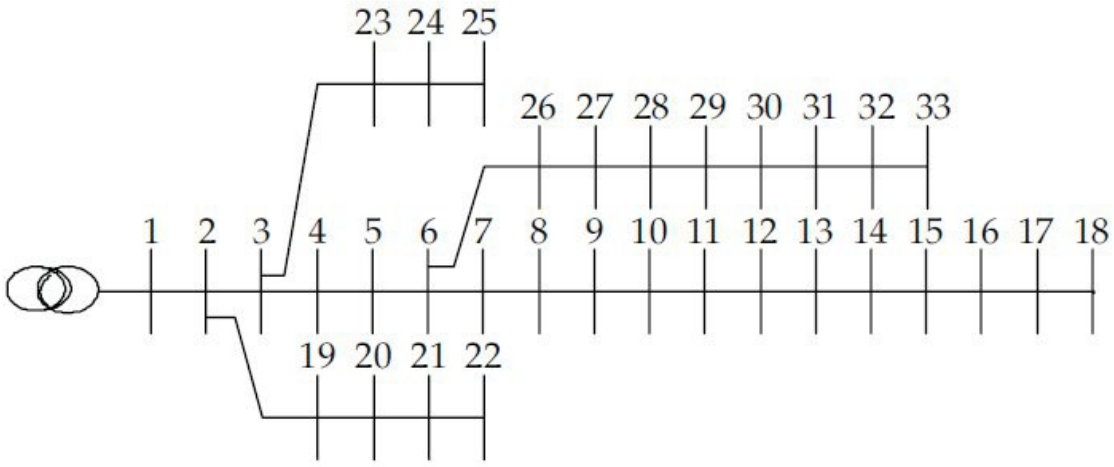

Figure 3.21: 32 bus radial test system

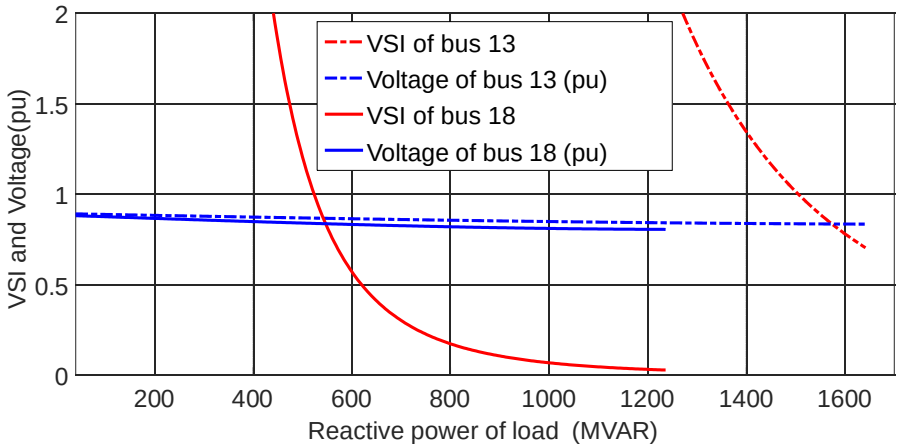

Figure 3.22: VSI and load voltage of 32 bus radial test system

3.6 Conclusion

A voltage stability index based on maximum loading capability is presented in this chapter. The index can be applied in a voltage and reactive power problem or a voltage stability analysis. The index can be calculated using load flow data or measurement data. Unlike previous indexes based on the similar method, this index can be applied in a transmission system. The index is formulated by reducing a transmission system into a 2 node system using a fast method of the Thevenin equivalent calculation. Instability detection using the proposed index has been shown

by implementing the method in IEEE 39 bus and IEEE 118 test system. The proposed method of monitoring of buses is implemented for secondary voltage control of power system and is presented in the next Chapter 6.

CHAPTER 4: VOLTAGE CONTROL AREA

4.1 Introduction

This chapter proposes a technique for partitioning power system into a number of coherent bus groups called voltage control area (VCA) for application in voltage stability assessment and optimal reactive power allocation. The voltage vulnerability and reactive power allocation in the power system depends on the balance of reactive power among generators and loads. Thus, this chapter presents partitioning of buses based on the sensitivity of reactive power of generators to reactive power of loads which is the direct measure between the production and consumption of reactive power in the system. The technique is implemented in IEEE 39 bus and IEEE 68 bus system for identifying VCAs. The results indicate that the application VCAs makes voltage vulnerability problem and reactive power allocation is efficient.

The chapter is organized as follows. Section 4.2 provides the literature review on the identification of VCAs. Section 4.3 describes few existing methods. Section 4.4, presents a iterative method for formation of reactive reserve generators and formation of VCA based on that. Section 4.5, describes the reactive power sensitivity and its formulation for VCA clustering. Case studies with the application of proposed method is shown in section 4.6. Section 4.7 discusses comparison of results with other methods. Conclusions are provided in section 4.8.

4.2 Voltage Control Area

Voltage stability problem is the inability of power system to maintain steady acceptable voltages at all the buses in the system under normal operating condition and after being subjected to a disturbance. The main factor causing instability is the

inability of the power system to meet the demand for reactive power [41]. Federal Energy Regulatory Commission (FERC) includes reactive power and voltage control as an ancillary service and requires voltage control problem to be addressed locally, since reactive power cannot be controlled globally.

It is a well known fact that for most system contingencies, the effect of outages on the system is of a local nature, which means the major effects of a perturbation are limited to a certain neighborhood close to the original perturbation [17]. For voltage security, if the area of a close neighborhood with reactive power deficiencies can be identified, then reactive power and voltage control can be implemented by establishing reactive power reserve. The areas of close neighborhood in power system prone to voltage instability under particular operating condition are referred as voltage control area (VCA). VCA is a group of buses which are connected to the rest of the system by a weak voltage boundary. They are sufficiently decoupled electrically from its neighboring areas and the buses exhibit similar voltage behavior patterns when the power system is subjected to perturbations that could originate voltage instability problems. VCA consists of a set of load and generator buses where voltages respond very similarly to the reactive load and generation changes outside this voltage control area [18]. The group of generators in the VCA is the primary reactive power reserve for that area.

Various literature has presented different methods for identification of VCAs. Reference [18, 19, 91] presented clustering method based on jacobian matrix to identify coherent bus group or VCA. The drawback of this method is the difficulty to determine coherency parameter α. The method of determining VCA based on an electrical distance between buses and clustering of buses using hierarchical clustering is presented in [20, 92] and its effectiveness is shown by applying in secondary voltage control of French grid. The concept of electrical distance along with power flow jacobian is used to determine VCAs under contingencies in [17, 92]. The electrical

distance is calculated from the matrix $[\partial(Q)/\partial(V)]$ which is a part of jacobian matrix and its inverse matrix $[\partial(V)/\partial(Q)]$, called the sensitivity matrix. After determining an electrical distance between all the buses, a hierarchical clustering algorithm is used to group the buses. A number of distances to be evaluated are $(n-1)X(n-1)$ where n is the number of buses. Evaluation of a large number of distances is time consuming further there are overlaps between groups which are decided based on a simple judgment which may decrease the accuracy of the technique. The variation of above is presented in [93] where full Newton-Raphson Load Flow (NRLF) Jacobian sensitives and voltage variations under contingencies is used to form VCAs. In [94], a similar method of identification of VCA is presented in the system with large wind power penetration.

Reference [95] presents a sensitivity-based method to determine VCA where a group has same reactive reserve basin generators if all the buses in the VCA are reactive reserve limited. Sensitivity in this paper is based on line flow Jacobian and power flow Jacobian. This method still requires computation of VQ curve which is a time-consuming process. VCA identification based on modal analysis to calculate participation factor at bifurcation point is presented in [96] for application in the dynamic security assessment. Similarly, a method using eigenvalue and eigenvector is performed in [97]. Here, coherency parameter similar to [19] is used to determine different areas so the accuracy of clustering depends upon the selection of the coherency parameter. Automatic voltage control of power grid is implemented using pilot nodes and control area which are grouped using hierarchical classification and put in operation in Italy [98] and China [99]. Robust clustering of voltage areas using fuzzy-c-means (FCM) algorithm has been implemented in [100]. Even though robustness for various operating conditions has been demonstrated, the method faces problem in initial data selection and FCM algorithm may group buses into multiple clusters without absolute clustering. Spectral clustering has been used to identify

VCAs by using Laplacian eigenvalues and eigenvectors associated with the matrix of the network [101–103].

Identification of voltage control areas is mainly implemented in voltage and reactive power control. The voltage and reactive power variation is a localized problem which is mainly due to a direct imbalance of reactive power or imbalance in the amount of reactive power generated by generators to that one consumed by loads. So, a new method is proposed in this paper to identify areas based on the direct relation between the reactive power of generator to the load. In this approach, first, a sensitivity matrix $\partial Q_g/\partial Q_m$ that gives the sensitiveness of generator to load bus in terms of reactive power is calculated. The elements of the matrix thus obtained is clustered using hierarchical clustering method.

4.3 Existing Methods of Identification of VCA

The literature on various techniques of identification of VCA are presented in section 4.2. Among them, the method based on Jacobian matrix and the method based on electrical distance are widely used and are presented in this section.

4.3.1 Method Based on Jacobian Matrix

Identification of VCA or coherent bus group based on Jacobian matrix J_{qv} are provided in [18] and [19]. Here, buses in coherent bus groups have similar VQ curve minima and have a set of exhausted generators at this VQ minima. The steps for identification of VCAs based on Jacobian matrix as in [19] is as follows.

1. Search for the largest diagonal element (d) of the reactive power voltage Jacobian J_{qv} that includes both load and generator buses
   d=max(J_{qv})

2. Normalize J_{qv} by dividing every element by d

3. For each row i of the normalized jacobian J_{qv}, the absolute values of the off diagonal Jacobian elements are ranked from the smallest to largest. The Jacobian

elements with the smallest absolute values are eliminated from each row i until the sum of the normalized Jacobian elements removed is close to but less than α, the coherency parameter chosenα.

4. The group of buses, that are still interconnected after the weakest branches connected to each bus are eliminated, are the buses in a voltage control area.

The method to obtain correct value for α has been demonstrated in [18], and this is important as it determines VCA. Reference [19] has pointed out difficulty in determining correct value of α and [95] argues that this method involves a fairly high degree of trial and error.

4.3.2 Method Based on Electrical Distance

The method of determination of zones in power system based on the structure of the network was presented in [20]. The concept of electrical distance was developed to identify coherent bus group in the system. The method involves two steps, first is the calculation of a electrical distance between the buses in the system and secondly, grouping of the buses. The method has been effective in determining the voltage control area in French power system. The method of finding electrical distance presented in [20] has been applied in [17, 92, 94, 104]. Here, the concept of electrical distance involves the matrix $[\partial(Q)/\partial(V)]$ which is part of jacobian matrix and its inverse matrix $[\partial(V)/\partial(Q)]$, called the sensitivity matrix. Both matrices are real and non-symmetrical. The magnitude of the coupling in terms of voltage, between two buses, can be quantified by the maximum attenuation of voltage variation between two buses. The attenuation can be obtained dividing the element of each column of $[\partial(V)/\partial(Q)]$ by the diagonal term.

$$\alpha_{ij} = (\partial(V_i)/\partial(Q_j))/(\partial(V_j)/\partial(Q_j)) \tag{4.1}$$

Generally,$\alpha_{ij} \neq \alpha_{ji}$. In order to have symmetry, the electrical distance between

two buses i and j is defined as below [20].

$$D_{ij} = D_{ji} = -Log(\alpha_{ij}.\alpha_{ji}) \tag{4.2}$$

The electrical distance D_{ij} between bus i and bus j has the properties of positivity and symmetry. The step-by-step method to obtain the separate coherent bus groups is given as follows. [92]

1. Calculate the Jacobian matrix J and hence obtain the submatrix J_4, where $J_4 = [\partial(Q)/\partial(V)]$
2. Invert J_4 to get sensitivity matrix $B = \partial(V)/\partial(Q)$ and the elements of matrix B are written as b_{ij}, where $b_{ij} = \partial(V_i)/\partial(Q_j)$
3. Obtain attenuation matrix,α_{ij}, between all the nodes as $\alpha_{ij} = -Log(\alpha_{ij}.\alpha_{ji})$
4. Calculate electrical distances $D_{ij} = -Log(\alpha_{ij}.\alpha_{ji})$
5. Normalize the electrical distances as follows: $D_{ij} = D_{ij}/Max(D_{ij}, ...D_{ij})$

After calculating electrical distance, a hierarchical classification algorithm is used to determine the areas. In this process, number of distances to be evaluated is $(n-1) \times (n-1)$ where n is the number of buses.

4.4 Proposed Iterative Method of Identification of VCA

The proposed method for determining coherent bus group by iterative method is based on the idea of sensitiveness of generator reactive power to the bus voltage. The generators which contribute to the bus have higher rate of change of reactive power with respect to the voltage of that bus i.e. $\Delta(Q_i)/\Delta(V_j)$, where, Q_i is the reactive power of generator including slack generator while V_j is the voltage of load bus j. The steps for determining coherent bus group by above iterative method is as follows:

1. For each load bus j, power flow is performed at different load points and the voltage of the bus and reactive power of generators are recorded.

2. Reactive power of each generator is plotted across the voltage of the test load bus

3. Slope for each generator is calculated in the region where it is not reactive power maximum or minimum

4. The generator with higher slope or rate of change of reactive power is considered as reserve generators for the load bus

5. The load buses with similar reserve generators are a group of load buses which belong to same coherent bus group.

The algorithm for identifying VCA is shown in Fig. 4.1. The method was implemented for various IEEE test system but computation burden and the time consuming iterative process doesn't justify for practical application.

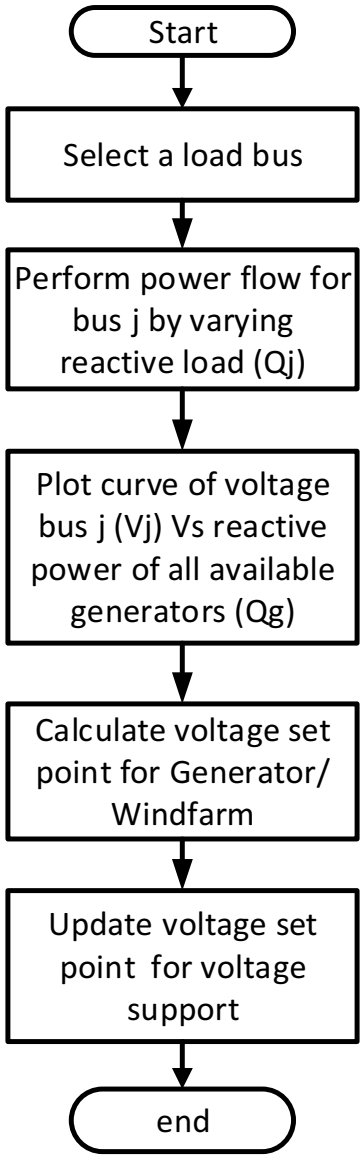

Figure 4.1: Flowchart of iterative method.

Some of the issues observed from the iterative method of identification of VCAs are as follows

1. A large number of power flow should be performed for wide range of load variation. Also, QV curve should be plotted for each bus. This increases the computation time.

2. Buses in same coherent bus group will have common reserve generators so con-

dition of reactive reserve limited introduced by [95] for buses of a coherent bus group with different coherent bus group generators does not apply here.

3. Need wisely decision to group buses based on the slope obtained and may lead to inaccuracies.

4.5 Proposed Method Based on Reactive Power Sensitivities

Reactive power and voltage control is a localized problem where voltage of a load bus is dependent on the available reactive power. Thus, voltage security is driven by the balance of reactive power in a system. To maintain voltage of a load bus there should be an adequate amount of reactive power supplied/received to/from load bus, which should be balanced by reactive power from a generator or other reactive power source. The level of reactive power in load bus balanced by generators or other sources governs the voltage level of the bus. We are establishing a relation between load and generator reactive power so other sources of reactive power can be omitted. Hence, we can identify set of generators which will be reactive power reserve to maintain a voltage level of a bus based on $Q - V$ relationship between generator and load bus. A generator or set of generators may cater reactive power to a group of load buses. These group of load buses should exhibit similar behavior in response to voltage disturbance as they have similar reactive power reserve. The group of buses related through Q-V curve to same set of generators can be identified as the buses in the same VCA. There might be some buses which will have reactive power reserve from different sets of generators. In such conditions, those buses can be grouped to the VCA with the generator having high Q-V sensitivity. We are interested in determining VCA based on the sensitivity of generator reactive power with respect to load voltage i.e. $\partial Q_g / \partial V_m$.

The relationship between reactive power and voltage of a load bus for constant active power can be shown by $Q - V$ curve as in Fig. 4.2. It can be seen that the

voltage stability limit is reached when the derivative is zero ie the minimum point. Thus the parts of $Q-V$ curves to the right of the minimum represent stable operation and the section to the left represents unstable operation [41]. Considering only the stable region, load voltage V_m is proportional to the reactive power Q_m. So, sensitivity of generator reactive power with respect to load reactive power $\partial Q_g/\partial Q_m$ can be considered instead of sensitivity of generator reactive power with respect to load voltage $\partial Q_g/\partial V_m$. With this we will formulate the problem that finds the sensitivity of the reactive power of generators to the load.

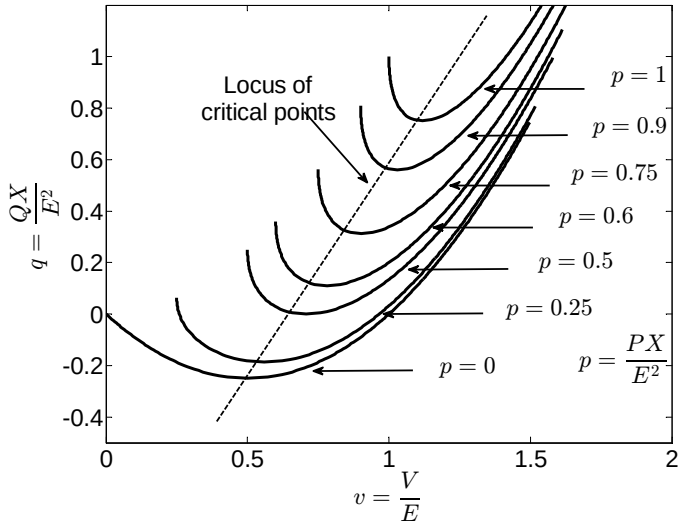

Figure 4.2: Relationship between voltage and the reactive power

The effect of static compensation on voltage stability has been studied in [105] . Minimum singular values of Jacobian matrix and total generated reactive power were calculated as indicators of stability margin and sensitivity methods were used for reactive support allocation. Here, the sensitivity of generated reactive power is analyzed with respect to active and reactive load requirements at various locations in the system. In the proposed approach, sensitivity factors of generated reactive power with respect to reactive load requirements developed and arranged using the Jacobian matrix.

4.5.1 Problem Formulation

Let the state vector of the power system be represented as

$$x = (\delta, V)^{\mathrm{t}} \tag{4.3}$$

Then from the Jacobian matrix of the power grid dynamic state space representation, jacobian vector can be calculated as

$$J_g = \left[\frac{\partial Q_g}{\partial x_j}\right] \tag{4.4}$$

where, g represents generator and j represents j^{th} bus In terms of the state vector then,

$$J_g = \begin{bmatrix} \dfrac{\partial Q_g}{\partial \delta_j} & \dfrac{\partial Q_g}{\partial V_j} \end{bmatrix} \tag{4.5}$$

We have load flow jacobian as

$$J = \left[\frac{\partial y_i}{\partial x_j}\right] \tag{4.6}$$

where $y_i = (P, Q)^t$

Considering, active and reactive power of load bus be P and Q, and active and reactive power of generator be P_g and Q_g. $y_i = (P_1..P_m, P_{g,1}...P_{g,n-1}, Q_1...Q_m)^t$

where, m is number of load bus and n is generator bus

Then,

$$J = \begin{bmatrix} \dfrac{\partial P_i}{\partial \delta_j} & \dfrac{\partial P_i}{\partial V_j} \\ \\ \dfrac{\partial Q_i}{\partial \delta_j} & \dfrac{\partial Q_i}{\partial V_j} \end{bmatrix} \tag{4.7}$$

and in full form

$$J = \begin{bmatrix} \frac{\partial P_1}{\partial \delta_j} & \frac{\partial P_1}{\partial V_j} \\ | & | \\ \frac{\partial P_m}{\partial \delta_j} & \frac{\partial P_m}{\partial V_j} \\ \\ \frac{\partial P_{g,1}}{\partial \delta_j} & \frac{\partial P_{g,1}}{\partial V_j} \\ | & | \\ \frac{\partial P_{g,n-1}}{\partial \delta_j} & \frac{\partial P_{g,n-1}}{\partial V_j} \\ \\ \frac{\partial Q_1}{\partial \delta_j} & \frac{\partial Q_1}{\partial V_j} \\ | & | \\ \frac{\partial Q_m}{\partial \delta_j} & \frac{\partial Q_m}{\partial V_j} \end{bmatrix} \tag{4.8}$$

The sensitivities of Q_g with respect to changes in load power y may be expressed as

$$S = \left[\frac{\partial Q_g}{\partial y_j}\right] = \left[\frac{\partial Q_g}{\partial x_j}\right]\left[\frac{\partial x_j}{\partial y_j}\right] = J_g J^{-1} \tag{4.9}$$

The element of vector S is obtained from (4.5) and (4.8)

$$S = \left[\frac{\partial Q_g}{\partial P_1} \cdots \frac{\partial Q_g}{\partial P_m}, \frac{\partial Q_g}{\partial P_{g1}} \cdots \frac{\partial Q_g}{\partial P_{g,n-1}}, \frac{\partial Q_g}{\partial Q_1} \cdots \frac{\partial Q_g}{\partial Q_m}\right] \tag{4.10}$$

and it can be partitioned into parts that correspond to active load requirements, active generation and reactive load requirements.

$$S = \Big[S_{pg} | S_{gg} | S_{qg}\Big] \tag{4.11}$$

For identification of VCA, we are interested only in elements of S_{qg} which represents the sensitivities of generator reactive power Q_g with respect to reactive power

requirement for load Q_m. The sensitivity S_{qg} can be easily calculated from modified load flow jacobian.

Once the sensitivities of all generators to load are determined, it can be used to identify the buses which belongs to same VCA. A hierarchical classification algorithm is used to determine the areas according to the sensitivities calculated. For each generator bus i, its sensitivity to all load buses j, S_{ij}, are classified into some ranges, Range1, Range2, Range3...which are in descending order. The relationship between them can be expressed as follows:

$$1 \geq Range1 \geq S_1$$

$$S_1 \geq Range2 \geq S_2$$

$$S_2 \geq Range3 \geq S_3$$

$$| \quad |$$

$$| \quad |$$

$$S_{n-1} \geq RangeN \geq S_n$$

where,

$$S_1 > S_2 > S_3 ... S_{n-1} > S_n$$

The classification is started from Range1. For each bus j, whose sensitivity to generator i is higher than S_1 it will belong to the same group as generator i. This grouping step is repeated with all the generator buses for Range1. If the buses doesn't belong to Range1 of any generator, the grouping steps is repeated for Range2, Range3,...RangeN until all the buses are at least in one of the groups. The buses may belong to different generator group in the same range or different range. Priority will be given to those generators where the bus lie in the higher range. Generators having common buses in higher ranges are grouped together in one VCA. Finally, all the buses will be grouped in different VCAs with at least one generator. There may be a few overlaps between groups, in other words, there may be a few buses belong to more than one groups. For this case, according to sensitivity to other buses, a

simple judgment can be done to classify it to one of the groups. The generators in the VCA will be the primary reactive power reserve for buses in that VCA group. Classification of buses into different VCAs using the proposed method is presented in section 4.4. The flowchart for identification of VCA group is shown in Fig. 4.3.

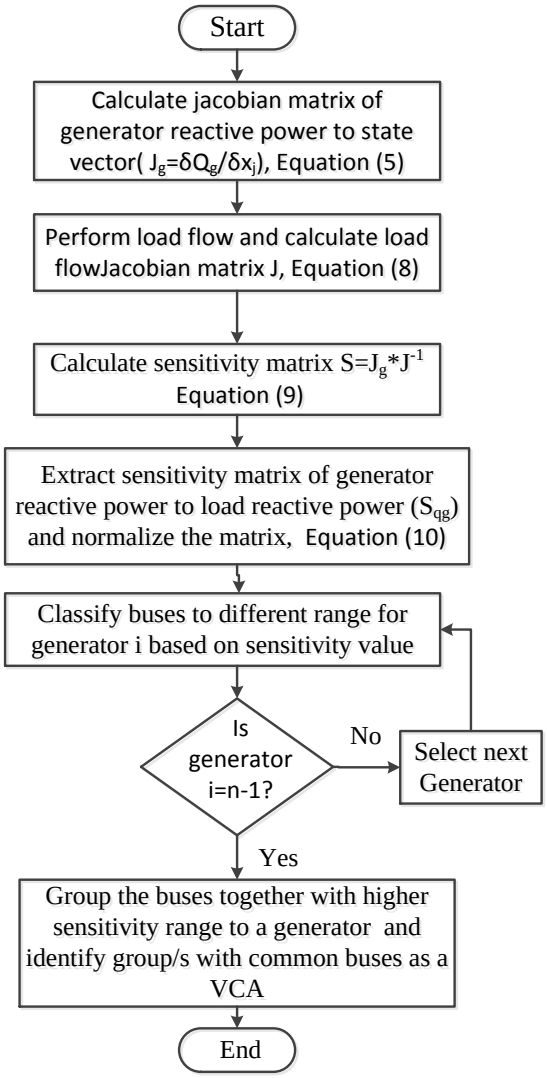

Figure 4.3: Flowchart for identification of VCAs using sensitivity method

4.6 Case Studies

The proposed sensitivity based technique for identifying voltage control areas have been performed in IEEE 39 bus system and IEEE 68 bus system. The studies are performed on Matlab. The results are compared with electrical distance method.

Similarly, voltage and reactive power responses with and without considering VCA are presented to state importance of VCA identification using reactive power sensitivities.

4.6.1 Test Case: New England 39 Bus System

New England 39 bus system is the 10 machine New England 39 bus system with parameters taken from [89]. The system comprises of 10 machines or generator buses and remaining 29 load buses. The 39 bus 10 machine system is shown in Fig. 4.4. The clustering of 39 buses into VCAs is performed in 2 steps, first reactive power sensitive matrix is calculated which is used as data for clustering in the second step. The reactive power sensitivity matrix S_q is the matrix of size $9X29$, as slack bus or swing generator which is bus 31 in the system is not considered for the sensitivity. Then hierarchical classification is used to group buses into various VCAs. The reactive power sensitivity matrix is shown in Appendix B. Classification of generators and load buses into various groups is shown in Table 4.1.

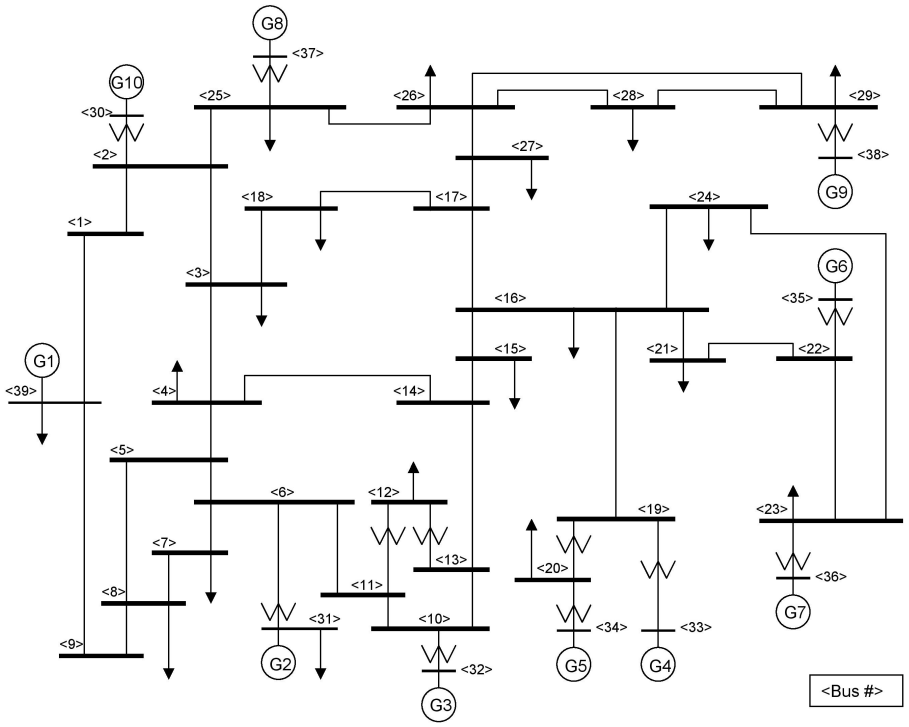

Figure 4.4: 39 Bus 10 machine system.

Table 4.1: VCA classification based on sensitivity method

VCA No	**Generators**	**Buses**
I	30,37	2,3,18,25
II	31,32,39	1,4,5,6,7,8,9,10,11,12,13,14
III	33,34	19,20
IV	35,36	15,16,17,21,22,23,24
V	38	26,27,28,29

Sensitivity of generators to load buses are shown in Fig. 4.5. The figure shows that generators have higher sensitivity to the buses which are in the same group. Load bus numbers 19 and 20 have very high sensitivity for generators 33 and 34 compare to other generators. Similarly, buses 26-29 have high sensitivity for generator 39. Hence, generators have high sensitivity to buses in the same VCA. The statement holds true in most of cases but some buses may have higher sensitivity to generators of other VCA than one of the generators from its VCA. Bus 18 belongs to VCA group number I with generators 30 and 37 but in Fig. 4.5, sensitivity of generator 33 is higher than generator 37. But, still the sensitivity of other generator in the VCA that is generator 30 has the highest sensitivity. There may be cases where bus overlaps into to two separate VCA groups with almost equal sensitivity to two generators. In these cases, based on the sensitivity of generators to bus, a simple judgment can be done to classify the bus into one of the group according to the topography of system and its need. All five VCA groups of New England 39 bus test system in shown in Fig. 4.6.

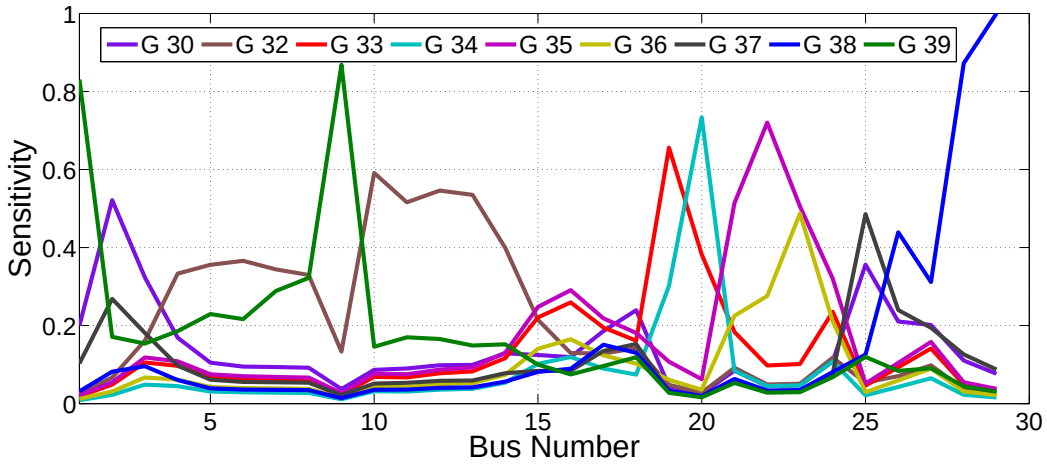

Figure 4.5: Sensitivity of generators to buses in 39 bus system

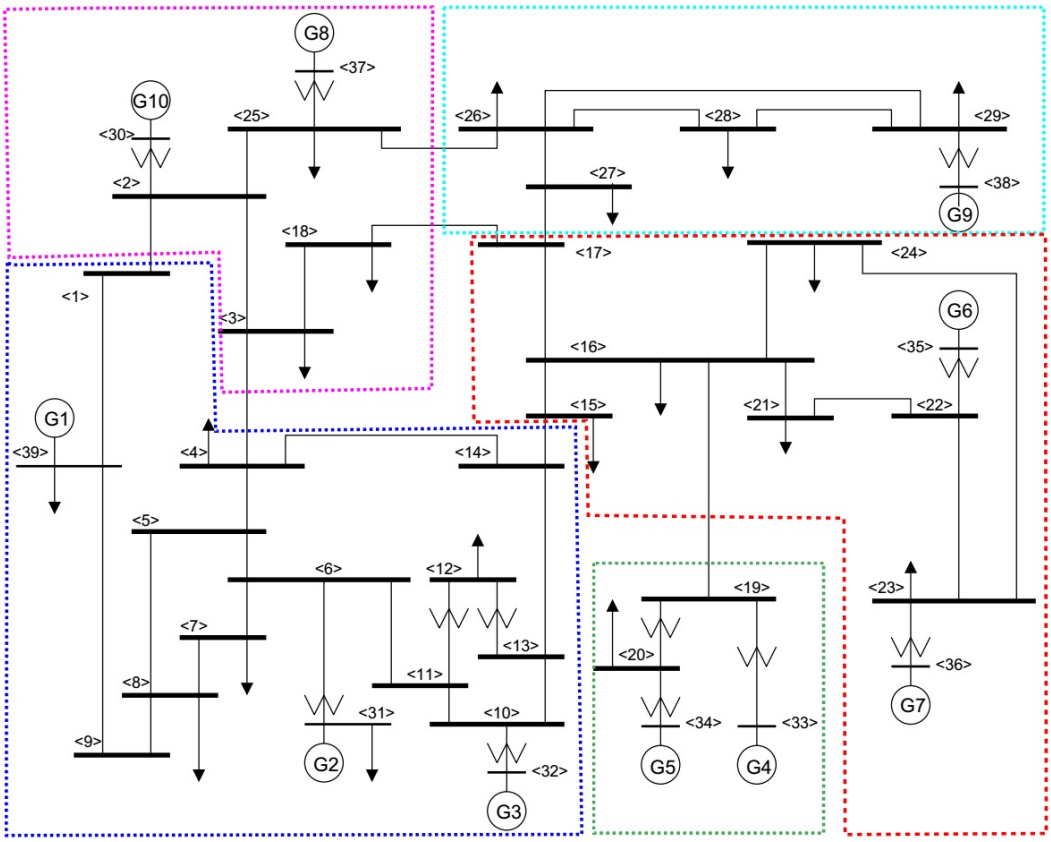

Figure 4.6: Graphical representation of VCAs of 39 bus system.

Fig. 4.7 shows the proportionality between load voltage and load reactive power with respect to generator reactive power. First plot in Fig. 4.7 is the stable region of

$Q-V$ curve for load bus 21 in New England 39 bus 10 machine test system Remaining figures are the plots of reactive power of generator G9 at bus 38 with respect to voltage and reactive power of load bus 21. The plots of voltage and reactive power of load bus with generator reactive power has similar trend showing that the voltage and reactive power of load bus are proportional and can be used interchangeably to get same sensitivity effect.

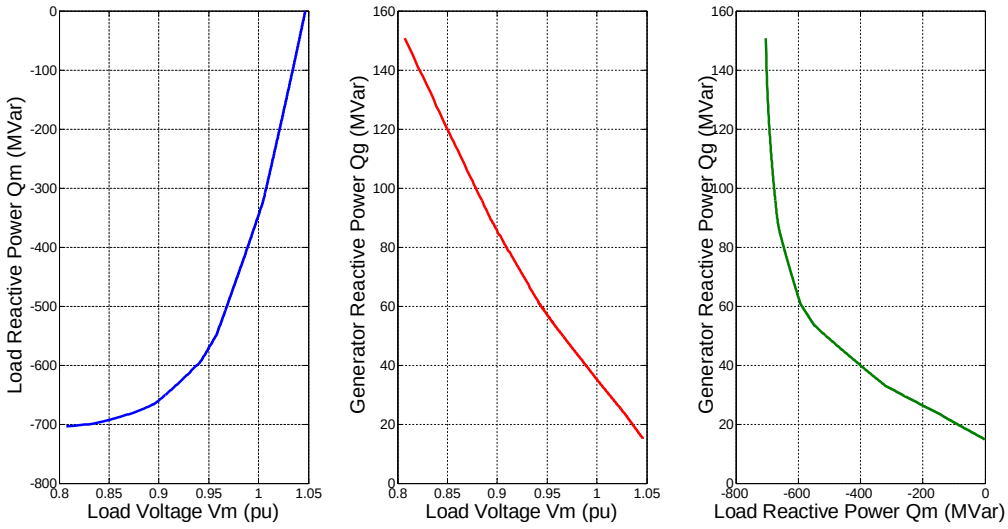

Figure 4.7: Plots of Q_g, Q_m and V_m.

Fig. 4.8 is the plots of generator reactive power Q_g of bus 38, load reactive power Q_m and bus voltage of bus 29 similar to Fig. 4.7. Maximum reactive power limit of generator 39 is 300 MVar from the loadflow data. In Fig. 4.8, generator supplies reactive power to its maximum limit and keeps the voltage of load bus 29 to acceptable limit. Once the generator saturates, the bus voltage starts depleting from 1.0 pu. In Q_g Vs Q_m plot, generator is supplying all reactive power for reactive power requirement of load. While in Fig. 4.7, generator is not supplying reactive power to its limit even though load voltage is depleting due to increase in reactive power requirement. From Fig. 4.6, we can see that load bus 29 is in the same VCA as generator 38 while load bus 21 is in different VCA group. Hence, we can conclude that generator in the VCA is the primary reactive power reserve of load. A proper reactive power control

within the VCA can prevent voltage instability and the subsequent voltage collapse.

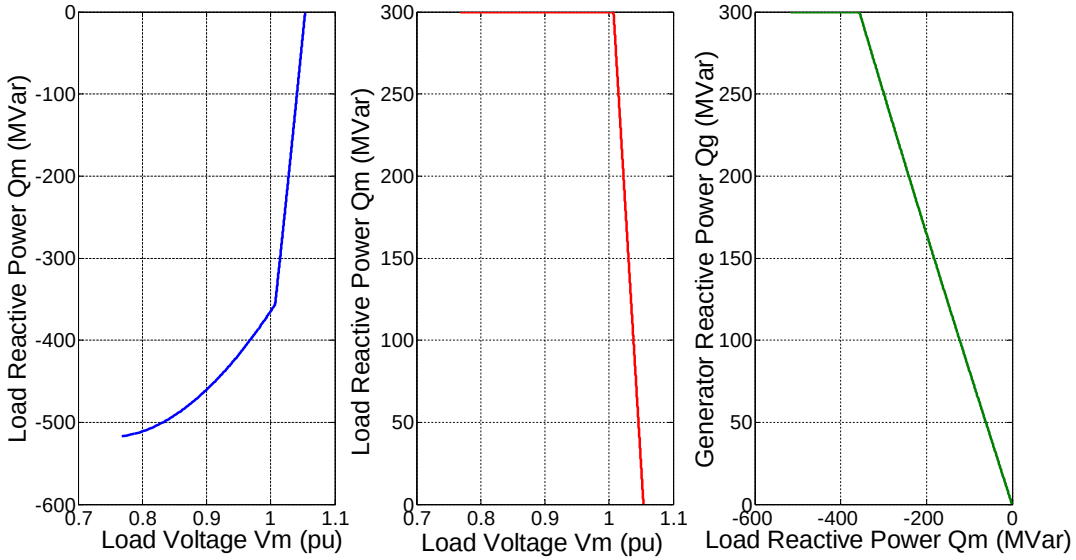

Figure 4.8: Plots of Q_g, Q_m and V_m for bus 29

To verify the local voltage and reactive power problem in the VCA, we change a load in a bus which eventually affects the reactive power in its vicinity inside the VCA. In the 39 bus system load of 250 KVA with power factor 0.90 is added to the bus number 8. Bus number 8 belongs to VCA II. The voltage profiles of the base case and system with added load in bus 8 is illustrated in Fig. 4.9.

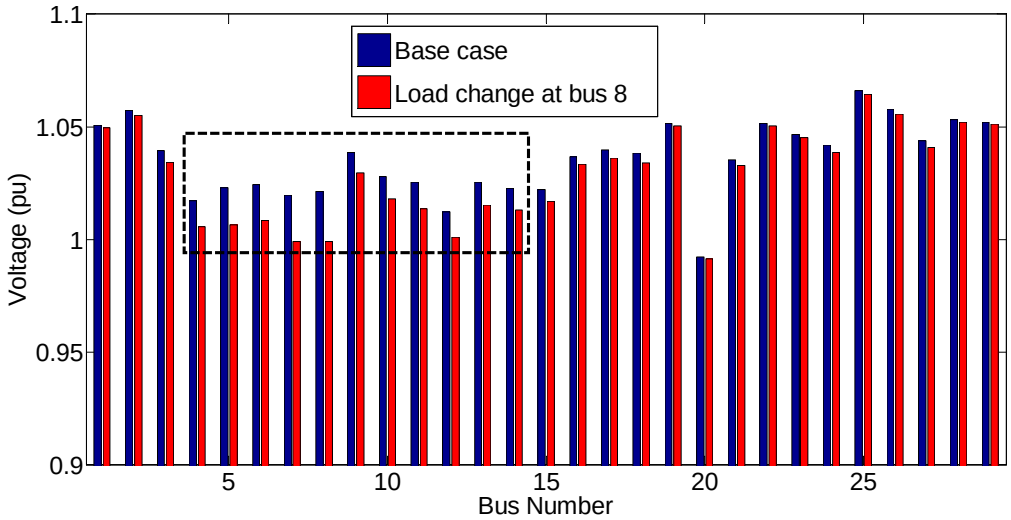

Figure 4.9: Voltage profile for IEEE 39 bus system

The figure illustrates that for load change in bus 8, buses in the VCA II has higher voltage drop compared to the buses in other VCA groups. In the VCA II, bus 8 has largest voltage drop of 0.023 pu while bus 9 has lowest voltage drop of 0.009 pu excluding bus 1 with the drop of 0.001 pu. The largest voltage drop outside of the VCA is 0.005 pu in bus number 3 which belongs to VCA I. Hence, the buses in a VCA group have higher voltage sensitivity.

The generators in a VCA are reactive reserve for the VCA. The generators in the VCA acts primarily to inject/absorb reactive power to bring the voltage profile back to tthe acceptable level. To show that the generators in the VCA are the primary reactive reserve, reactive/voltage control in response to the voltage drop due to load change in PQ bus is activated in individual generator only.

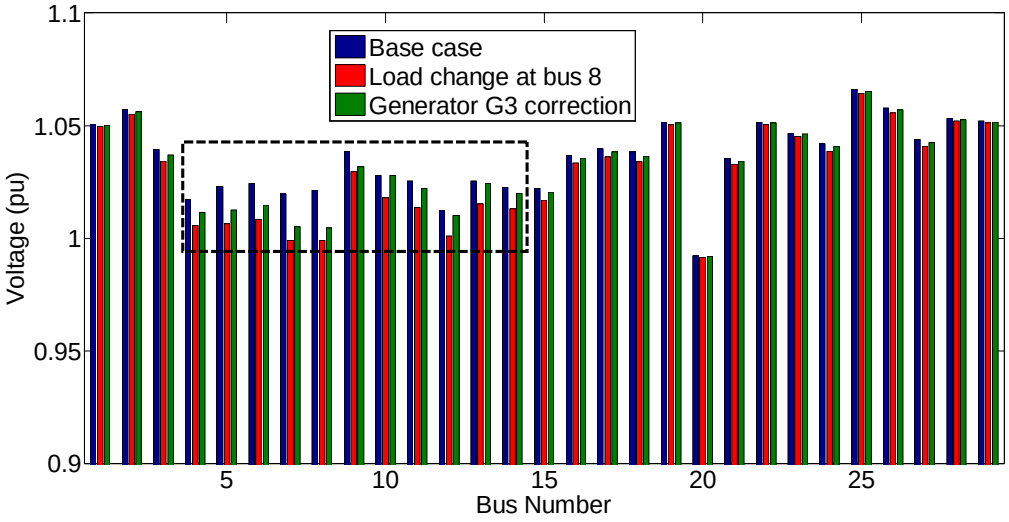

Figure 4.10: Voltage profile after reactive control by generator G3

Generators G1 and G3 belongs to VCA II. The reactive control of generator G3 at bus number 32 is activated in response to voltage drop due to disturbance in bus 8. The voltage profile after the correction control from G3 is shown in Fig. 4.10. The voltage profile after the correction reactive control shows that voltage level in buses in VCA II is improved but is still below the one compared to the base case. Fig. 4.11 shows the voltage profile after the reactive control from generator G1. The voltage

correction in the buses of VCA II is better compared to the correction from generator G3. This is due to higher reactive sensitivity of G1 to bus 8 compared to sensitivity of G3 to bus 8 as shown in Fig. 4.5. The sensitivity values of different generators to the bus is illustrated in Table 5.1.

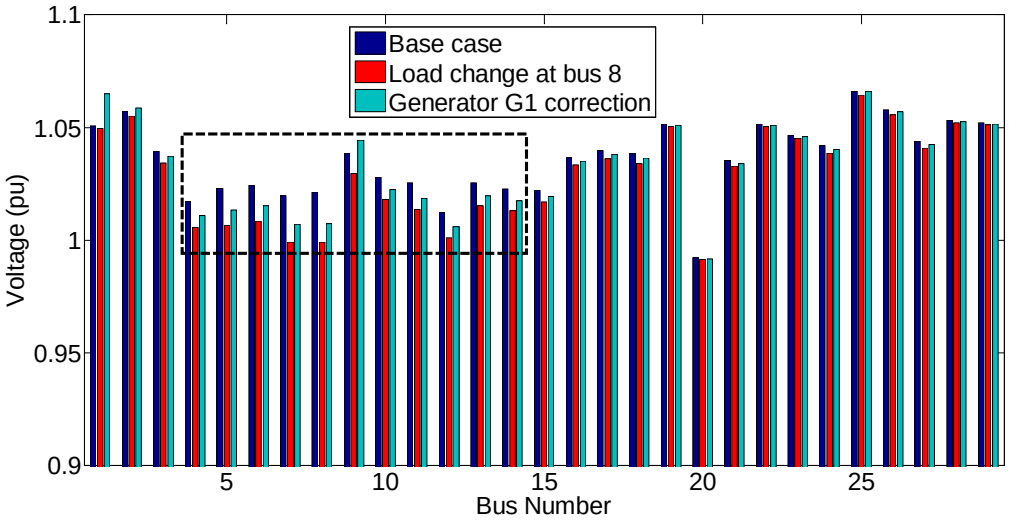

Figure 4.11: Voltage profile after reactive control by generator G1

Table 4.2: Reactive sensitivity of generators to bus 9

Generator ID	**Sensitivity value**
G10	0.037
G2	0.133
G3	0.024
G4	0.011
G5	0.027
G6	0.015
G7	0.021
G8	0.013
G9	0.869

Now, reactive/voltage control in generator G4 belonging to VCA III is activated

to correct the voltage drop in bus 8 and neighboring buses due to load change in the bus 8. Voltage profile after the reactive control from G4 is shown in Fig. 4.12. The reactive power control from G4 is not able to correct the voltage level in the buses of VCA II but overcorrects reactive power of buses 19 and 20 which belongs to VCA III.

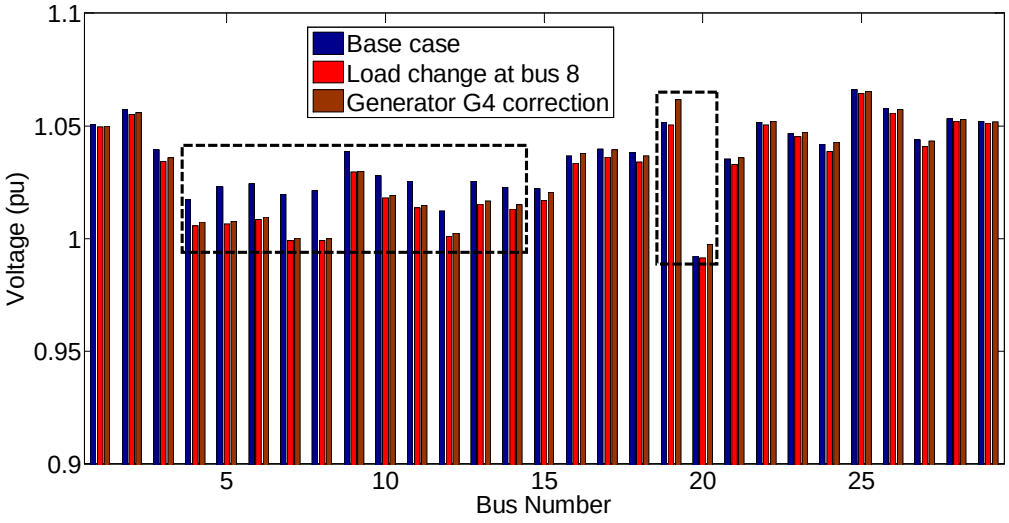

Figure 4.12: Voltage profile after reactive control by generator G4

The simulation results above shows that the buses in VCA grouped based on the reactive power sensitivity have similar voltage nature and generator in the VCA acts as the primary reactive reserve responsible to inject/absorb reactive power to correct voltage level.

4.6.2 Test Case: IEEE 68 Bus System

VCA identification by sensitivity method has been applied to identify VCA groups in 68-Bus, 16-Machine system which is the reduced order equivalent of the interconnected New England test system (NETS) and New York Power System (NYPS) [106]. The clustering of 68 buses into VCAs is performed in 2 steps, first reactive power sensitive matrix is calculated which is used as data for clustering in the second step. The reactive power sensitivity matrix S_q is the matrix of size $15X29$, as slack bus or swing generator which is bus 16 in the system is not considered for the sensitivity.

Then hierarchical classification is used to group buses into various VCAs. The reactive power sensitivity matrix is shown in Appendix B. Classification of generators and load buses into various groups is shown in Table 4.3. Fig 4.13 is the schematic diagram of 68-Bus, 16-Machine system with VCA groups identified using the sensitivity method.

Table 4.3: VCA classification based on sensitivity method for 68 bus system

VCA No	**Generator No**	**Bus No**
I	14	41
II	15	42
III	16	18
IV	1,6,7,8	21,22,23,24,25,27,37,52,54,55,68
V	2,3	56,57,58,59,60,62,63,64,65,66,67
VI	4,5	19,20
VII	9	26,28,29
VIII	10,11	30,31,32,33,38,40,46,47,48,49,53
IX	12,13	17,34,35,36,39,43,44,45,50,51,61

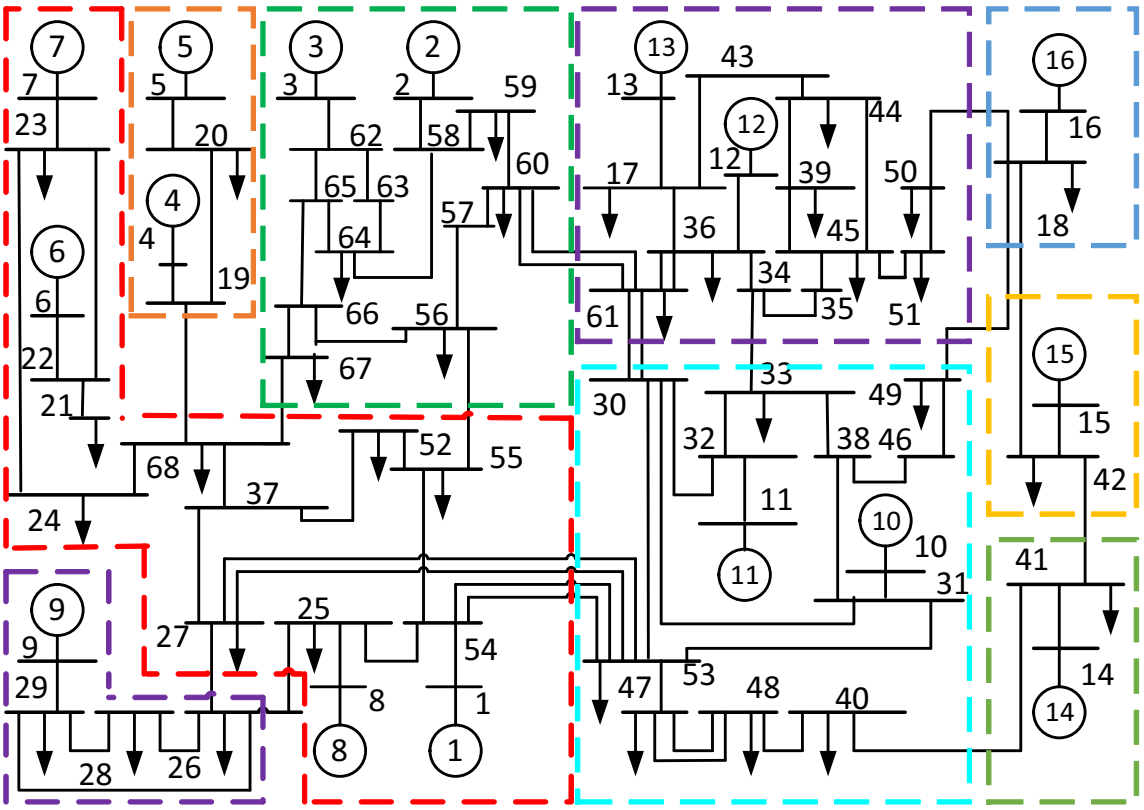

Figure 4.13: Graphical representaion of VCAs of 68 bus system.

4.7 Comparison With Other Techniques

The comparison between the clustering of power systems into VCAs by reactive power sensitivity technique and clustering based on electrical distance is shown here. The algorithm of identificatio of votlage control area based on electrical distance in presented in Section 4.3.2. The comparison of VCA classification based on sensitivity method and electrical distance is shown in Table 4.4 The VCA groups obtained from the proposed method is compared to the electrical distance method. The VCA groups from electrical distance method is shown in Table 4.4. Comparing Tables 4.1 and 4.4, it can be seen that the both method yields same number of VCA groups with same buses in each group.

Table 4.4: VCA classification based on distance method

Group No	**Generator ID**	**Bus No**
I	G8,G10	2,3,18,25
II	G3,G1	1,4,5,6,7,8,9,10,11,12,13,14
III	G4,G5	19,20
IV	G6,G7	15,16,17,21,22,23,24
V	G9	26,27,28,29

Comparison of VCA grouping using sensitivity method and electrical distance method for IEEE 68 bus system is shown in Table 4.5. According to the table, both methods yield equal number of VCA groups but buses in some of the VCAs are different. There are the buses which overlaps between the VCAs and are mostly in the boundary between two VCAs.

Table 4.5: Comparison of VCAs for 39 bus system

VCA No.	Sensitivity		Distance	
	Generator No	**Load bus NO**	**Generator No**	**Load bus No.**
I	14	41	14	41
II	15	42	15	42
III	16	18	16	18
IV	1,6,7,8	21,22,23,24,25,27 37,52,54,55,68	1,6,7,8	21,22,23,24,25,37 52,54,55,67,68
V	2,3	56,57,58,59,60,62 63,64,65,66,67	2,3	56,57,58,59,60,62 63,64 65,66
VI	4,5	19,20	4,5	19,20
VII	9	26,28,29	9	26,27,28,29
VIII	10,11	30,31,32,33,38,40 46,47,48,49,53	10,11	30,31,32,33,38,40 46,47,48,49,53,61
IX	12,13	17,34,35,36,39,43 44,45,50,51,61	12,13	17,34,35,36,39,43 44,45 50,51

4.8 Conclusion

The identification of voltage control area of a power system using reactive power sensitivity of the generator to the load is proposed in this chapter. The effectiveness of the proposed method is demonstrated by implementing in the IEEE test cases. A number of elements to be evaluated in the proposed method is less compared to the electrical distance method. Only $mX(n-m-1)$ sensitivities are required to be evaluated in proposed method compared to $(n-1)X(n-1)$ distances where n is the number of buses and m is a number of generator buses. In the proposed method clustering is done by hierarchical classification algorithm which can be replaced by

some clustering technique based on machine learning for effective online application of the method. In the next chapter, an algorithm for the identification of VCA using a clustering technique based on machine learning will be presented.

CHAPTER 5: ONLINE IDENTIFICATION OF VOLTAGE CONTROL AREA

5.1 Introduction

This chapter presents the online identification of VCAs of power system using a machine learning technique. The identification of VCA is based on the reactive power sensitivities presented in Chapter 4 but uses an unsupervised machine learning technique of k-means clustering instead of the hierarchical clustering algorithm. K-means clustering is modified with an initial estimation of an optimal number of clusters and centroids. The initial estimation increases the accuracy and computation of clustering thus allowing the k-means method for online clustering of VCAs. The technique is implemented in IEEE 39 bus and IEEE 68 bus system for identifying VCAs.

Few literatures have used machine learning methods for identification of VCAs based on different parameters. Unlike hierarchical clustering in previous literatures for identifying VCA using electrical distance, [107] used machine learning technique of k-means clustering to identify VCA. Spectral clustering algorithm is employed to identify contingency cluster which along with influential buses obtained from sensitive buses are used to identify VCA [108].

The chapter is organized as follows. Section 5.2 provides a brief description of clustering and various methods of clustering employed in machine learning. Section 5.3 describes k-means method for clustering. Section 5.4, presents estimation methods of initial values which allow k-means technique for online application. Section 5.5, describes algorithm of online k-means clustering. Case studies with the application of proposed online clustering method presented in section 5.6. Conclusions are provided in section 5.7.

5.2 Clustering

The objective of clustering or cluster analysis is to assign observations to groups so that observations within each group are similar to one another with respect to variable or attributes of interest, and the group themselves stand apart from one another. In other words, the objective is to divide the observations into homogeneous and distinct groups. Clustering process seeks to discover the number and composition of the groups unlike the classification problem where each observation is known to belong to one of a number of groups and the objective is to predict the group to which a new observation belongs. So, clustering is unsupervised learning process while classification is supervised learning process [109–111]. Many clustering methods have been developed using different induction principle and the main reason for having many clustering methods is the fact that the notion of 'cluster' is not precisely defined [111,112]. Many kinds of literature has suggested dividing the clustering methods into two main groups viz 1) hierarchical and 2) partitioning methods [113–115].

5.2.1 Hierarchical Methods

Hierarchical clustering method finds clusters by recursively partitioning the instances either in top-down or bottom-up fashion resulting in a dendrogram like structure, representing the nested grouping of objects and similarity levels at which groupings change. There are various methods of hierarchical clustering which are the variant of single-link [116], complete-link [117], and minimum-variance [118] algorithms. In the hierarchical clustering number of cluster is not required to define but solution highly depends on the definition of the inter-cluster distance. Further , the method is computationally intensive limiting its application to relatively small datasets.

5.2.2 Partitioning Methods

Partitioning method of clustering directly divides data points into some prespecified number of clusters without the hierarchical structure. The process usually accompa-

nies the optimization of criterion function. For a given data set X of n objects, partitioning clustering algorithm partitions them into k clusters while maximizing or minimizing a prespecified criterion function J. The basic idea is to find a clustering structure that minimizes a certain error criterion which measures the distance of each instance to its representative value. One of such criterion function is Sum of Squared Error (SSE) which is most frequently used as they tend to work well with isolated and compact clusters [119]. However, this criterion may be sensitive to the existence of outliers and therefore may incorrectly divide a large cluster into small pieces. The simplest and most commonly used algorithm, employing a squared error criterion is the k-means algorithm [120, 121].

5.3 K-Means Clustering

K-means algorithm is a simple iterative method to partition datasets into a prespecified number of clusters employing squared error criterion. The algorithm was first presented in [122, 123] and since then been applied in different disciplines in a different variant. The clustering process starts by selecting k points in the data sets as initial cluster centers or centroids and objects of datasets are randomly assigned to clusters initially. The objects are then successively reassigned to other clusters to minimize the within-cluster variation, which is basically the squared Euclidean distance from each observation to the centroid. The squared euclidean distance can be expressed as

$$D(x_i, x_{i'})_{=}||\mathrm{x}_i - x_{i'}||^2 \tag{5.1}$$

If the reallocation of an object to another cluster decreases the within-cluster variation, this object is reassigned to that cluster. The process is repeated until there is no reassignment of the object and final k clusters of data sets obtained. The algorithm aims at minimizing the objective function that is, the squared error function. For a dataset X divided into K clusters C_k and centroids m_k, the objective function is

expressed as

$$Minimize \sum_{k=1}^{K} \sum_{C(i)=k} ||\mathrm{x}_i - m_k||^2 \tag{5.2}$$

The steps for k-means clustering are as follows:

1. Initialize number of cluster k and cluster centroids m_j for dataset X with objects $x_i \in \Re$, where, $j = 1, 2....k$ and $i = 1, 2, ..., N$

2. Calculate euclidean distance D_{ij} between m_j centroids and x_i observation points as in (5.1).

3. Assign each observations in the data set to the nearest cluster C_l

$$x_j \in C_l, if ||x_j - m_l|| < ||x_j - m_i|| \tag{5.3}$$

   for j=1,....,N,i≠l, and i=1,...,K

4. Calculate cluster centroids using the observations in each clusters

$$m_i = \frac{1}{N_i} \sum_{x_j \in C_j} x_j \tag{5.4}$$

5. Repeat steps 2 to 4 until there is not change in each cluster.

With the hierarchical methods, an object remains in a cluster once it is assigned to it, but with k-means, cluster affiliations can change in the course of the clustering process. Consequently, k-means does not build a hierarchy which is why the approach is also frequently labeled as non-hierarchical.

The advantage and disadvantage of k means clustering over hierarchical clustering and in general are presented below [124, 125].

Advantages of k means

- Computationally efficient, basically linear in the number of data points so can be applied to large data sets.

- k-means is superior to hierarchical methods as it is less affected by outliers and the presence of irrelevant clustering variables.

Disadvantages of k means

- Number of cluster k should be specified in advance
- Since k-means can converge to a local optimum, different initial points lead to different final solution.
- Not good when clusters are of very different sizes or very non-spherical.
- Based on squared error criterion so may be sensitive to the existence of outliers and therefore may incorrectly divide a large cluster into small pieces.

5.4 Initial Estimate For K Means Clustering

Cluster analysis is an important tool for unsupervised learning. A major challenge in cluster analysis is the estimation of the optimal number of clusters and initial centroids. These drawbacks restrict the online application of k-means method for clustering. Estimation of k using gap static and centroids using k- means++ is augmented to modify the standard k-means clustering in an iterative fashion for online application. Overview of gap static and k-means++ algorithm are presented below and algorithm for online application of k-means will be provided in Section 5.5

5.4.1 Estimation of K Using Gap Statistic

The recently proposed gap statistic method compares the curve $logW_k$ (W_k is within the cluster dispersion defined below)to the curve obtained from data uniformly distributed over a rectangle containing the data. It estimates the optimal number of clusters to be the place where the gap between the two curves is largest.It also works reasonably well when the data fall into a single cluster, and in that case will tend to estimate the optimal number of clusters to be one. This is the scenario where

most other competing methods fail [126]. Previously, the methods of estimating the number of clusters were divided into global and local method [127]. The global method evaluates some measure over the entire data set and optimist it as function of the number of clusters while ;oacal method considering pairs of clusters and test whether they should be amalgamated. The gap method us a global procedure. A global method was proposed in [128] with quantity $W_k k^2/p$ as a criterion for choosing number of cluster following the proposal by [129] who used the determinant, rather than the trace, of the within sum of square matrix. The estimation of k based on the computation of the number of connected components of an estimate of set $f > c$ where f denoted the underlying density function and c is given constant is presented in [130] but the high dimensionality is not acceptable in general.

The gap static method is presented in [131] which can be used to estimate the number of cluster to virtually any clustering method. The dataset $x_{ij}, i = 1, 2, ..n, j = 1, 2, ..p$ consist of p as features measured and n as independent observations. Let $d_{ii'}$ denote the distance between observations i and i'.Let us assume data x_{ij} be clustered into k clusters $C_1, C_2, ..., C_r$, with C_r denoting the indices of observations in cluster r, and n_r=$|C_r|$. The sum of the pairwise distances fo all points in cluster r be represented as

$$D_r = \sum_{i,i' \in C_r} d_{ii'} \tag{5.5}$$

Then, W_k be the pooled within -cluster sum of squares around the cluster means.

$$W_k = \sum_{r=1} k \frac{1}{2n_r} D_r \tag{5.6}$$

The idea behind their approach was to find a way to standardize the comparison of $logW_k$ with a null reference distribution of the data, i.e. a distribution with no obvious clustering. Then, the estimate of the optimal number of clusters is the value for which $logW_k$ falls the farthest below this reference curve. Hence, gap static is

defined as:

$$Gap_n(k) = E_n^*(logW_k) - logW_k \tag{5.7}$$

where, E_n^* denotes expectation under a sample of size n from the reference distribution. The estimate k will be the value maximizing g$Gap_n(k)$ after we take the sampling distribution into account. The estimate is very general and applicable to any clustering method and distance measure $d_{ii'}$. The reference distribution is generated by sampling uniformly over the range of the observed values. $E_n^*(logW_k)$ is estimated by the average of B copies of $log(W_k^*)$, each of which is computed from a Monte Carlo sample from the reference distribution. Now, (5.7) can be restated as following.

$$Gap_n(k) = (1/B)\sum_b(logW_{kb}^*)) - logW_k \tag{5.8}$$

Let, $sd(k)$ denote the standard deviation of the B Monte Carlo replicates of $log(W_k^*)$. The term, after accounting for the simulation error in $E_n^*(logW_k)$, will result into following quantity:

$$s_k = \sqrt{(}1 + 1/B)sd(k) \tag{5.9}$$

The optimal number of clusters is the smallest k such that $Gap(k) \geq Gap(k+1) - s_{k+1}$.

The computation of the gap statistic involves the following steps

1. Cluster the observed data, varying the number of clusters from $k = 1, ..., K$, and compute the corresponding W_k

2. Generate B reference data sets and cluster each one giving within -dispersion measure W_{kb}^*, where $b = 1, 2, .., B$ and $k = 1, 2, .., K$ compute estimated gap statistic

$$Gap(k) = (1/B)\sum_b(logW_{kb}^*) - logW_k \tag{5.10}$$

3. Let, $w = (1/B)\sum_b logW^*_{kb}$, compute the standard deviation

$$sd(k) = [(1/B)\sum_b (logW^*_{kb} - w)^2]^(0.5) \tag{5.11}$$

and define

$s_k = sd_k\sqrt{1 + 1/B}$

4. Choose the number of clusters as the smallest k such that

$Gap(k) \geq Gap(k+1) - s_{k+1}$.

5.4.2 Estimation of Centroids Using K-Means++ Algorithm

Clustering of data using k-means algorithm begins with k arbitrary centroids, typically chosen uniformly at random from the data points. New centroids are recomputed closer to the center of the cluster mass until the process stabilizes. The process will always terminate and the algorithm is much faster but there is no theoretical guarantee of getting close to the minimum that is accuracy is compromised for simplicity and speed. Initialization of centroids for k-means algorithm is proposed in [132] with higher probability of accuracy by using k-means++ algorithm with precise theoretical guarantee. The steps for choosing centroids in a datasets X of n points using k-means++ algorithm are as follows [132].

1. Choose an initial center c_1 uniformly at random from X.

2. Compute the vector containing the square distances between all points in the dataset and c_1 i.e. $D_i^2 = ||\mathrm{x}_i - c_1||^2$

3. Choose a second center c_2 from X randomly drawn from the probability distribution $D_i^2 / \sum_j D_j^2$

4. Recompute the distance vector as $D_i^2 = \min\left(||\mathrm{x}_i - c_1||^2, ||\mathrm{x}_i - c_2||^2\right)$

5. Choose a successive center c_l and recompute the distance vector as $D_i^2 = \min\left(||\mathrm{x}_i - c_1||^2, \ldots, ||\mathrm{x}_i - c_l||^2\right)$

6. Continue until k centers are chosen and $c_1, c_2, ..c_k$ are initial centroids for k-means algorithm

[132] has shown that the estimated set of centers using k-means++ algorithm is probably close to the optimal solution and increases both speed and accuracy of k-means algorithm. Thus initial seeding is done using heuristic method of k-means++ algorithm which improves the running time and final solution of k-means algorithm [132].

5.5 Algorithm for Identification of VCA Using Clustering

The goal of clustering is to assign the observations into different groups such that the dissimilarities between those in the same group is smaller than those in different groups. k-means clustering algorithm is utilized to group the buses into different clusters to form VCA based on reactive power sensitivities. The reactive power sensitivity is used to define similarity between buses. The algorithmic procedure involved in grouping buses using k-means clustering is given in the following steps.

1. Jacobian matrix and Sensitivity matrix: Jacobian matrix of generator reactive power to state vector,J_g from Equation (4.5) is calculated and load flow is performed to calculate load flow jacobian matrix J. Then, the both matrices are used to calculate sensitivity of reactive power to change in load. The sensitivity matrix S_{qg} is of size $mXp, p = (n - m - 1)$ where, n is number of bus, m is number of PV generators

2. Preliminary Cluster: Once the sensitivity matrix is calculated, the transpose of sensitivity matrix S_{qg} is obtained to get dataset X of size $p \times m$. Data set X contains x_{ij} observations where i=1,2,..,p are points and j=1,2..,m are variables.

Here,the load buses are represented as row or the points and generator are represented by column or variables. Hence, clustering of sensitivity will cluster load buses into different groups or voltage control area. The generators will be grouped in the VCA which has highest sensitivity values.

3. k-means clustering: The steps for clustering given dataset with reactive sensitivities using k-means algorithm is as follows:

   (a) Select initial estimate of k using gap statistic algorithm and use K-means++ algorithm for initial seeding of centroids C_{ij} where i=1,2,..,k and k is the number of cluster estimated using gap statistic and j=1,2..,m are variables.

   (b) Calculate the euclidean distance D_{ij} between C_j centroids and x_{ij} observation points.

$$D_{ij} = \sum_{j=1}^{k} \sum_{i=1}^{n} \mid x_{ij} - C_j \mid^2 \tag{5.12}$$

   (c) Assign the sensitivity observations into k clusters based on the minimum distance

   (d) Compute k new centroids using average of the points in each cluster

   (e) Repeat b) through d) until cluster assignment is unchanged

4. Clustering validation: The quality of clusters obtained by above algorithm can be evaluated by various cluster evaluation techniques like Davies-Bouldin index, Dunn index, average silhouette value, etc. Here, the silhouette value is used to evaluate the clustering results as it works well with k-means clustering. The value ranges from -1 to 1, where higher values indicates optimal clustering and lower value indicates that the points are poorly clustered [133]. The silhouette value can

be expressed as following

$$f(n) = \begin{cases} 1 - a(i)/b(i), & \text{if } a(i) < b(i) \\ 0 & \text{if } a(i) = b(i) \\ b(i)/a(i) - 1, & \text{if } a(i) > b(i) \end{cases} \tag{5.13}$$

where, $a(i)$ is average dissimilarity within the same cluster and $b(i)$ is the lowest average dissimilarity to any other cluster. The accuracy of clusteres formed can be measured in terms of average silhoutte value. An average silhouette value greater than 0.5 indicates reasonable clustering of data and a value less than 0.2 indicates the data groups formed do not exhibit cluster structure [108].

5. Generator buses: After completion of k-means clustering of load buses, a coherent groups of load buses are obtained. Load buses in each cluster have higher sensitivity to one generator or group of generators. These generators will be part of the voltage control area and serve as the primary reactive reserve of the area.

The overall algorithmic flowchart for VCA identification is shown in Fig. 5.1.

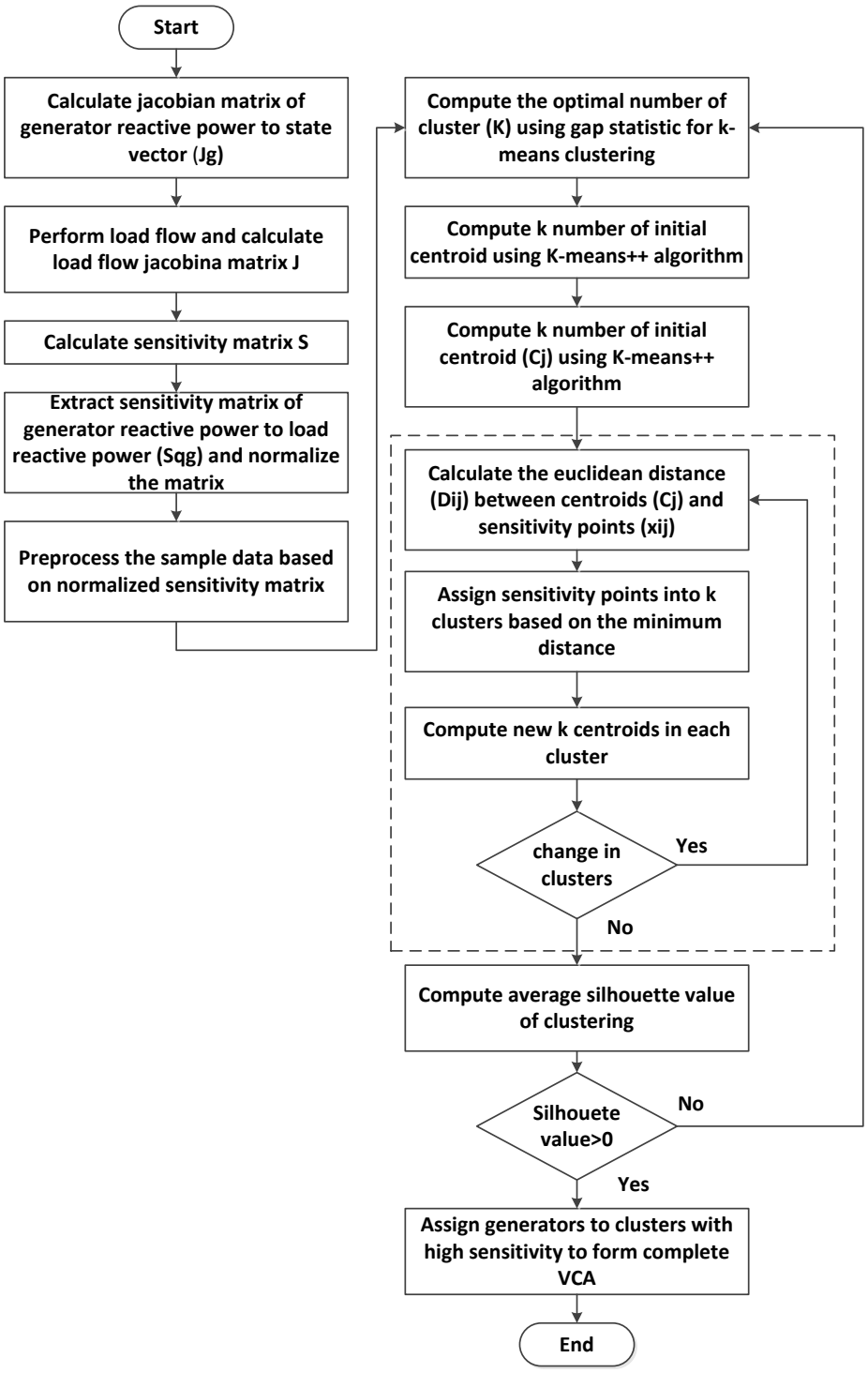

Figure 5.1: Identification of VCAs using k-means clustering

5.6 Test Cases

The identification of VCA based on sensitivities presented in Chapter 4 is implemented for online application using the k-means clustering technique. The algorithm is implemented in IEEE 39 bus and IEEE 68 bus sytem test cases and compared with the hierarchical method presented in Chapter 4.

5.6.1 Test Case: IEEE 39 Bus System

IEEE 39 bus system comprises of 10 machines or generator buses and remaining 29 load buses. The clustering of 39 buses into VCAs is performed in 2 steps, first reactive power sensitive matrix is calculated which is used as dataset for online clustering in the second step. The reactive power sensitivity matrix S_{qg} is the matrix of size $9X29$, as slack bus or swing generator which is bus 31 in the system is not considered for the sensitivity. The sensitivity matrix is normalized and preprocessed for k-means clustering by taking the transpose of the matrix. The data set for clustering will be of size $p \times m$ with p=29 points representing rows and m=9 variables as columns. The data set for 39 bus system is shown in Table B.1 of Appendix B.

Prior to clustering of the above data set using k-means algorithm, the optimal number of clusters k is decided using gap statistic algorithm. The plot of within-cluster sum of squares W_k from (5.6) is shown in Fig. 5.2a where, elbow of the curve suggests the optimal number of clusters which can be proved in subsequent plots. The comparison of $\log W_k$ with a null reference distribution of data represented by (5.7) is shown in Fig. 5.2b. The estimated gap static computed from the two curves for different number of cluster values are shown in Fig. 5.3a. The optimal number of clusters is the smallest value of k satisfying $Gap(k) \geq Gap(k+1) - s_{k+1}$. In Fig. 5.3b the barplot of gap change which is $Gap(k) - (Gap(k+1) - s_{k+1})$ shows the first positive value for $k = 5$ confirming the optimal k as 5.

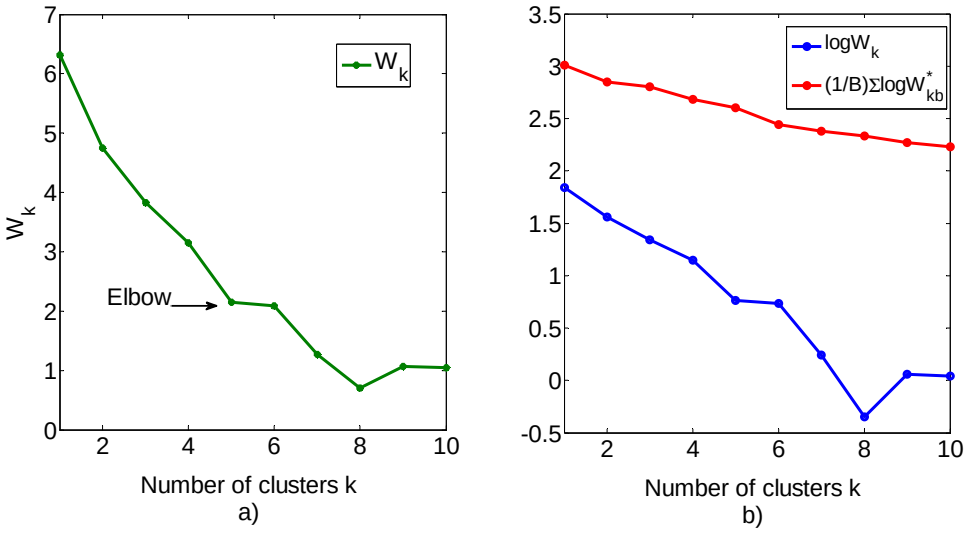

Figure 5.2: Plot of a) W_k and b)comparison of curves for IEEE 39 bus system

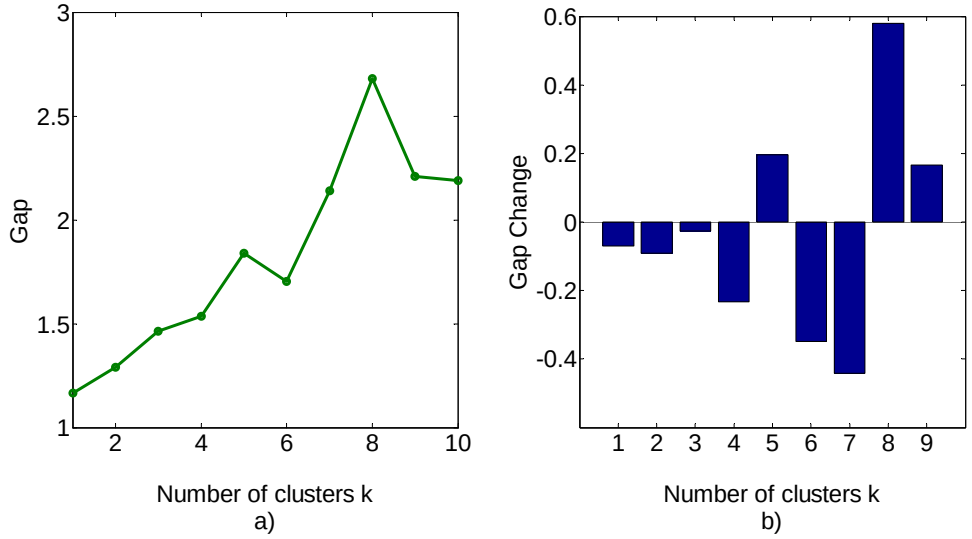

Figure 5.3: Plot of a) gap and b) gap change for for IEEE 39 bus system

The solution of k-means clustering is effected by the initial seeding of cluster centroid so, the optimal seeding is important to avoid bad clustering. K-means++ algorithm used for initial seeding of cluster centroids highly improves the accuracy of k-means clustering compared to random selection of centroids as there is no theoretical guarantee of getting close to the minimum. The optimal numbe of cluster obtained from gap statistic is used to estimate initial centroids. The k-means++ al-

gorithm generates 5 sets of centroids with p observations, hence the size of centroids is $k \times p$. With the initial values of k and centroids, clustering of 29 load buses data set results into 5 distinct groups of VCA based on reactive power sensitivities. The initial result of clustering is as shown in the Table 5.1.

Table 5.1: Clustering of 39 bus system

Cluster No.	**Bus No.**
I	2,3,18,25
II	1,4,5,6,7,8,9,10,11,12,13,14
III	19,20
IV	15,16,17,21,22,23,24
V	26,27,28,29

The clustering solution of dataset shown in Table can be verified using average silhouette value. Generally, average silhouette value above 0.5 is considered good as it exhibit cluster structure. To demonstrate the validity of result obtained above, silhouette values of clusters when the dataset is clustered to 4 and 6 cluster using the above method is shown in Fig. 5.4. The average silhouette values are shown in Table 5.2. Since, average value for all three cluster numbers are above 0.5, the clusters formed in all three cases exhibit cluster structure. But, higher the value greater is the uniformity of observations in data and clustering solution with 5 cluster is the best as it has highest value. The uniformity of observations can be compared in the silhouette plot of each observation in cluster in Fig.5.4. Silhouette plot with k=6 has silhouette value for a observation going negative showing poor cluster formation. Hence, average silhouette value validates the clusters formed by k-means method.

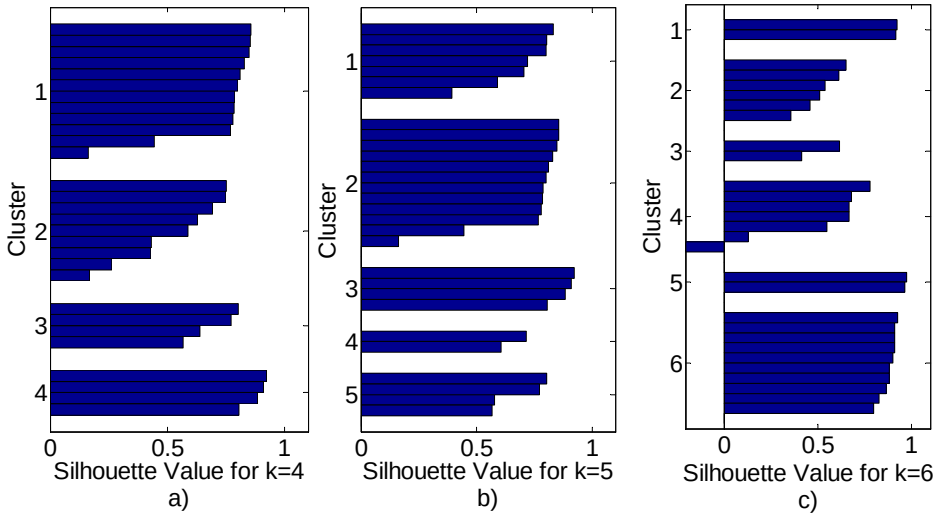

Figure 5.4: Plot of silhoutte values for a) k=4 b) k=5 and c) k=6

Table 5.2: Average silhouette values

Number of clusters (k)	**Average Silhoutte Value**
4	0.6797
5	0.7283
6	0.6895

Once the clustering of the buses is completed, generators are assigned to each clusters based on the sensitivity values. Generator is assigned to a cluster where reactive power sensitivity value to its buses is higher. The generators in the cluster are the reactive reserve basin. The grouping of buses and generators completes the formation of VCA. After, allocation of generators the complete VCA for 39 bus system is as shown in Table 5.3.

Table 5.3: VCA of 39 bus system

VCA No	Bus No	Generator ID
I	2,3,18,25	G8, G10
II	1,4,5,6,7,8,9,10,11,12,13,14	G1,G2,G3
III	19,20	G4, G5
IV	15,16,17,21,22,23,24	G6,G7
V	26,27,28,29	G9

The results of identification of VCA of IEEE 39 bus system is similar to the hierarchical method presented in Chapter 4. The comparison of identification of VCA using hierarchical method and online clustering method is shown in Table 5.4.

Table 5.4: Comparison of VCAs for 39 bus system

VCA No.	Hierarchical		K-means Clustering	
	Generator	Load bus No	Generator ID	Load bus No.
I	G8,G10	2,3,18,25	G8,G10	2,3,18,25
II	G1,G2,G3	1,4,5,6,7,8,9,10, 11,12,13,14	G1,G2,G3	1,4,5,6,7,8,9,10, 11,12,13,14
III	G4, G5	19,20	G4, G5	19,20
IV	G6,G7	15,16,17,21,22, 23,24	G6,G7	15,16,17,21,22, 23,24
V	G9	26,27,28,29	G9	26,27,28,29

5.6.2 Test Case: IEEE 68 Bus System

IEEE 68 bus system is reduced order equivalent of the inter-connected New England test system (NETS) and New York power system, with 5 geographical regions out of which NETS and NYPS are represented by a group of generators while remain-

ing 3 areas are approximated by equivalent generator models [106]. Preliminary data set for clustering IEEE 68 bus system yields matrix of size 52×15. Besides, group of generators of NETS and NYPS, the remaining groups are approximated with equivalent generator models and can be considered as separate VCA on its own. To identify the these neighboring groups as separate VCA, sensitivity of these generators to its adjoining buses can be compared with sensitivity with other buses. According to [106] generators 14, 15 and 16 are equivalent generator models and since, generator 16 is considered as swing generator, the comparison will be shown for generators 14 and 15 only. The sensitivity of generators 14 and 15 to load buses are shown in Fig. 5.5. The figure shows that the generators have very high reactive sensitivity to adjoining buses that is bus 41 for generator 14 and bus 42 for generator 15 compared to other buses. The sensitivity values of these generators and buses in data set for clustering are outliners in the data set and may influence the solution of k-means clustering. Hence, to get optimal clustering results, the generators 14, 15 and 16 and load buses 41, 42 and 18 are excluded from the data set for clustering.

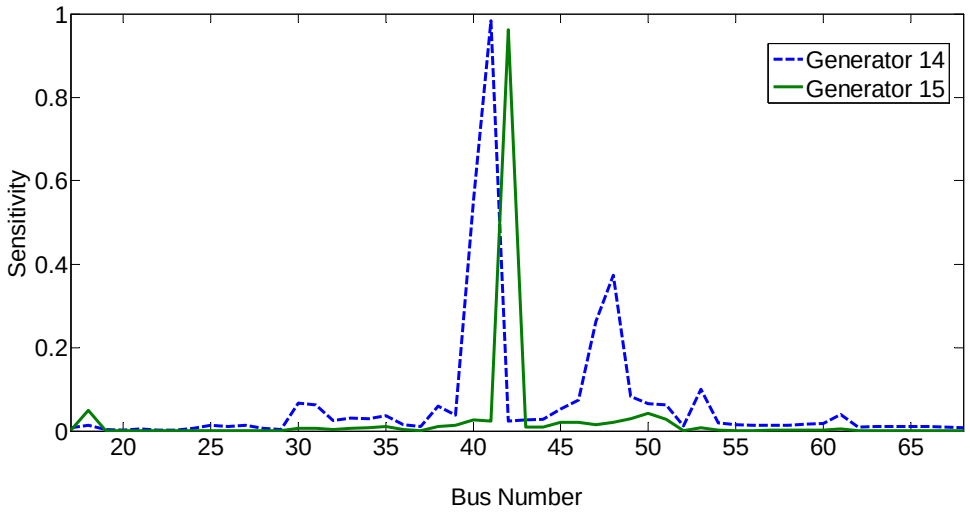

Figure 5.5: Sensitivity of generators in IEEE 68 bus system

The data set for clustering of IEEE 68 bus systems is reduced to matrix of size 49×12. The data set will result in additional clusters to the three determined already

and the total number of VCAs will be the sum of two. The data set is used to estimate optimal number of cluster using gap statistic algorithm. Plot of within-clusters sum of squares W_k and comparison of logW_k is shown in Fig. 5.6. The elbow in the plot of W_k suggests that the optimal number of cluster is 6. Fig. 5.7 shows the plots of gap and gap change and the optimal number of clusters is 6 as the first positive gap change is for $k = 6$.

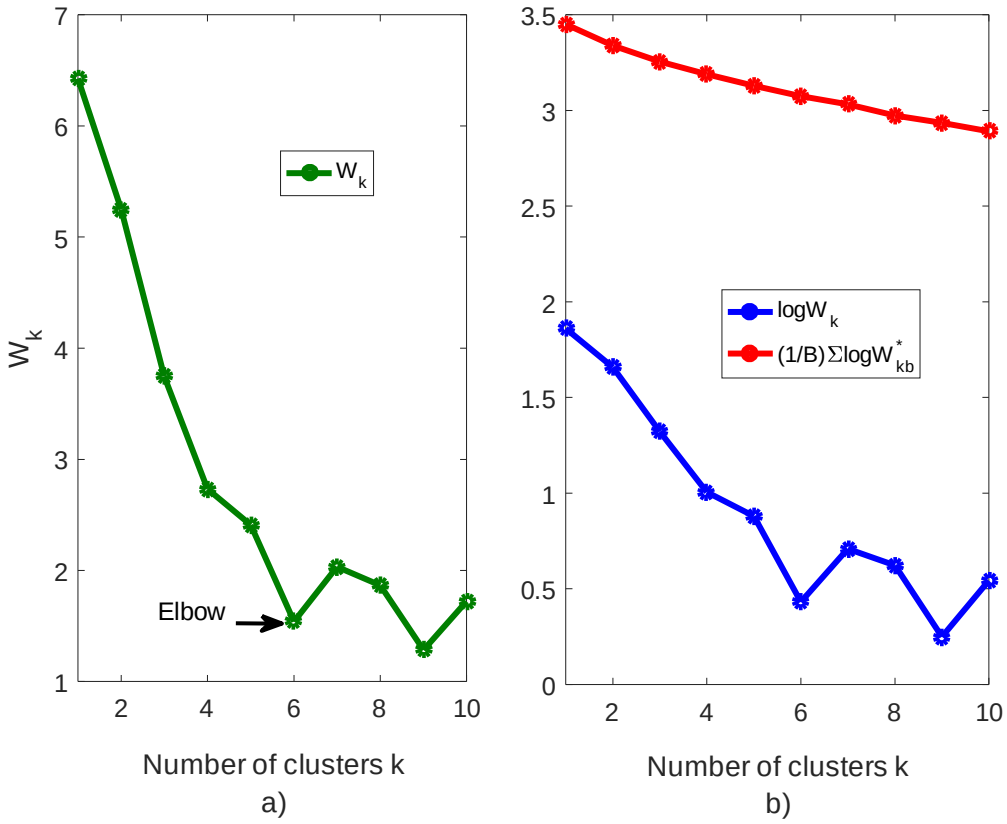

Figure 5.6: Plot of a) W_k and b) comparison of curves for IEEE 68 bus system

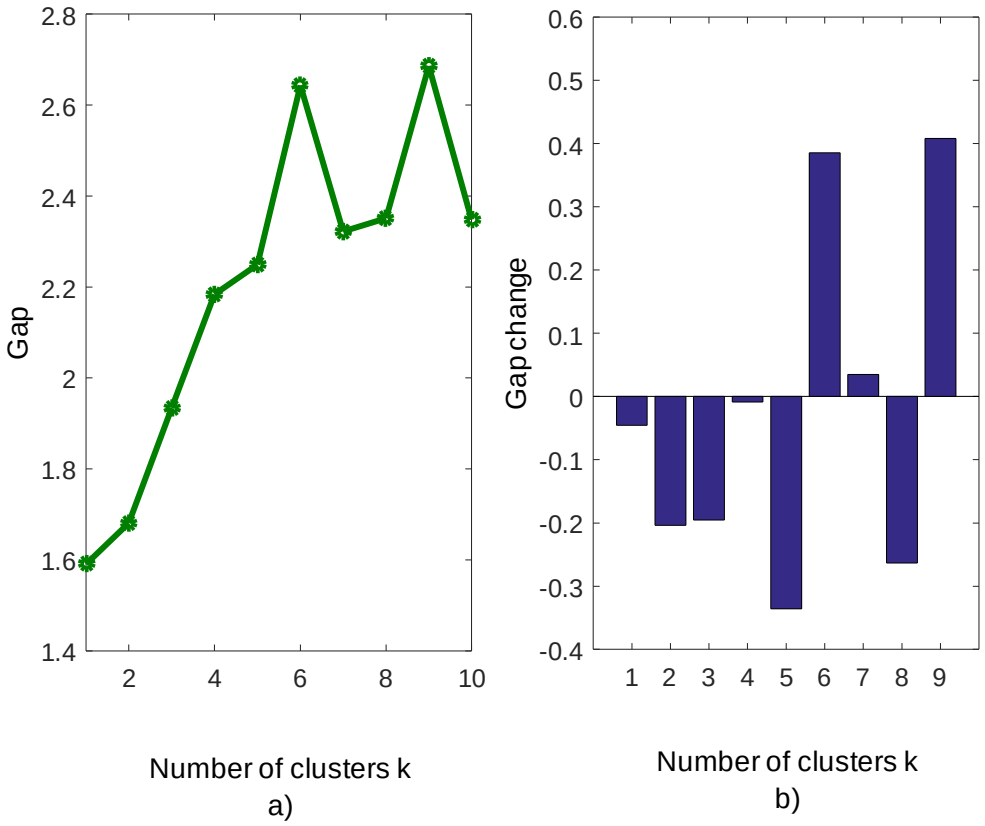

Figure 5.7: Plot of a) gap and b) gap change for IEEE 68 bus system

K-means++ algorithm is used for the initial seeding of 5 clusters to start clustering process using k-means technique. The result of clustering of data set of 68 bus system is as shown in Table 5.5.

Table 5.5: Clustering of IEEE 68 bus data set

Group No	**Bus No**
1	21 22 23 24 37 52 55 67 68
2	56 57 58 59 60 62 63 64 65 66
3	19 20
4	25 26 27 28 29 54
5	30 31 32 33 38 40 46 47 48 49 53
6	17 34 35 36 39 43 44 45 50 51 61

The result of clustering is verified with the average silhoutte values. The plot of silhoutte values for k=6 along with k=5 and k=7 for comparison are shown in Fig. 5.8 and average sihoutte values are shown in Table 5.6. Since, the average silhouette value for k=6 is greater than 0.5 and lower than that for other values of k, the optimal value of k=6 is verified. The final groups formed by k-means clustering for the data set of IEEE 68 bus system is as shown in Table 5.5.

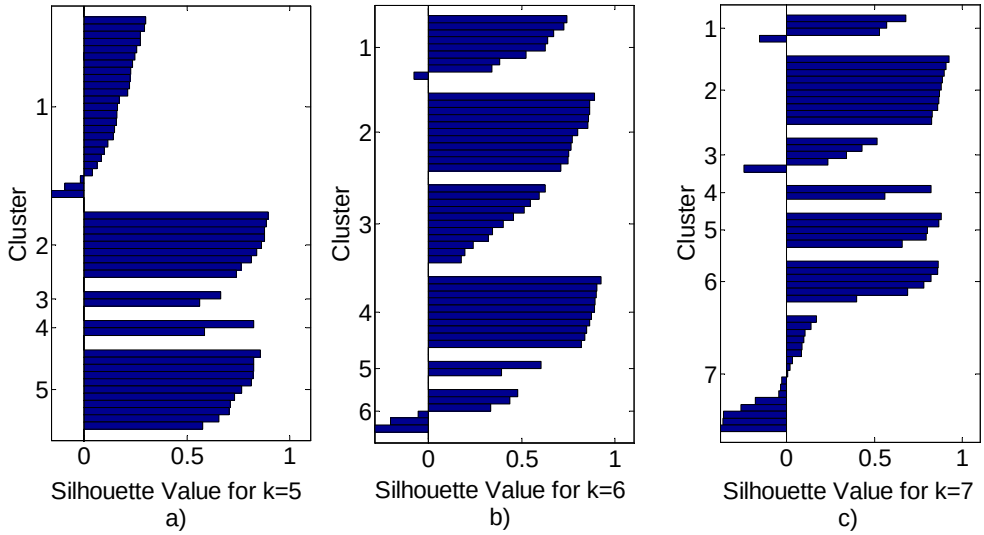

Figure 5.8: Plot of silhoutte values for a) k=5 b) k=6 and c) k=7

Table 5.6: Average silhouette values

Number of clusters (k)	**Average silhouette Value**
5	0.4557
6	0.5775
7	0.4193

VCAs for IEEE 68 bus system is completed with combination of three VCAs defined earlier and the six VCAs identified using the k-means clustering. To identify the reactive reserve generators for the VCAs, the sensitivity matrix is used. The generators with higher sensitivity to the buses of a VCA belongs to the particular

VCA. Complete allocation of generator and load buses into the identified VCAs are shown in Table 5.7.

Table 5.7: VCAs of IEEE 68 bus system

VCA No	**Load Bus No**	**Generator No**
I	14	41
II	15	42
III	16	18
IV	21,22,23,24,37,52,55,67,68	6,7
V	56,57,58,59,60,62,63,64,65,66	2,3
VI	19,20	4,5
VII	25,26,27,28,29,54	1,8,9
VIII	30,31,32,33,38,40,46,47,48,49,53	10,11
IX	17,34,35,36,39,43,44,45,50,51,61	12,13

Graphical representation of identification of VCAs in IEEE 68 bus system is shown in Fig. 5.9. The figure clearly shows that each of equivalent generator model is grouped in as a separate VCA while remaining two system viz NYPS and NETS are subdivided to 4 and 2 VCAs respectively.

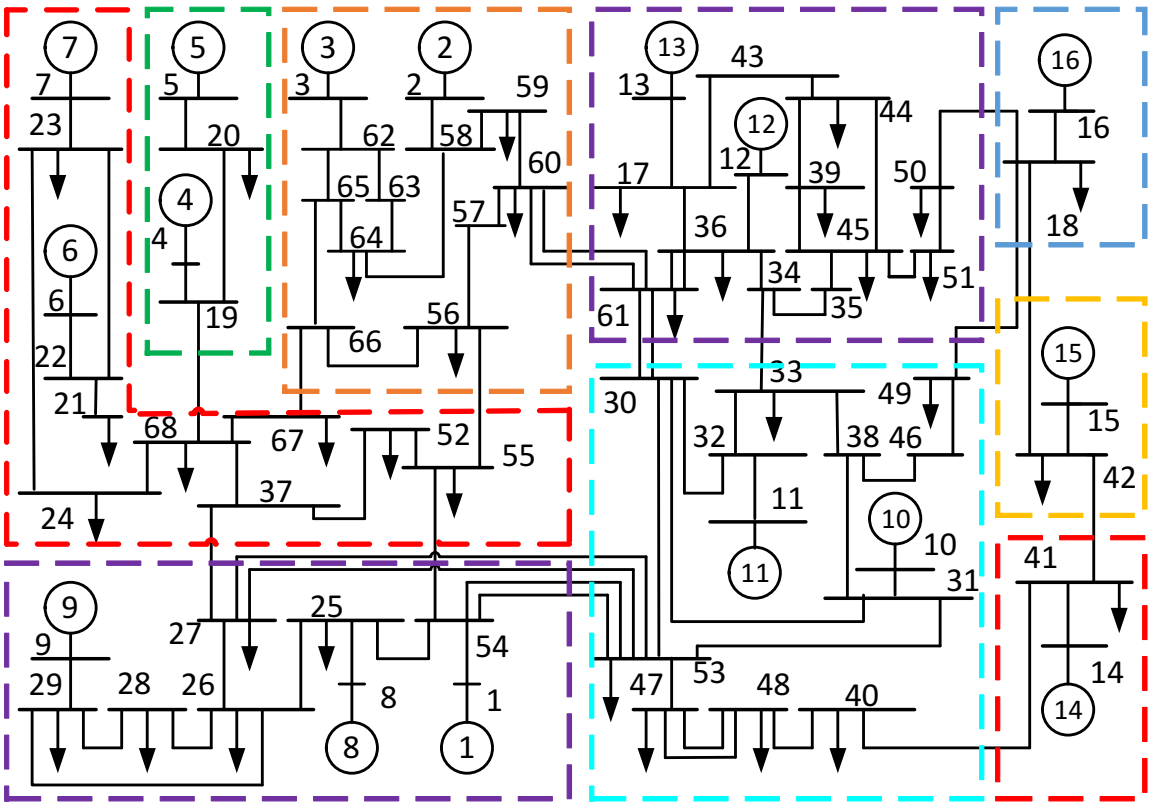

Figure 5.9: VCA of IEEE 68 bus system

The comparison of identification of VCAs based on reactive power sensitivities using hierarchical method and clustering technique is shown in Table. 5.8. Both technique resulted in equal number of VCAs but with minor variation in VCAs. Buses 25 and 54 belonged to VCA IV but k-means clustering method grouped it in VCA VIII along with load buses 25,26,27,28,29 and 54 with reactive reserve generators 1,8 and 9. The reactive power sensitivity of generator 9 to buses 25 and 54 is higher than that of generator 6 and 7. Beside this, bus 61 changes from VCA VIII to IX and from the sensitivity value shown in appendix, sentivity of generator 12 and 14 to bus 44 is higher than that of generators 10 and 11.

Table 5.8: Comparison of VCAs for 68 bus system

VCA No.	Hierarchical		K-means Clustering	
	Generator	Load bus No.	Generator ID	Load bus No.
I	14	41	14	41
II	15	42	15	42
III	16	18	16	18
IV	1,6,7,8	21,22,23,24,25,37 52,54 55,67,68	6,7	21,22,23,24,37,52 55,67,68
V	2,3	56,57,58,59,60,62 63,64,65,66	2,3	56,57,58,59,60,62 63,64,65,66
VI	4,5	19,20	4,5	19,20
VII	9	26,27,28,29	1,8,9	25,26,27,28,29,54
VIII	10,11	30,31,32,33,38,40 46,47,48,49,53,61	10,11	30,31,32,33,38,40 46,47,48,49,53
IX	12,13	17,34,35,36,39,43 44,45 50,51	12,13	17,34,35,36,39,43 44,45,50,51,61

5.7 Conclusion

An online identification of VCA using reactive power sensitivity and an unsupervised machine learning technique of k-means clustering is proposed in this chapter. The k-means method is augmented with gap statistic method and k-means++ algorithm for initial estimation of an optimal number of clusters and centroid respectively. The initial estimation improves the accuracy and computational efficiency of k-means algorithm and thus it is suitable for the online clustering. The proposed method is implemented for online identification of VCAs in IEEE test cases of 39 and 68 bus system. This method allows effective online voltage control and reactive power alloca-

tion by identifying the localized area for the voltage problem. The implementation of the proposed method of identification of VCA for secondary voltage control is shown in the next chapter.

CHAPTER 6: VOLTAGE CONTROL OF WIND INTEGRATED POWER GRID

6.1 Introduction

This chapter proposes a secondary voltage control of power system by based on the partitioning of the system using the online identification of VCAs presented in chapter 5 and voltage monitoring using VSI proposed in chapter 3. The secondary voltage control is achieved by changing the set-point of the reference voltage of the generator. The new set-point of the reference voltage is calculated using the voltage difference of the vulnerable bus and the participation factor of the generator. The comparison of voltage control for wind integrated power grid is shown with the conventional power grid. Voltage control capability of a wind generator is normally used for terminal voltage control as a primary voltage control only. In this chapter, the voltage capability of the wind generator is shown for regional voltage control through secondary voltage control with simulation results.

The chapter is organized as follows. Section 6.2 provides brief description of of voltage control of power system. Various aspects of secondary voltage control is discussed in section 6.3. Proposed voltage control using VSI and VCA is presented in section 6.4. Application of proposed control in the conventional power system of IEEE 39 bus test system with simulation results is shown in section 6.5. The wind integrated power is grid is explained in section 6.6. Proposed voltage control is applied in wind integrated power grid in section followed by conclusion in section .

6.2 Voltage Control of Power System

For the security, reliability and economical operation of the electric power grid, control of bus voltages and reactive power flows is essential [134]. Voltage control

of power system is operated in different ways in different countries. In North America, much of voltage control actions are coordinated by operators by switching in or out shunt capacitor or reactor banks, as well as by adjusting transformer taps as needed [25]. In 1980 and 1990s various hierarchical voltage control schemes were proposed in European countries and they were defined as primary, secondary, tertiary voltage control similar to emulate hierarchical levels of frequency control. Primary control is a local control and its main role is to maintain the voltage at the generator buses performed by AVRs or exciter of renewable generation sources. As per NERC command, the primary voltage control by generator including wind generators are required as per grid connection code in most power systems including in North America. Secondary voltage control is a slower level of control in which several AVRs together perform the control actions in a regional sense. Secondary voltage control is slower level of control which updates the primary control set points to improve voltage of buses in an area based on the information from the control area. Most of the secondary control schemes use voltage control area as a regional control zone and pilot buses as reference bus. Tertiary voltage control is designed for optimal power transfer while considering security constraints and provides set points for the controllers in the other two levels.

6.3 Secondary Voltage Control

Primary voltage control functions to maintain the voltages at the generator buses at their reference values through AVRs. Due to local nature of reactive power, the primary control action is not sufficient to maintain voltage profiles and prevent voltage instability in an area of the system. Secondary voltage control regulates the voltage control of buses farther from generator buses. Traditionally secondary voltage control actions consist of one or more of following [135].

- Changing reference voltage values at the generators and/or synchronous compensator buses

- Switching of capacitors and/or inductors
- Switching of load tap changer transformer
- Load shedding in a critical situation
- Using of FACTS devices

The secondary control scheme is implemented in European countries with the concept of pilot bus [26–28]. A pilot bus is the representative of buses of control area with voltage profile reflecting the pattern of other buses in the area. There are various techniques to select pilot bus like the one with the greatest short circuit capacity [20, 29] or with optimization problem to minimize voltage deviation after random disturbance [30]. Once the pilot bus was selected, all the control actions were aimed at regulating the voltage at this bus. Thus, the AVR's set-points were changed as needed to meet the set-point voltage at the pilot buses.

6.4 Voltage Control Using VSI and VCA

The pilot bus selection was important due to the lack of measurements of buses and inability to handle large amounts of data coming from different buses. But with the large installations of synchrophasor across the power systems around the world and advanced technique enabling control centers to handle a large amount of data, monitoring of individual buses is feasible instead of a single pilot bus in the area. This increases accuracy in the monitoring of the voltage instability level of the system. In North America and other countries, operator switches shunt capacitor or reactor banks and adjusts transformer taps for voltage control action. But better communication technology enables to relay the voltage instability index of buses and take control action in AVRs of generators for voltage control as a secondary voltage scheme instead of switching of additional reactive power compensator. Hence, we present a voltage and reactive power control of area based on the monitoring of all

the load buses using VSI proposed in Chapter 3. Online VCA identification presented in Chapter 5 is used to define an area for secondary voltage control. The volage vulnerability of all the buses is monitored using the VSI. The VSI below the value of 1 is the proximity to voltage instability. Hence, if any bus VSI drops below 1, secondary voltage control action started. The first step of secondary voltage control is to identify the VCA and reactive reserve generators of the venerable bus. The identification of VCA and reactive reserve generator is done by the VCA identification method proposed here. Then, a control signal is calculated. The control signal is the difference between the base voltage level and the current voltage level of the vulnerable bus.

$$C^* = Vbase_i - V_i \tag{6.1}$$

where,C* is control signal.

V_{basei} and V_i are base voltage and current voltage of bus i. Then, participation factor K_j of generators are determined based on the reactive power sensitivities of generators to the bus.

$$K_j = \frac{S_{ij}}{\sum_{j=1}^{k} S_{ij}} \tag{6.2}$$

where,

S_{ij} is reactive power sensitivity of generator j to bus i

k is the number of reactive reserve generators in the VCA of bus i Now,new reference voltage for AVR or exciter of generator is given as

$$Vref_{new} = Vref_{old} + K_j * C^* \tag{6.3}$$

where, Vref is reference voltage of AVR

The overall algorithmic flowchart for voltage control using VSI and VCA identification is shown in Fig. 6.1.

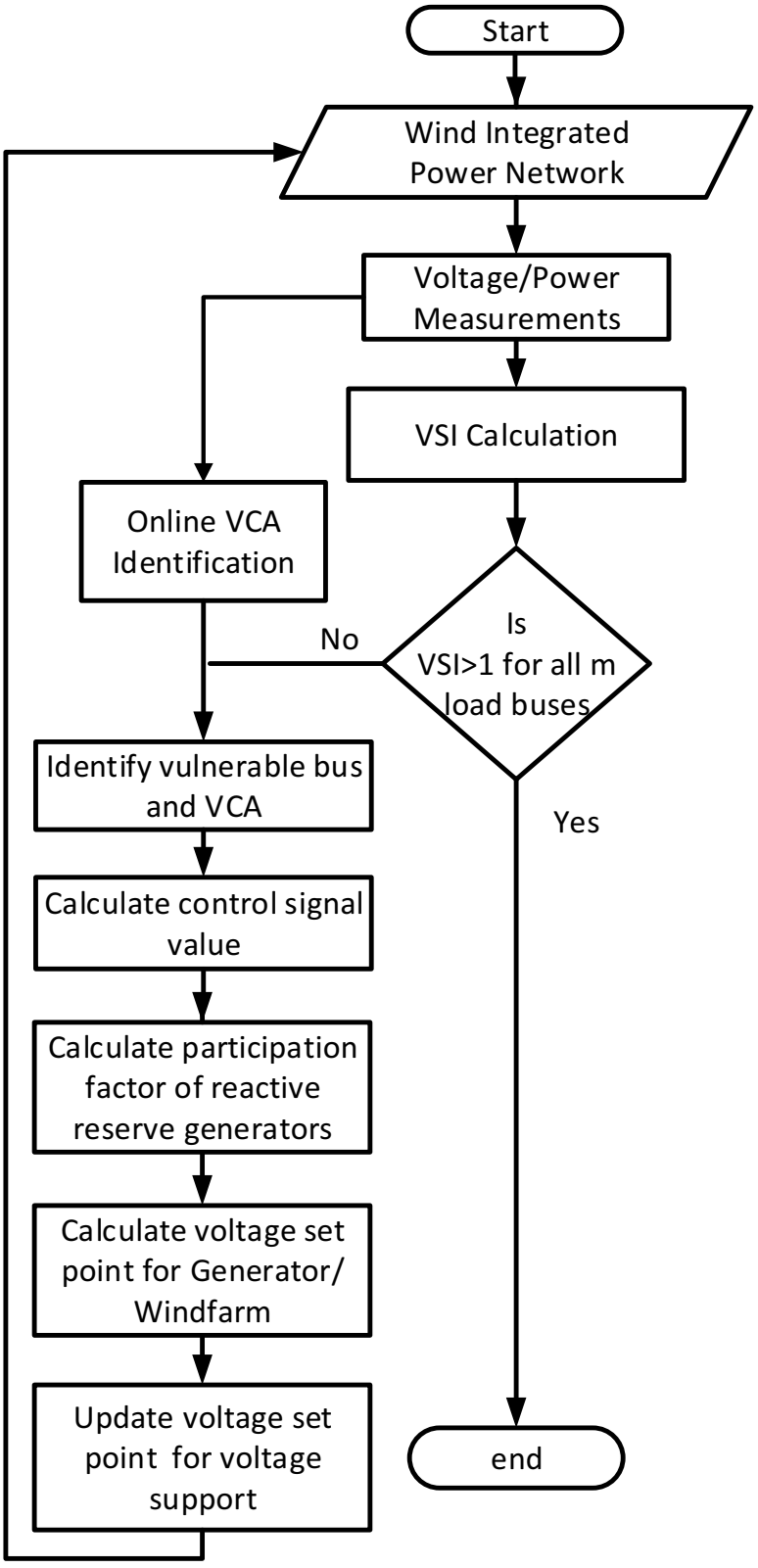

Figure 6.1: Algorithmic flowchart for voltage control using VSI and VCA identification

Organization of proposed voltage control concept using VSI and VCA identification is shown in Fig. 6.2.

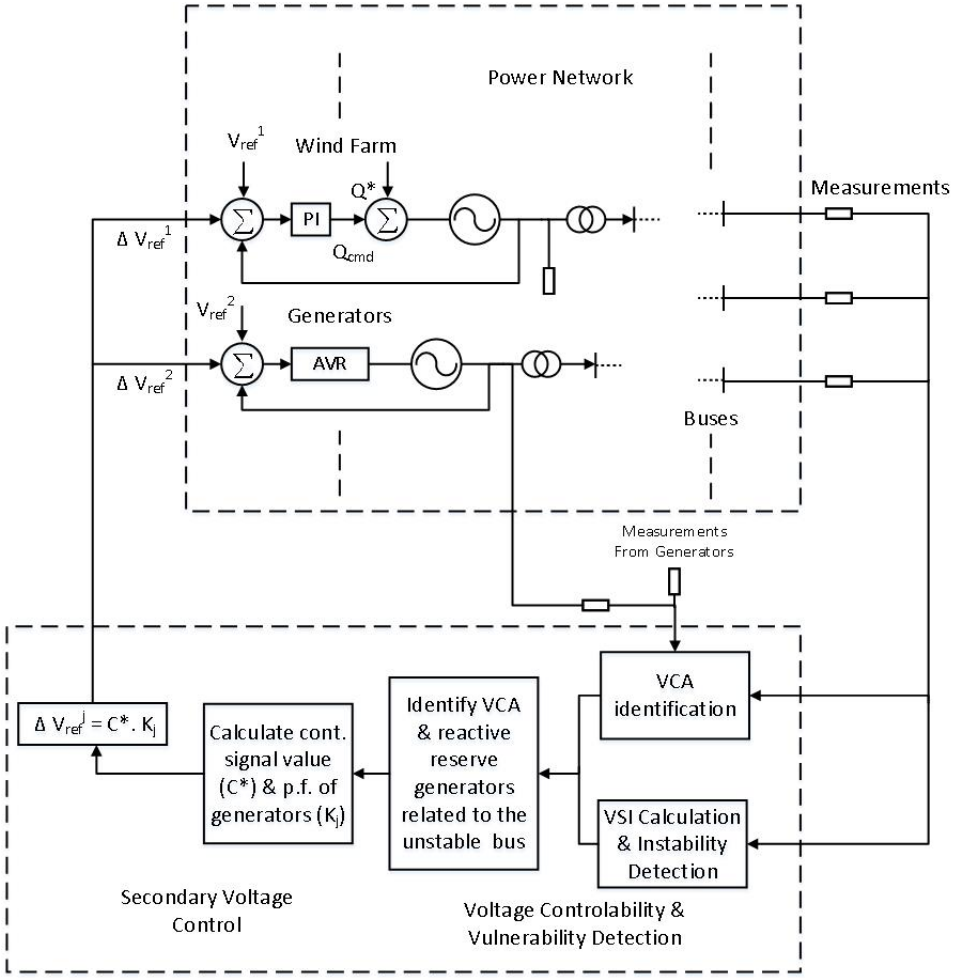

Figure 6.2: Organization of proposed voltage control concept

6.5 Voltage Control in IEEE 39 Bus System

The IEEE 10-machine 39 bus system is used to implement the proposed scheme of voltage control. The one-line diagram of the system is shown is Fig. 4.4 and identification of VCA for the base case is shown is Fig. 4.6. Load in the system is active power load. Here, load bus no. 21 is subjected to disturbance by increasing the load. Voltage monitoring of buses is conducted through measurement units like synchrophasor and VSI is calculated to check the violation and proximity to voltage collapse. The load change profile of bus 21 is shown in Fig. 6.3.

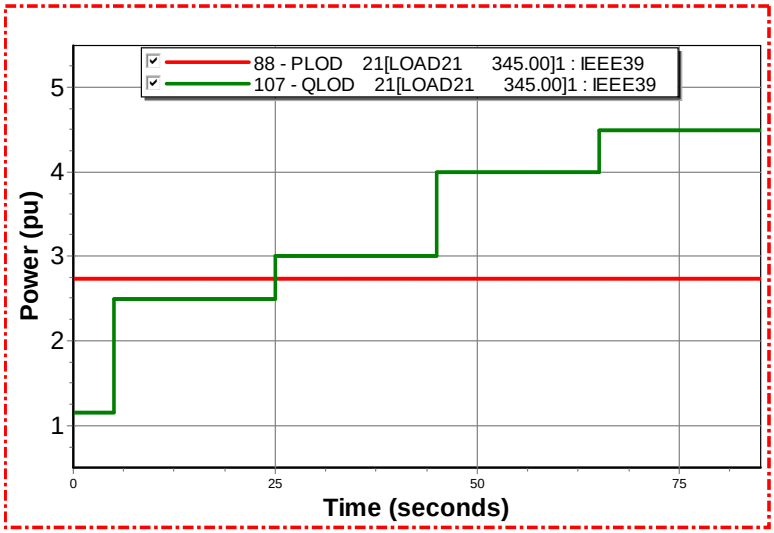

Figure 6.3: Load in bus 21

Corresponding voltage of bus 21 for load change is shown in Fig. 6.4.

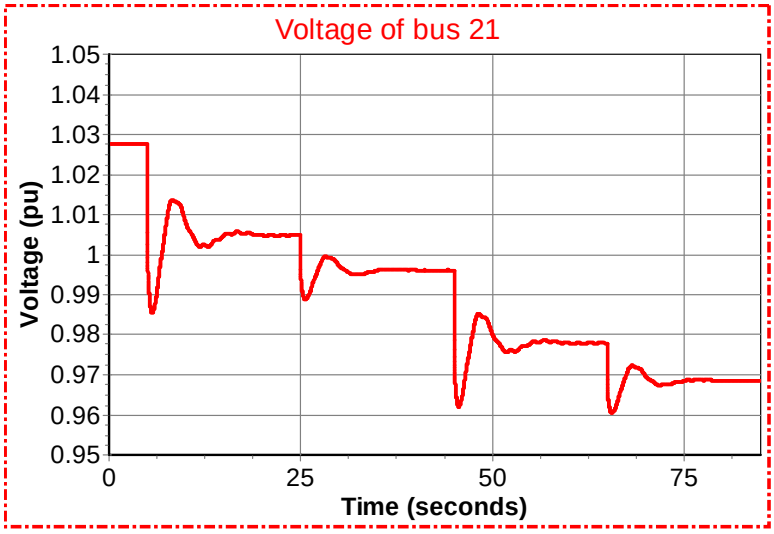

Figure 6.4: Voltage of bus 21

Similarly, voltage in other buses are shown in Fig. 6.5. Buses 15, 23 and 24 which are in the same VCA as that of bus 21 has higher voltage drop compared to buses 15 and 26.

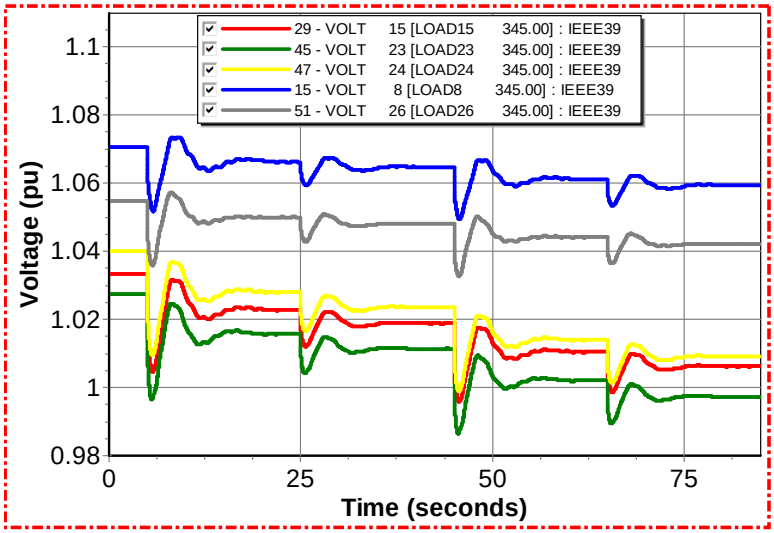

Figure 6.5: Voltage of surrounding bus of bus 21

The AVRs of generators are employed for the primary voltage control action. Reactive power generation increase to support terminal voltages by generators are shown in Fig. 6.6. The load increase disturbance in bus 21 is causing voltage drop not only in the surrounding buses but in other buses as well. But, the voltage drop in distant buses is of less magnitude. Generators 35 and 36 are reactive reserve generators. Hence, primary voltage control operated by AVR increases the reactive power generation for voltage control.

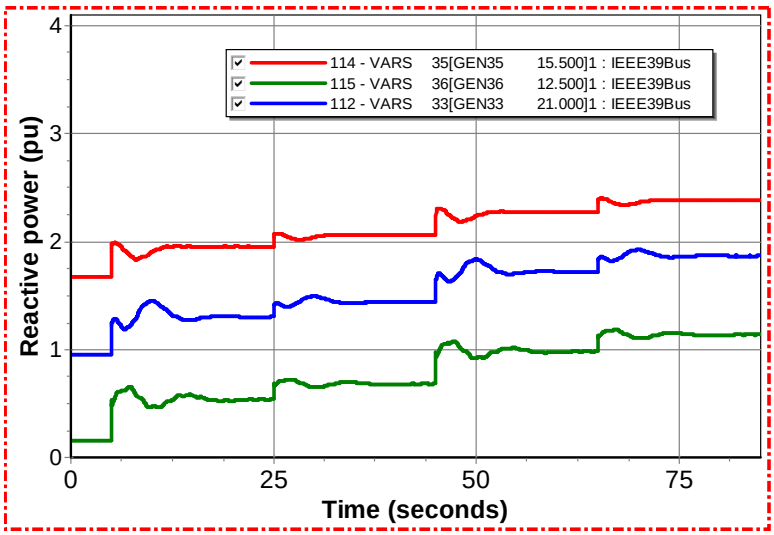

Figure 6.6: Reactive power of generators

The terminal voltages of generators are maintained to the reference voltage of AVR by the AVR primary control but as the load increases further the generators in VCA are not able to maintain the reference voltage as shown in Fig. 6.7. Generator 33 is not a reactive reserve generator which is able to maintain terminal voltage with the AVR action.

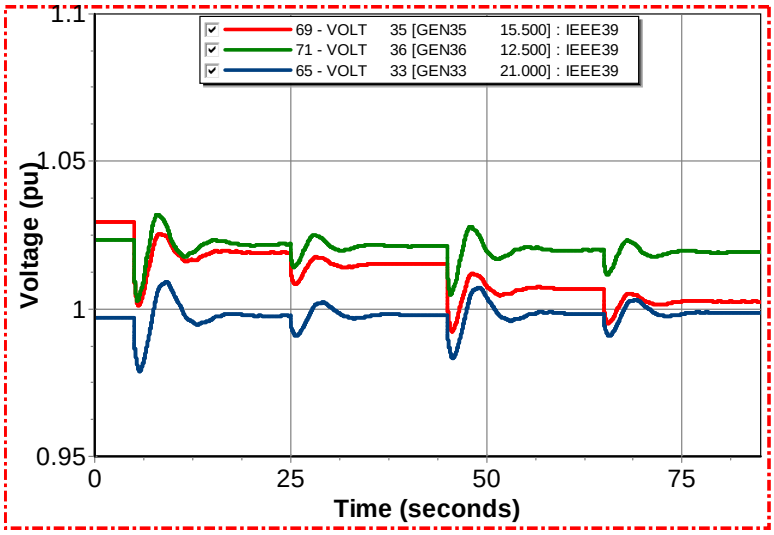

Figure 6.7: Terminal voltage of generators

The voltages of bus 21 and surrounding buses are decreasing as the reactive power load increases. The AVR of generators are not able to control the voltage with the fixed reference voltage. The monitoring of buses provide following VSI for load bus 21 and surrounding bus is shown in Fig. 6.8.

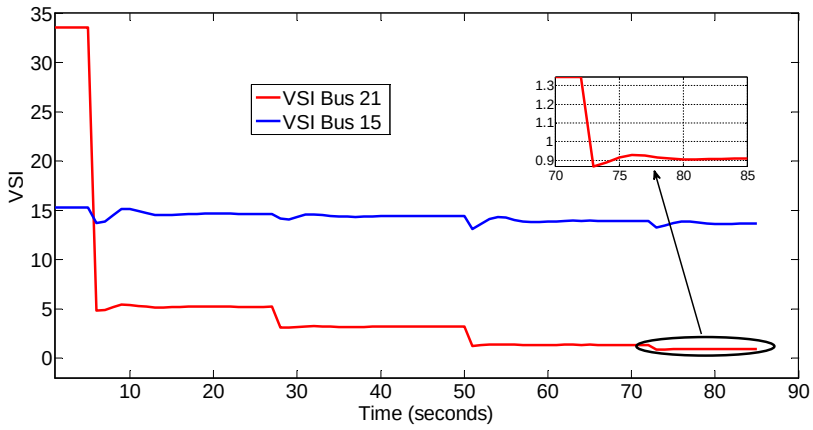

Figure 6.8: VSI of bus 21 during load disturbance

The VSI plot shows that the VSI of bus 21 gradually decreases as load increases and VSI drops below 1 when reactive power load is increased to 4.5 pu indicating that the bus is close to voltage instability. Once the bus passes the control criteria, secondary control is activated. The control signal is calculated with reference to base voltage and current voltage of bus 21. From Fig. 6.4 the base voltage value and current voltage are 1.028 pu and 0.969 pu respectively. Bus 21 belongs to VCA no IV with reactive reserve generators as generator buses 35 and 36. Since, the area contains only 2 generators for simplicity we assign equal participation factor of 1. The reference voltage of AVRs of generators are updated as given by (6.3). Secondary voltage control changes the reference votlag of AVR and forces generators to inject more reactive power the in VCA, which increases the voltage of buses in the area. The improvement in the voltage level of bus after secondary voltage control is shown in Fig. 6.9.

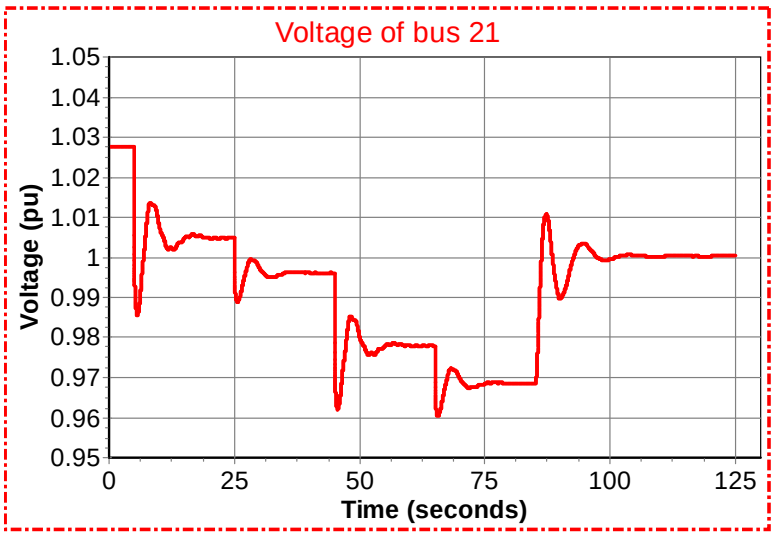

Figure 6.9: Voltage of bus 21 after voltage control

The voltage level of bus 21 is improved to 1.0 pu after secondary voltage control. The voltage vulnerability of the bus can be checked using VSI. The VSI value of bus 21 after secondary voltage control is shown in Fig 6.10. The VSI is greater than 1 which is above voltage instability zone.

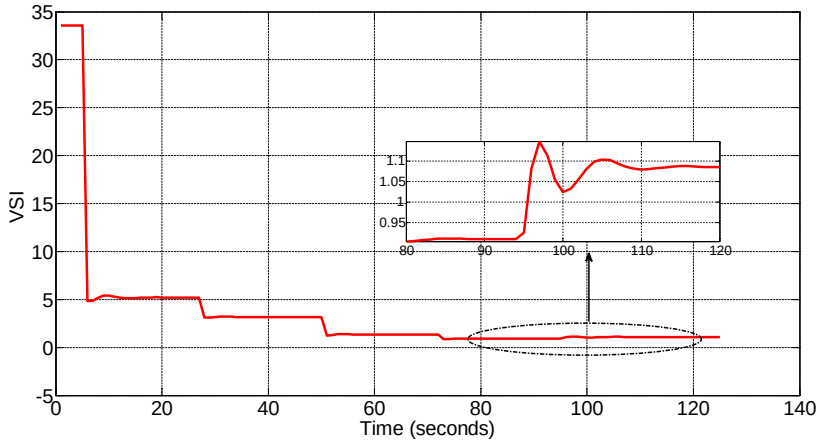

Figure 6.10: VSI of bus 21 during after voltage control

The reactive power generation of generators participating in secondary voltage control increases. The reactive power of generators after voltage control are shown in Fig. 6.11. The reactive power of reactive reserve generator that is generator 35

and 36 increases while the reactive power of other generators like generator 33 shown decreases as the total load remain constant and AVR reference points are unchanged.

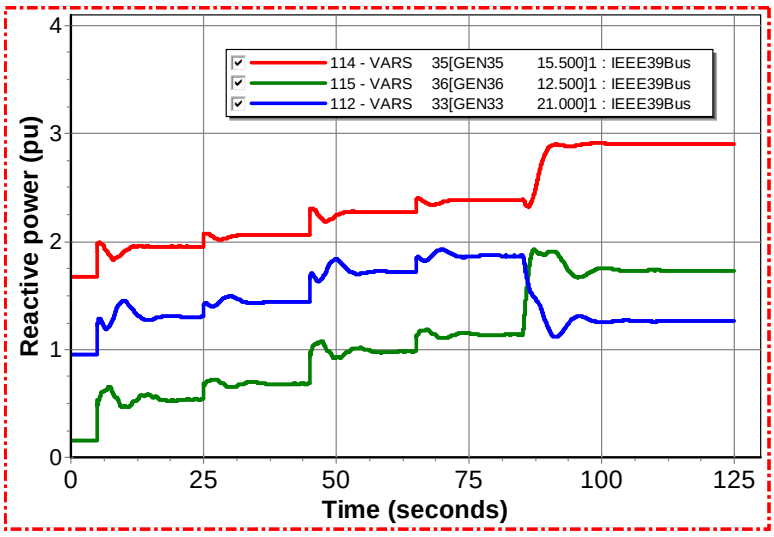

Figure 6.11: Reactive power generators after voltage control

The voltage of buses in the VCA and buses outside of VCA after the voltage control is shown in Fig 6.12.

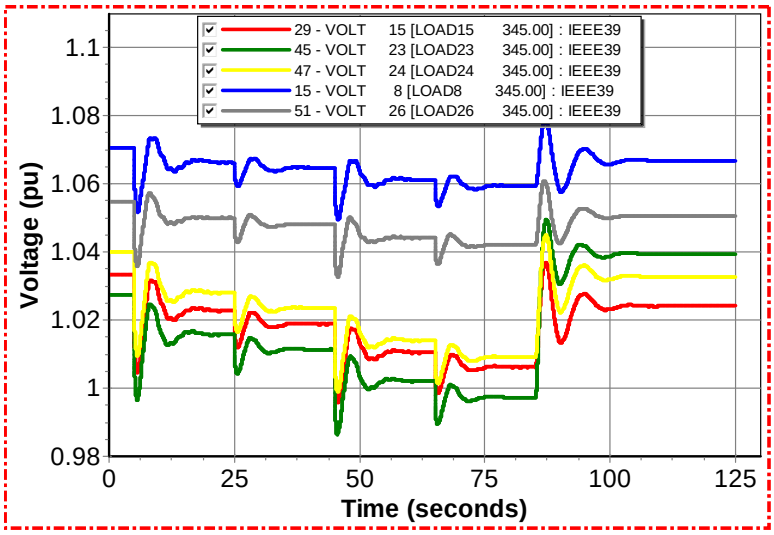

Figure 6.12: Bus voltages after voltage control action

The reactive power of generators in the VCA with secondary voltage control increases while other generators reactive power in the system are decreased as shown

in Fig 6.13. The reactive power of generator 32 is very high and have very negligible change so it is not shown in the plot. The voltage profile of the area and the system as whole is improved with secondary voltage profile.

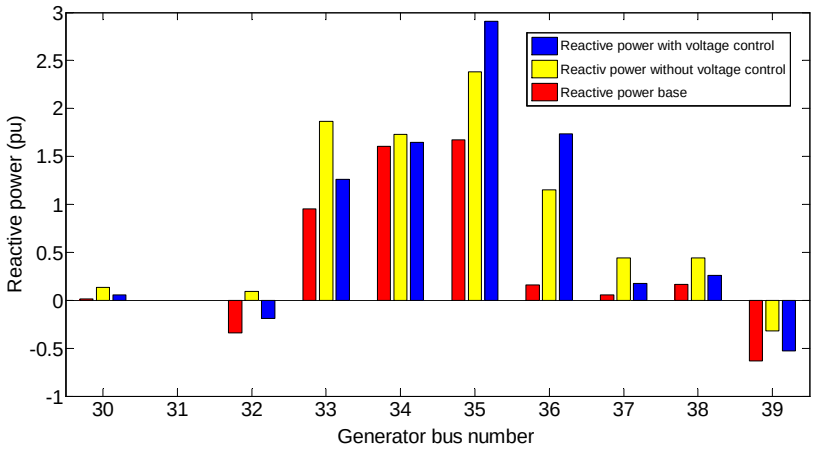

Figure 6.13: Generator reactive powers

6.6 Wind Integrated Power Grid

Wind integrated power grid is the power grid with wind farms injecting power to the system as a dispatcher source. A windfarm will typically include several wind turbine generators which are connected to each other though a collector bus. The collector bus is connected to grid at the point of common coupling (PCC). Typically, the wind farm is represented by a single suitably-sized equivalent interconnected to the grid at the point of interconnection. The response of the equivalent machine accurately describes the aggregate behavior of individual wind turbine generators with respect to the system at the interconnection point [40]. Here, the wind integrated power grid is formed by replacing generator 35 of IEEE 39 system with a wind generator. Generic wind farm model available in PSSE software is used for wind integrated power grid simulation [136]. A 670 units of 1.5MW wind generator type WT3G1 is clustered to provide power through collector bus. WT3E1 is the exciter used for terminal voltage control with reference voltage as a input. The dynamic data of wind generator and exciter along with generic drive train model and pitch control mode is provided in

Appendix A.

6.7 Voltage Control of Wind Integrated Power Grid

The modified IEEE 39 bus system consists of 9 conventional machines and 1 wind generator. All of the machine are controlled by exciters for primary voltage control to regulate terminal bus voltage. Since, the topology of the system is not changed even though the generator 25 is replaced by wind generator, the VCA classification will remain same. A in the above section, bus 21 is subjected to disturbance by increasing reactive power load. The load change profile of bus 21 is shown in Fig 6.14.

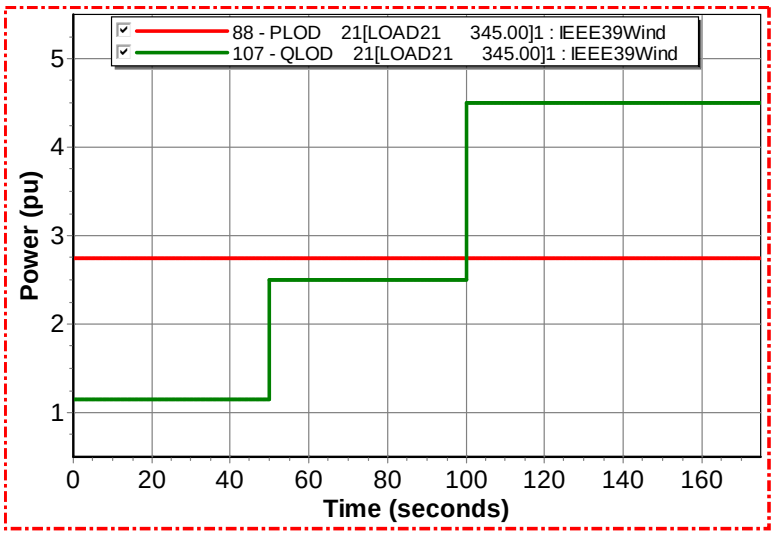

Figure 6.14: Load in bus 21

Corresponding voltage of bus 21 for the above load change is shown in Fig. 6.15.

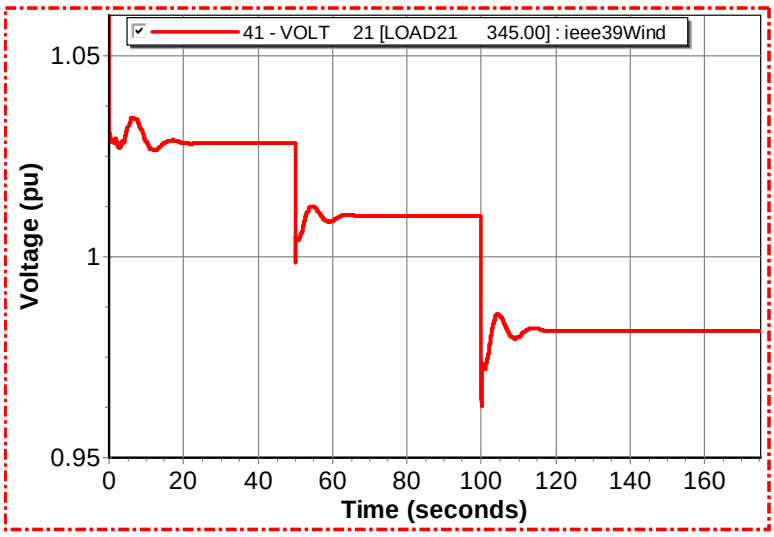

Figure 6.15: Voltage of bus 21

Similarly, voltage in other buses are shown in Fig. 6.16. Buses 15, 23 and 24 which are in the same VCA as that of bus 21 has higher voltage drop compared to buses 15 and 26.

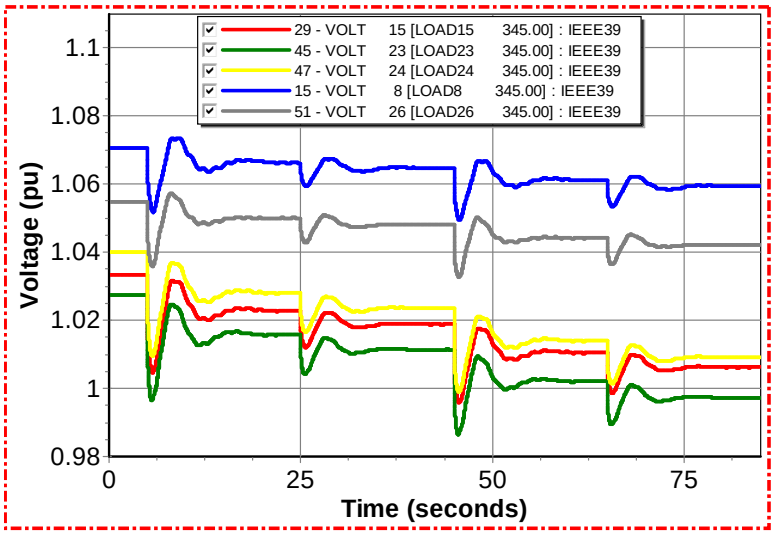

Figure 6.16: Voltage of surrounding bus of bus 21

The AVRs of generators and converter controller of wind generator sare employed for the primary voltage control action. Reactive power generation increase to regulate the reference terminal voltages of generators are shown in Fig. 6.17. The load increase in bus 21 is causing voltage drop not only in the surrounding buses but in other buses

as well. But, the voltage drop in distant buses are in less magnitude. Generators 35 and 36 are reactive reserve generators. Hence, primary voltage control operated by AVR and converter controller of wind generator results in the increase in the reactive power generation for voltage regulation.

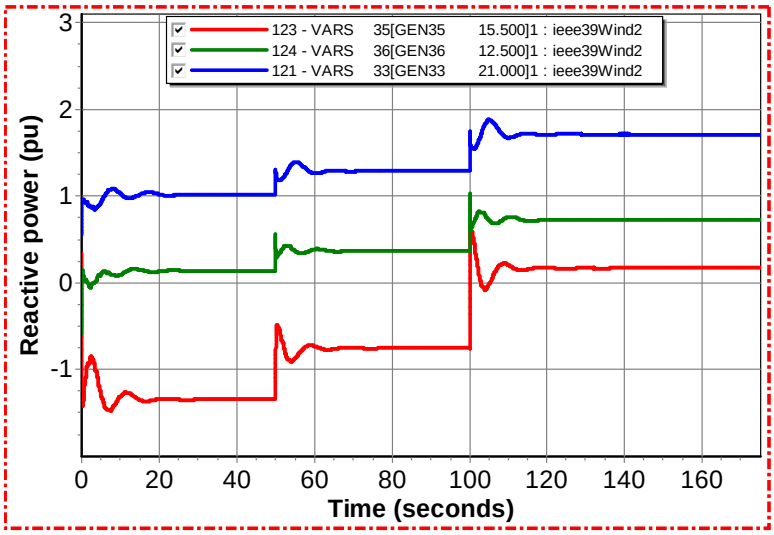

Figure 6.17: Reactive power of generators

The terminal voltages of generators are maintained to the reference voltage by the exciter and converter controller as a primary control as shown in Fig. 6.18.

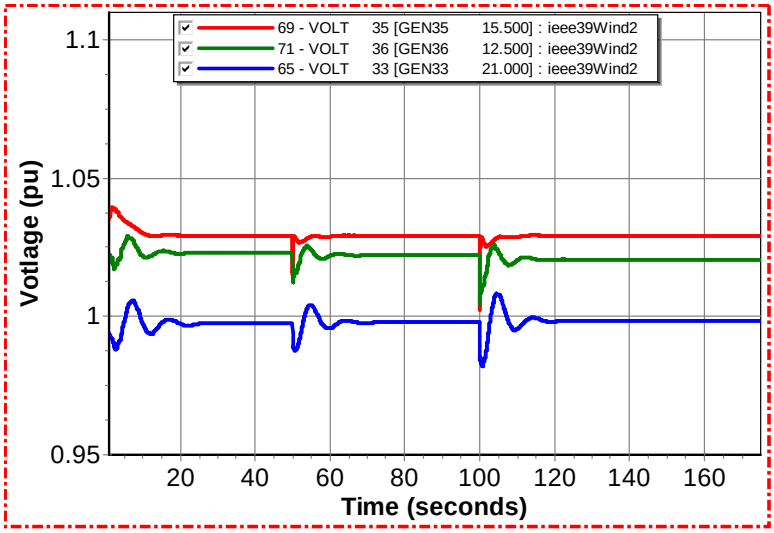

Figure 6.18: Terminal voltage of generators

The voltages of bus 21 and surrounding buses are decreasing as the reactive power

load increases. The reactive power and voltage regulation by exciters and converter controllers are not able to control the voltage with the fixed reference voltage. The monitoring of buses provide following VSI for load bus 21 and surrounding bus as shown in Fig. 6.19.

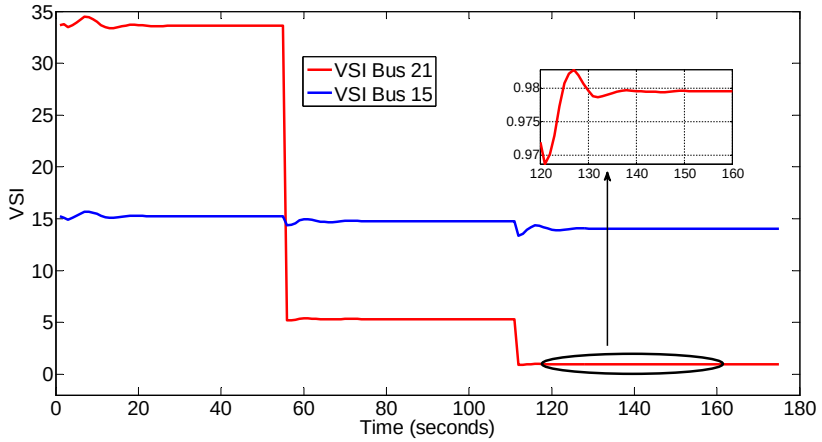

Figure 6.19: VSI of bus 21 during load disturbance

The VSI plot shows that the VSI of bus 21 gradually decreases as load increases and VSI drops below 1 when reactive power load is increased to 4.5 pu indicating that the bus is close to voltage instability. Once the bus passes the control criteria, secondary control is activated. The control signal is calculated with reference to base voltage and current voltage of bus 21. From Fig. 6.15 the base voltage value and current voltage are 1.064 pu and 0.982 pu respectively. Bus 21 belongs to VCA no IV with reactive reserve generators as generator buses 35 and 36. Since, the area contains only 2 generators for simplicity we assign equal participation factor of 0.5. The reference voltage of AVRs of generators are updated as given by (6.3). Secondary voltage control changes the reference votlag of AVR and forces generators to inject more reactive power the in VCA, which increases the voltage of buses in the area. The improvement in the voltage level of bus after secondary voltage control is shown in Fig. 6.20.

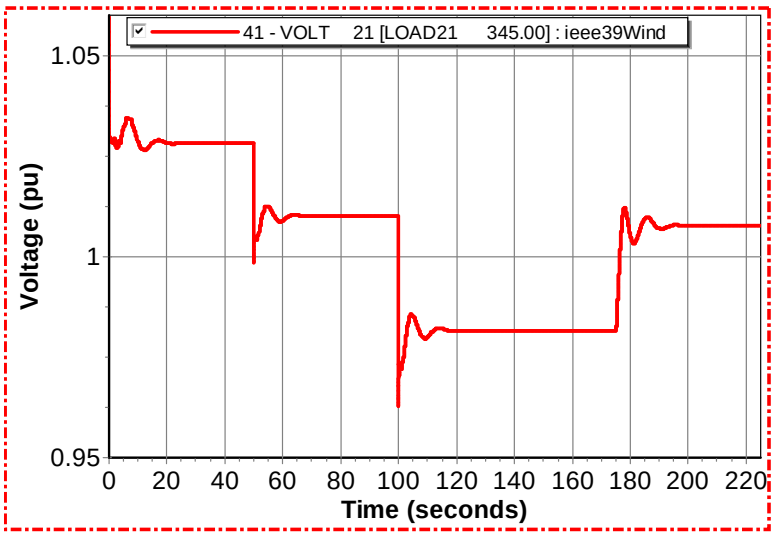

Figure 6.20: Voltage of bus 21 after voltage control

The voltage level of bus 21 is improved to 1.0 pu after secondary voltage control. The voltage vulnerability of the bus can be checked using VSI. The VSI value of bus 21 after secondary voltage control is shown in Fig 6.21. The VSI is greater than 1 which is above voltage instability zone.

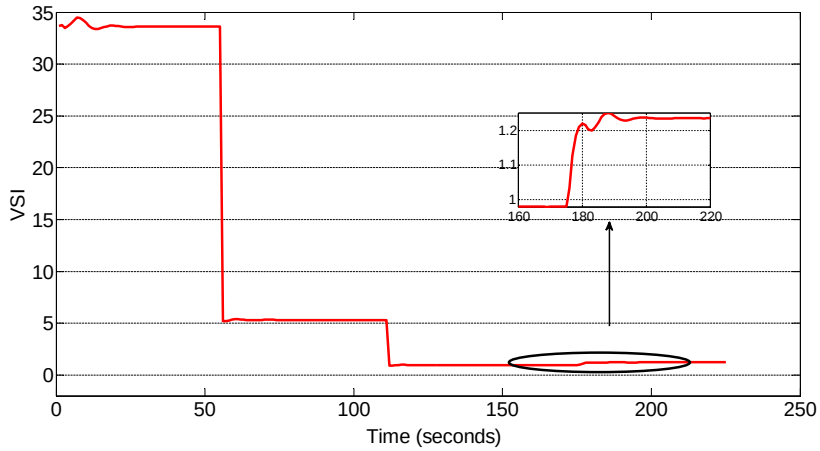

Figure 6.21: VSI of bus 21 during after voltage control

The reactive power generation of generators participating in secondary voltage control increases. The reactive power of generators after voltage control are shown in Fig. 6.22. The reactive power of reactive reserve generator that is generator 35

and 36 increases while the reactive power of other generators like generator 33 shown decreases as the total load remain constant and AVR reference points are unchanged.

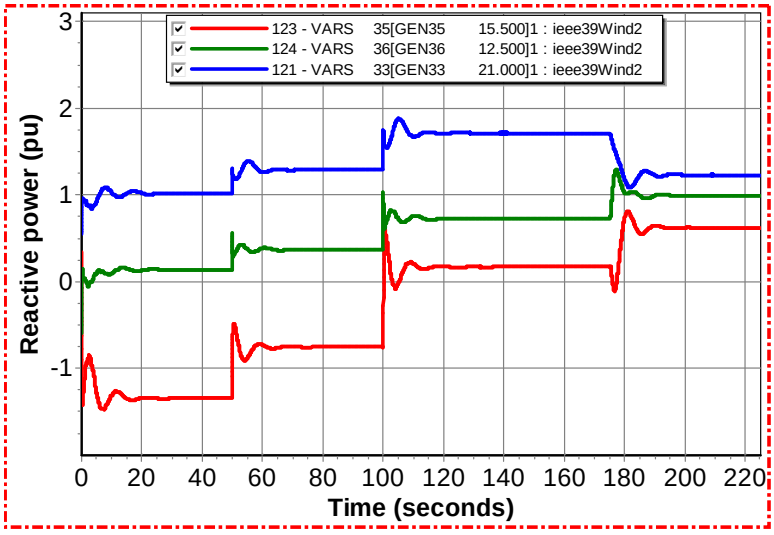

Figure 6.22: Reactive power generators after voltage control

The voltage of buses in the VCA and buses outside of VCA after the voltage control is shown in Fig 6.23.

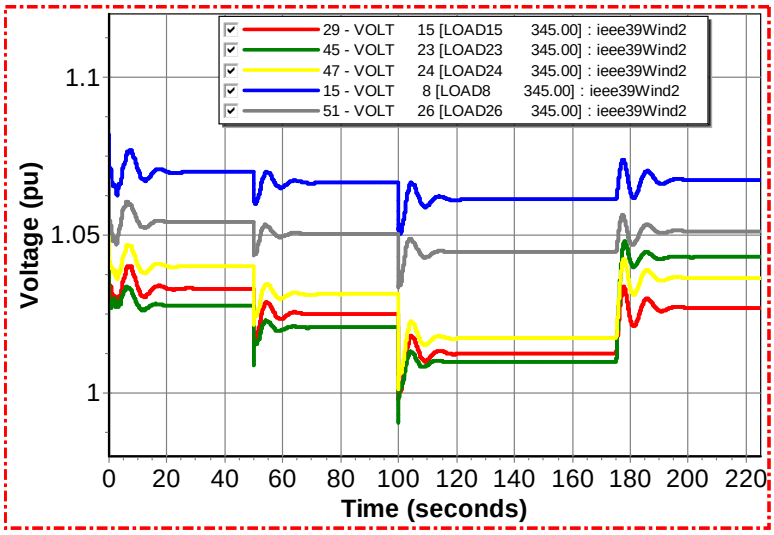

Figure 6.23: Bus voltages after voltage control action

6.8 Conclusion

The secondary voltage control of wind integrated power grid using VSI and VCA is proposed in this chapter. The control is achieved by updating setpoint of the reference voltage of a generator. The new setpoint is calculated using the control signal from the vulnerable bus and participation factor of the generator. The online identification of VCA is used to partition the grid into a number of regions and reflect the changes in the power grid topography in the VCAs. Vulnerability criterion for voltage control is determined by monitoring VSI of a bus. The proposed control scheme effectively improves the voltage level and prevents from voltage instability with a reactive power support from the reactive reserve generators of VCA belonging to the vulnerable bus.

CHAPTER 7: CONCLUSIONS

7.1 Introduction

This chapter summarizes the research conducted in this dissertation and presents the concluding remarks. The main contributions of this work are listed and several opportunities for future research are suggested.

7.2 Concluding Remarks

This dissertation is focused on the secondary control of wind integrated power system to prevent it from voltage instability by using voltage controllability and vulnerability detection. Secondary voltage control scheme is used to regulate the voltage in a control area. The adaptive control area is identified using online clustering method based on reactive power sensitivities. The reactive power sensitivities provide a direct relation between load and generator reactive power. K-means clustering is used to cluster the sensitivities and the system is divided into control areas. Each control area will have buses with common voltage characteristics. The effectiveness of identification of VCAs by the proposed method is validated through dynamic simulation studies and comparisons with other identification methods as shown in Chapters 4 and 5. Vulnerability studies of bus voltage are performed by online monitoring of buses and the criteria for the vulnerability is established by proposed VSI. The proposed VSI is based on the maximum loading capability and can be calculated with simple measurement of states at each power system bus. The VSI represents bus vulnerability in a scalar form. The effectiveness of the index is illustrated in Chapter 3. Voltage control of a power grid based on the control area and VSI is proposed in Chapter 6. A simple approach based on participation factor is used to update the

reference of exciter or converter controller for voltage regulation. The effectiveness of proposed method to regulate the voltage in a conventional power grid and a wind integrated power grid is illustrated with the simulation results in IEEE test systems. The capability of a wind generator to participate in reactive power and voltage control of a given area using the secondary voltage control scheme is also presented. The VCA partitioning of the system helped to identify a range of a generator for voltage control without additional reactive power sources.

7.3 Summary of Research Contributions

The main contributions of this thesis are summarized below:

- Formulation of simple voltage stability index based on maximum power loading. The VSI is a scalar measure that predicts the proximity of bus to the voltage collapse. Since, the proposed index can be calculated using system measurements and employs fast Thevenin method, the method can be used for online bus monitoring for secondary voltage regulation. The effectiveness of the index as voltage vulnerability criteria is shown with simulation results. Further, it can be an effective tool for voltage stability assessment.

- A novel identification method of voltage control area based on reactive power sensitivities is formulated. A simple yet direct relationship between consumer and supplier of reactive power provided a good criteria to divide a system for voltage and reactive power control. Only general information of systems as a requirement and direct approach for sensitivity calculation along with clustering technique allows the operator to use this tool for online application. This is a big step that can be used in modern power grid compared to the current state-of-the-art which uses conventional offline methods.

- A secondary voltage control scheme is proposed. The secondary voltage control is based on the voltage controllability and vulnerability detection for smooth

operation of power grid and prevention from voltage collapse leading to blackouts. The function of reactive reserve generator is extended beyond the terminal voltage regulation and is used for voltage control of a area to prevent voltage collapse without switching the other additional reactive power sources. The capability of wind generator for voltage control of system using voltage control area is presented.

7.4 Future Work

Several suggestions and considerations for future research work are listed below.

1. In this research, an index is calculated using the maximum loadability by reducing a system to Thevenin equivalent. Though fast method of Thevenin equivalent is used based on required calculation of impedance matrix the method could be modified to make it faster. An alternative method of Thevenin equivalent calculation with iterative methods should be considered.

2. The proposed identification method of VCAs based on reactive power sensitivities considers the reactive power of generators only. Fixed shunt devices and even switched shunt can be included in the formulation of VCA.

3. For secondary voltage control simple approach based on participation factor for variation of exciter or converter controller reference in used. An adaptive approach or an outer controller can be formulated to control reference values.

4. The proposed control scheme is limited to small disturbance only. It can be extended to various other small disturbances including active power and large disturbance as well. The large disturbances will be better validation for voltage vulnerability test using VSI.

5. Voltage control of an area is proposed without considering any optimization. An optimal control approach can be introduced with additional shunt and FACTS

devices.

6. The wind integrated power grid is shown with a signal wind generator. The grid can be expanded with high wind penetration with numerous wind generators in a control area as well as outside of the control area. Further, wind farm types can be varied and their controllability which varies with reactive power capability and converter types can be studied.

REFERENCES

[1] J. W. Simpson-Porco, F. Dorfler, and F. Bullo, "Voltage collapse in complex power grids," *Nature Communications*, vol. 10790, no. doi:10.1038/ncomms10790, February 2016.

[2] C. D. Brummitt, P. D. H. Hines, I. Dobson, C. Moore, and R. M. D'Souza, "Transdisciplinary electric power grid science," *Proceedings of the National Academy of Sciences*, vol. 110, no. 30, p. 12159, 2013.

[3] J. H. Eto, M. Parashar, B. C. Lesieutre, and N. J. Lewis, "California iso real time voltage security assessment (vsa) summary report (real-time grid reliability management pier final project report appendix b)," p. 50, 10/2008 2008.

[4] S. Lindahl, "Case studies of recent blackouts," in *CRIS International Workshop on Power System Blackouts Causes, Analyses, and Countermeasures , Lund, Sweden*, May 2004.

[5] Final Report on the August 14, 2003 Blackout in the United States and Canada: Causes and Recommendations, U.S. Canada Power System Outage Task Force, April 5, 2004.

[6] Power failure in Eastern Denmark and Southern Sweden on 23 September 2003, Final report on the course of events, Ekraft System, November 4, 2003.

[7] Technical Summary on the Athens and Southern Greece Blackout of July 12,2004.

[8] *Report on failure inquiry in UES of Russia that took place at May 25,2005 in Russian.*

[9] Report on the grid disturbance on 30th July 2012 and grid disturbance on 31st July 2012.

[10] T. van Cutsem and C. Vournas, *Voltage Stability of Electric Power Systems*. Springer US, 1998.

[11] K. Vu, M. Begovic, D. Novosel, and M. Saha, "Use of local measurements to estimate voltage-stability margin," *Power Systems, IEEE Transactions on*, vol. 14, no. 3, pp. 1029–1035, Aug 1999.

[12] D. E. Julian, R. Schulz, K. T. Vu, W. Quaintance, N. Bhatt, and D. Novosel, "Quantifying proximity to voltage collapse using the voltage instability predictor (vip)," in *Power Engineering Society Summer Meeting, 2000. IEEE*, vol. 2, 2000, pp. 931–936 vol. 2.

[13] I. Smon, G. Verbic, and F. Gubina, "Local voltage-stability index using tellegen's theorem," *Power Systems, IEEE Transactions on*, vol. 21, no. 3, pp. 1267–1275, Aug 2006.

[14] M. Glavic and T. V. Cutsem, "A short survey of methods for voltage instability detection," in *2011 IEEE Power and Energy Society General Meeting*, July 2011, pp. 1–8.

[15] P. Kessel and H. Glavitsch, "Estimating the voltage stability of a power system," *Power Delivery, IEEE Transactions on*, vol. 1, no. 3, pp. 346–354, July 1986.

[16] M. Haque, "A fast method for determining the voltage stability limit of a power system," *Electric Power Systems Research*, vol. 32, no. 1, pp. 35 – 43, 1995.

[17] H. Liu, A. Bose, and V. Venkatasubramanian, "A fast voltage security assessment method using adaptive bounding," *Power Systems, IEEE Transactions on*, vol. 15, no. 3, pp. 1137–1141, Aug 2000.

[18] R. Schlueter, I.-P. Hu, M. Chang, J. Lo, and A. Costi, "Methods for determining proximity to voltage collapse," *Power Systems, IEEE Transactions on*, vol. 6, no. 1, pp. 285–292, Feb 1991.

[19] R. Schlueter, "A voltage stability security assessment method," *Power Systems, IEEE Transactions on*, vol. 13, no. 4, pp. 1423–1438, Nov 1998.

[20] P. Lagonotte, J.-C. Sabonnadiere, J. Leost, and J. Paul, "Structural analysis of the electrical system: application to secondary voltage control in france," *Power Systems, IEEE Transactions on*, vol. 4, no. 2, pp. 479–486, May 1989.

[21] H. Sun, Q. Guo, B. Zhang, W. Wu, and B. Wang, "An adaptive zone-division-based automatic voltage control system with applications in china," *IEEE Transactions on Power Systems*, vol. 28, no. 2, pp. 1816–1828, May 2013.

[22] T. V. Cutsem, "Voltage instability: phenomena, countermeasures, and analysis methods," *Proceedings of the IEEE*, vol. 88, no. 2, pp. 208–227, Feb 2000.

[23] S. Corsi, P. Marannino, N. Losignore, G. Moreschini, and G. Piccini, "Coordination between the reactive power scheduling function and the hierarchical voltage control of the ehv enel system," *IEEE Transactions on Power Systems*, vol. 10, no. 2, pp. 686–694, May 1995.

[24] M. D. Ilic, X. Liu, G. Leung, M. Athans, C. Vialas, and P. Pruvot, "Improved secondary and new tertiary voltage control," *IEEE Transactions on Power Systems*, vol. 10, no. 4, pp. 1851–1862, Nov 1995.

[25] V. Venkatasubramanian, J. Guerrero, J. Su, H. Chun, X. Zhang, F. Habibi-Ashrafi, A. Salazar, and B. Abu-Jaradeh, "Hierarchical two-level voltage controller for large power systems," *IEEE Transactions on Power Systems*, vol. 31, no. 1, pp. 397–411, Jan 2016.

[26] H. Vu, P. Pruvot, C. Launay, and Y. Harmand, "An improved voltage control on large-scale power system," *IEEE Transactions on Power Systems*, vol. 11, no. 3, pp. 1295–1303, Aug 1996.

[27] J. P. Paul, J. Y. Leost, and J. M. Tesseron, "Survey of the secondary voltage control in france : Present realization and investigations," *IEEE Transactions on Power Systems*, vol. 2, no. 2, pp. 505–511, May 1987.

[28] J. V. Hecke, N. Janssens, J. Deuse, and G. F. Promel, "Coordinated voltage control experience in belgium," in *CIGRE Session 2000 Paris France*, 2000.

[29] V. Arcidiacono, "Automatic voltage and reactive power control in transmission systems," in *IFAC Symp. on Power Systems, Florence*, 1983.

[30] J. L. Sancha, J. L. Fernandez, A. Cortes, and J. T. Abarca, "Secondary voltage control: analysis, solutions and simulation results for the spanish transmission system," in *Power Industry Computer Application Conference, 1995. Conference Proceedings., 1995 IEEE*, May 1995, pp. 27–32.

[31] Heier, S., *Grid Integration of Wind Energy Conversion Systems*. John Wiley and Sons, 2006.

[32] AWEA U.S. Wind Industry Second Quarter 2015 Market Report.

[33] 20Electricity Supply, DOE Report, DOE/GO-102008-2567, July 2008.

[34] FERC-Interconnection of Wind Energy, 18 CFR Part 35, Docket No. RM05-4-001;Order No. 661-A December 12, 2005.

[35] M. Tsili and S. Papathanassiou, "A review of grid code technical requirements for wind farms," *IET Renewable Power Generation*, vol. 3, no. 3, pp. 308–332, Sept 2009.

[36] MATLAB, MathWorks.

[37] PSS/E, Siemens.

[38] P. Kundur, J. Paserba, V. Ajjarapu, G. Andersson, A. Bose, C. Canizares, N. Hatziargyriou, D. Hill, A. Stankovic, C. Taylor, T. V. Cutsem, and V. Vittal, "Definition and classification of power system stability ieee/cigre joint task force on stability terms and definitions," *IEEE Transactions on Power Systems*, vol. 19, no. 3, pp. 1387–1401, Aug 2004.

[39] C. Canizares, "Voltage stability assessment : concepts, practices and tools," Special Publication of IEEE Power System Stability Subcommittee, C. Canizares (editor/coordinator), Tech. Rep., 2002.

[40] Venkataramana Ajjarapu, *Computational Techniques for Voltage Stability Assessment and Control*. Springer US, 2006.

[41] P. Kundur, *Power System Stability and Control*. McGraw-Hill, 1994.

[42] B. Gao, G. K. Morison, and P. Kundur, "Voltage stability evaluation using modal analysis," *Power Systems, IEEE Transactions on*, vol. 7, no. 4, pp. 1529–1542, Nov 1992.

[43] N. Flatabo, R. Ognedal, and T. Carlsen, "Voltage stability condition in a power transmission system calculated by sensitivity methods," *Power Systems, IEEE Transactions on*, vol. 5, no. 4, pp. 1286–1293, Nov 1990.

[44] A. Berizzi, P. Finazzi, D. Dosi, P. Marannino, and S. Corsi, "First and second order methods for voltage collapse assessment and security enhancement," *Power Systems, IEEE Transactions on*, vol. 13, no. 2, pp. 543–551, May 1998.

[45] A. de Souza, C. Canizares, and V. Quintana, "New techniques to speed up voltage collapse computations using tangent vectors," *Power Systems, IEEE Transactions on*, vol. 12, no. 3, pp. 1380–1387, Aug 1997.

[46] N. Hatziargyriou and T. Van Cutsem, "Indices predicting voltage collapse including dynamic phenomena," 1994.

[47] M. V. Suganyadevia and C. Babulal, "Estimating of loadability margin of a power system by comparing voltage stability indices," in *Control, Automation, Communication and Energy Conservation, 2009. INCACEC 2009. 2009 International Conference on*, June 2009, pp. 1–4.

[48] M. H. Haque, "Use of local information to determine the distance to voltage collapse," in *Power Engineering Conference, 2007. IPEC 2007. International*, Dec 2007, pp. 407–412.

[49] M. Moghavvemi and G. Jasmon, "New method for indicating voltage stability in power system," in *IEEE International Conference on Power Engineering*, 1997, pp. 223–227.

[50] A. Mohamed, G. Jasmon, and S. Yusoff, "A static voltage collapse indicator using line stability factors," *Journal of industrial technology*, vol. 7, no. 1, pp. 73–85, 1989.

[51] I. Musirin and T. K. A. Rahman, "Novel fast voltage stability index (fvsi) for voltage stability analysis in power transmission system," in *Research and Development, 2002. SCOReD 2002. Student Conference on*, 2002, pp. 265–268.

[52] M. Moghavvemi and O. Faruque, "Real-time contingency evaluation and ranking technique," *Generation, Transmission and Distribution, IEE Proceedings-*, vol. 145, no. 5, pp. 517–524, Sep 1998.

[53] B. Leonardi and V. Ajjarapu, "An approach for real time voltage stability margin control via reactive power reserve sensitivities," *Power Systems, IEEE Transactions on*, vol. 28, no. 2, pp. 615–625, May 2013.

[54] L. Bao, Z. Huang, and W. Xu, "Online voltage stability monitoring using var reserves," *Power Systems, IEEE Transactions on*, vol. 18, no. 4, pp. 1461–1469, Nov 2003.

[55] A. de Souza, J. C. S. De Souza, and A. Leite da Silva, "On-line voltage stability monitoring," *Power Systems, IEEE Transactions on*, vol. 15, no. 4, pp. 1300–1305, Nov 2000.

[56] M. Glavic and T. Van Cutsem, "Wide-area detection of voltage instability from synchronized phasor measurements. part i: Principle," *Power Systems, IEEE Transactions on*, vol. 24, no. 3, pp. 1408–1416, Aug 2009.

[57] K. Vu, M. Begovic, D. Novosel, and M. Saha, "Use of local measurements to estimate voltage-stability margin," *Power Systems, IEEE Transactions on*, vol. 14, no. 3, pp. 1029–1035, Aug 1999.

[58] L. Fu, B. Pal, and B. Cory, "Phasor measurement application for power system voltage stability monitoring," in *Power and Energy Society General Meeting - Conversion and Delivery of Electrical Energy in the 21st Century, 2008 IEEE*, July 2008, pp. 1–8.

[59] M. H. Haque, "Use of v-i characteristic as a tool to assess the static voltage stability limit of a power system," *Generation, Transmission and Distribution, IEE Proceedings-*, vol. 151, no. 1, pp. 1–7, Jan 2004.

[60] M. Zima, M. Larsson, P. Korba, C. Rehtanz, and G. Andersson, "Design aspects for wide-area monitoring and control systems," *Proceedings of the IEEE*, vol. 93, no. 5, pp. 980–996, May 2005.

[61] W. Li, Y. Wang, and T. Chen, "Investigation on the thevenin equivalent parameters for online estimation of maximum power transfer limits," *Generation, Transmission Distribution, IET*, vol. 4, no. 10, pp. 1180–1187, October 2010.

[62] B. Milosevic and M. Begovic, "Voltage-stability protection and control using a wide-area network of phasor measurements," *Power Systems, IEEE Transactions on*, vol. 18, no. 1, pp. 121–127, Feb 2003.

[63] G. Verbic and F. Gubina, "Fast algorithm for voltage collapse protection based on local phasors," in *Power Engineering Society Summer Meeting, 2002 IEEE*, vol. 3, July 2002, pp. 1650–1655 vol.3.

[64] ——, "A new concept of voltage-collapse protection based on local phasors," *Power Delivery, IEEE Transactions on*, vol. 19, no. 2, pp. 576–581, April 2004.

[65] B. Genet and J.-C. Maun, "Voltage-stability monitoring using wide-area measurement systems," in *Power Tech, 2007 IEEE Lausanne*, July 2007, pp. 1712–1717.

[66] V. Balamourougan, T. Sidhu, and M. Sachdev, "Technique for online prediction of voltage collapse," *Generation, Transmission and Distribution, IEE Proceedings-*, vol. 151, no. 4, pp. 453–460, July 2004.

[67] Y. Gong, N. Schulz, and A. Guzman, "Synchrophasor-based real-time voltage stability index," in *Power Systems Conference and Exposition, 2006. PSCE '06. 2006 IEEE PES*, Oct 2006, pp. 1029–1036.

[68] V. A. Venikov, V. Stroev, V. I. Idelchick, and V. I. Tarasov, "Estimation of electrical power system steady-state stability in load flow calculations," *Power Apparatus and Systems, IEEE Transactions on*, vol. 94, no. 3, pp. 1034–1041, May 1975.

[69] P. Lof, G. Andersson, and D. Hill, "Voltage stability indices for stressed power systems," *Power Systems, IEEE Transactions on*, vol. 8, no. 1, pp. 326–335, Feb 1993.

[70] A. Sinha and D. Hazarika, "A comparative study of voltage stability indices in a power system," vol. 22, no. 8, pp. 589–596, Feb 2000.

[71] V. Balamourougan, T. Sidhu, and M. Sachdev, "Technique for online prediction of voltage collapse," *Generation, Transmission and Distribution, IEE Proceedings-*, vol. 151, no. 4, pp. 453–460, July 2004.

[72] Y. Tamura, H. Mori, and S. Iwamoto, "Relationship between voltage instability and multiple load flow solutions in electric power systems," *Power Apparatus and Systems, IEEE Transactions on*, vol. PAS-102, no. 5, pp. 1115–1125, May 1983.

[73] O. Crisan and M. Liu, "Voltage collapse prediction using an improved sensitivity approach," *Electric Power Systems Research*, vol. 28, no. 3, pp. 181 – 190, 1994.

[74] B. Avramovic and L. Fink, "Real-time reactive security monitoring," *Power Systems, IEEE Transactions on*, vol. 7, no. 1, pp. 432–437, Feb 1992.

[75] R. Schlueter, I.-P. Hu, M. W. Chang, J. C. Lo, and A. Costi, "Methods for determining proximity to voltage collapse," *Power Systems, IEEE Transactions on*, vol. 6, no. 1, pp. 285–292, Feb 1991.

[76] T. Lie, R. Schlueter, P. Rusche, and R. Rhoades, "Method of identifying weak transmission network stability boundaries," *Power Systems, IEEE Transactions on*, vol. 8, no. 1, pp. 293–301, Feb 1993.

[77] P. Vijayan, S. Sarkar, and V. Ajjarapu, "A novel voltage stability assessment tool to incorporate wind variability," in *Power Energy Society General Meeting, 2009. PES '09. IEEE*, July 2009, pp. 1–8.

[78] E. Vittal, M. O'Malley, and A. Keane, "A steady-state voltage stability analysis of power systems with high penetrations of wind," *Power Systems, IEEE Transactions on*, vol. 25, no. 1, pp. 433–442, Feb 2010.

[79] A. Tamimi, A. Pahwa, and S. Starrett, "Effective wind farm sizing method for weak power systems using critical modes of voltage instability," *Power Systems, IEEE Transactions on*, vol. 27, no. 3, pp. 1610–1617, Aug 2012.

[80] C. Zheng and M. Kezunovic, "Impact of wind generation uncertainty on power system small disturbance voltage stability: A pcm-based approach," *Electric Power Systems Research*, vol. 84, no. 1, pp. 10 – 19, 2012.

[81] R. Pena, J. Clare, and G. Asher, "Doubly fed induction generator using back-to-back pwm converters and its application to variable-speed wind-energy generation," *Electric Power Applications, IEE Proceedings* -, vol. 143, no. 3, pp. 231–241, 1996.

[82] Vijay Vittal,Raja Ayyanar, *Grid Integration and Dynamic Impact of Wind Energy.* Springer-Verlag New York, 2013.

[83] C. Reis and F. Barbosa, "A comparison of voltage stability indices," in *Electrotechnical Conference, 2006. MELECON 2006. IEEE Mediterranean*, May 2006, pp. 1007–1010.

[84] B. Singh and S. N. Singh, "Voltage stability assessment of grid-connected offshore wind farms," *Wind Energy*, vol. 12, no. 2, pp. 157–169, 2009.

[85] C. Zheng and M. Kezunovic, "Distribution system voltage stability analysis with wind farms integration," in *North American Power Symposium (NAPS), 2010*, Sept 2010, pp. 1–6.

[86] V. Ajjarapu and C. Christy, "The continuation power flow: a tool for steady state voltage stability analysis," *Power Systems, IEEE Transactions on*, vol. 7, no. 1, pp. 416–423, Feb 1992.

[87] A. Chebbo, M. Irving, and M. Sterling, "Voltage collapse proximity indicator: behaviour and implications," *Generation, Transmission and Distribution, IEE Proceedings C*, vol. 139, no. 3, pp. 241–252, May 1992.

[88] B. Venkatesh, R. Ranjan, and H. Gooi, "Optimal reconfiguration of radial distribution systems to maximize loadability," *Power Systems, IEEE Transactions on*, vol. 19, no. 1, pp. 260–266, Feb 2004.

[89] M. A. Pai , *Energy Function Analysis for Power System Stability.* Springer US, 1989.

[90] A. Augugliaro, L. Dusonchet, and S. Mangione, "Voltage collapse proximity indicators for radial distribution networks," in *Electrical Power Quality and Utilisation, 2007. EPQU 2007. 9th International Conference on*, Oct 2007, pp. 1–6.

[91] T. Lie, R. A. Schlueter, P. A. E. Rusche, and R. H. Rhoades, "Method of identifying weak transmission network stability boundaries," *IEEE Transactions on Power Systems*, vol. 8, no. 1, pp. 293–301, Feb 1993.

[92] J. Zhong, E. Nobile, A. Bose, and K. Bhattacharya, "Localized reactive power markets using the concept of voltage control areas," *Power Systems, IEEE Transactions on*, vol. 19, no. 3, pp. 1555–1561, Aug 2004.

[93] M. Verma and S. Srivastava, "Approach to determine voltage control areas considering impact of contingencies," *IEE Proceedings - Generation, Transmission and Distribution*, vol. 152, pp. 342–350(8), May 2005.

[94] W. Villa, J. Rueda, S. Torres, and W. Peralta, "Identification of voltage control areas in power systems with large scale wind power integration," in *Transmission and Distribution: Latin America Conference and Exposition (T D-LA), 2012 Sixth IEEE/PES*, Sept 2012, pp. 1–7.

[95] C. Aumuller and T. Saha, "Determination of power system coherent bus groups by novel sensitivity-based method for voltage stability assessment," *Power Systems, IEEE Transactions on*, vol. 18, no. 3, pp. 1157–1164, Aug 2003.

[96] K. Morison, X. Wang, A. Moshref, and A. Edris, "Identification of voltage control areas and reactive power reserve; an advancement in on-line voltage security assessment," in *Power and Energy Society General Meeting - Conversion and Delivery of Electrical Energy in the 21st Century, 2008 IEEE*, July 2008, pp. 1–7.

[97] R. Prada, J. Ceballos Infantes, and J. Passes Filho, "Identifying voltage control areas based on the interdependence of control equipment," in *EUROCON, 2013 IEEE*, July 2013, pp. 1227–1234.

[98] S. Corsi, M. Pozzi, C. Sabelli, and A. Serrani, "The coordinated automatic voltage control of the italian transmission grid-part i: reasons of the choice and overview of the consolidated hierarchical system," *IEEE Transactions on Power Systems*, vol. 19, no. 4, pp. 1723–1732, Nov 2004.

[99] H. Sun, Q. Guo, B. Zhang, W. Wu, and B. Wang, "An adaptive zone division based automatic voltage control system with applications in china," in *2013 IEEE Power Energy Society General Meeting*, July 2013, pp. 1–1.

[100] H. Mehrjerdi, E. Ghahremani, S. Lefebvre, M. Saad, and D. Asber, "Authenticated voltage control of partitioned power networks with optimal allocation of statcom using heuristic algorithm," *IET Generation, Transmission Distribution*, vol. 7, no. 9, pp. 1037–1045, Sept 2013.

[101] H. Li, G. W. Rosenwald, J. Jung, and C. ching Liu, "Strategic power infrastructure defense," *Proceedings of the IEEE*, vol. 93, no. 5, pp. 918–933, May 2005.

[102] H. Mehrjerdi, S. Lefebvre, M. Saad, and D. Asber, "A decentralized control of partitioned power networks for voltage regulation and prevention against disturbance propagation," *IEEE Transactions on Power Systems*, vol. 28, no. 2, pp. 1461–1469, May 2013.

[103] R. J. SÃ¡nchez-GarcÃa, M. Fennelly, S. Norris, N. Wright, G. Niblo, J. Brodzki, and J. W. Bialek, "Hierarchical spectral clustering of power grids," *IEEE Transactions on Power Systems*, vol. 29, no. 5, pp. 2229–2237, Sept 2014.

[104] E. Nobile and A. Bose, "A new scheme for voltage control in a competitive ancillary service market," *Proceedings of PSCC'02, 14th Power System Computation Conference*, June 2002.

[105] M. Begovic and A. Phadke, "Control of voltage stability using sensitivity analysis," *Power Systems, IEEE Transactions on*, vol. 7, no. 1, pp. 114–123, Feb 1992.

[106] A. K. Singh and B. C. Pal, "Report on the 68-bus, 16-machine, 5-area system," *IEEE PES Task Force on Benchmark Systems for Stability Controls*, vol. Version 3.3, pp. 1–41, Feb 2013.

[107] S. Satsangi, A. Saini, and A. Saraswat, "Voltage control areas for reactive power management using clustering approach in deregulated power system," in *Sustainable Energy and Intelligent Systems (SEISCON 2011), International Conference on*, July 2011, pp. 409–415.

[108] M. Paramasivam, S. Dasgupta, V. Ajjarapu, and U. Vaidya, "Contingency analysis and identification of dynamic voltage control areas," *IEEE Transactions on Power Systems*, vol. 30, no. 6, pp. 2974–2983, Nov 2015.

[109] P. Tryfos, *Methods for Business Analysis and Forecasting Text & Cases*. John Wiley and Sons, 1998, ch. Cluster Analysis, pp. 1–23.

[110] R. Xu and D. Wunsch, *Clustering*. Wiley-IEEE Press, 2008.

[111] L. Rokach and O. Maimon, *Clustering Methods*. Boston, MA: Springer US, 2005, pp. 321–352.

[112] V. Estivill-Castro and J. Yang, *Fast and Robust General Purpose Clustering Algorithms*. Berlin, Heidelberg: Springer Berlin Heidelberg, 2000, pp. 208–218.

[113] D. M. L. D. D. S. Brian S. Everitt, Dr Sabine Landau.

[114] P. Hansen and B. Jaumard, "Cluster analysis and mathematical programming," *Mathematical Programming*, vol. 79, no. 1, pp. 191–215, 1997.

[115] A. K. Jain, M. N. Murty, and P. J. Flynn, "Data clustering: A review," *ACM Comput. Surv.*, vol. 31, no. 3, pp. 264–323, Sep. 1999.

[116] S. P. H. A and S. R. Rl., "Numerical taxonomy the principles and practice of numerical classification," p. 573p, 1987.

[117] K. B., "Step-wise clustering procedures," pp. 86–101, 1967.

[118] J. H. Ward, "Hierarchical grouping to optimize an objective function," *Journal of the American Statistical Association*, vol. 58, no. 301, pp. 236–244, 1963.

[119] R. O. Duda, P. E. Hart, and D. G. Stork, *Pattern Classification*, 2nd ed. New York: Wiley, 2001.

[120] S. Theodoridis and K. Koutroumbas, *Pattern recognition*, 3rd ed. San Diego, CA: Academic Press, 2001.

[121] T. Hastie, R. Tibshirani, and J. Friedman, *The Elements of Statistical Learning: Data Mining, Inference, and Prediction.* New York, NY: Springer New York, 2009, ch. Unsupervised Learning, pp. 485–585.

[122] J. B. MacQueen, "Some methods for classification and analysis of multivariate observations," in *Proc. of the fifth Berkeley Symposium on Mathematical Statistics and Probability*, L. M. L. Cam and J. Neyman, Eds., vol. 1. University of California Press, 1967, pp. 281–297.

[123] E. W. Forgy, "Cluster analysis of multivariate data: efficiency versus interpretability of classifications," *Biometrics*, vol. 21, pp. 768–769, 1965.

[124] F. Rameshkhah, M. Abedi, and S. H. Hosseinian, "Clustering of voltage control areas in power system using shuffled frog-leaping algorithm," *Electrical Engineering*, vol. 92, no. 7, pp. 269–282, 2010.

[125] M. Sarstedt and E. Mooi, *A Concise Guide to Market Research.* Springer-Verlag Berlin Heidelberg, 2014.

[126] J. F. Trevor Hastie, Robert Tibshirani, *The Elements of Statistical Learning.* Springer New York, 2009.

[127] A. D. Gordon, *Null Models in Cluster Validation.* Berlin, Heidelberg: Springer Berlin Heidelberg, 1996, pp. 32–44.

[128] W. J. Krzanowski and Y. T. Lai, "A criterion for determining the number of groups in a data set using sum-of-squares clustering," *Biometrics*, vol. 44, no. 1, pp. 23–34, 1988.

[129] F. H. C. Marriott, "Practical problems in a method of cluster analysis," *Biometrics*, vol. 27, no. 3, pp. 501–514, 1971.

[130] F. M. Cuevas, Antonio and F. Ricardo, "Authenticated voltage control of partitioned power networks with optimal allocation of statcom using heuristic algorithm," *The Canadian Journal of Statistics La Revue Canadienne De Statistique*, vol. 28, no. 2, pp. 367–382, Jun 2000.

[131] R. Tibshirani, G. Walther, and T. Hastie, "Estimating the number of clusters in a data set via the gap statistic," *Journal of the Royal Statistical Society: Series B (Statistical Methodology)*, vol. 63, no. 2, pp. 411–423, 2001.

[132] D. Arthur and S. Vassilvitskii, "K-means++: The advantages of careful seeding," in *Proceedings of the Eighteenth Annual ACM-SIAM Symposium on Discrete Algorithms*, ser. SODA '07. Philadelphia, PA, USA: Society for Industrial and Applied Mathematics, 2007, pp. 1027–1035.

[133] L. Kaufman and P. J. Rousseeuw, *Finding Groups in Data.* John Wiley Sons, Inc., 2008.

[134] C. W. Taylor, *Power System Voltage Stability.* McGraw-Hill, Inc., 1994.

[135] M. D. Amadou, H. Mehrjerdi, S. Lefebvre, M. Saad, and D. Asber, "Area voltage control analysis in transmission systems based on clustering technique," *IET Generation, Transmission Distribution*, vol. 8, no. 12, pp. 2134–2143, 2014.

[136] "Psse 33.4 model library," Siemens PTI Ltd,, Tech. Rep., March 2013.

[137] "Wecc wind power plant dynamic modeling guide," *WECC Renewable Energy Modeling Task Force, Western Electricity Coordinating Council*, 2014.

APPENDIX A: WIND GENERATOR MODEL

This appendix contains data for the dynamic model of the wind machines used in PSSE simulations throughout this dissertation. WECC adopted guideline for using generic dynamic model for wind power plants and Siemens PTI PSSE has implemented it in its simulation platform [137]. Generic model of type 3 wind generator based on DFIG known as WT3 Generic wind model is used as wind generator in this dissertation. The WT3 Generic wind model comprises models as follows

1. WT3G: generator/converter model
2. WT3E: electrical control model
3. WT3T: mechanical control (wind turbine) model
4. WT3P: pitch control model

The data used for the above models are presented below in Tables A.1-A.4.

A.1 Wind Model Parameters

Table A.1: Generic wind turbine generator/converter model WT3G1

Symbol	**Description**	**Value**
X_{eq}	Equivalent reactance for current injection (pu)	0.8
K_{pll}	PLL first integrator gain	30
K_{ipll}	PLL second integrator gain	0.0
P_{llmax}	PLL maximum limit	0.10
P_{rated}	Turbine MW rating	1.5

Table A.2: Electrical control for type 3 wind generator WT3E1

Symbol	**Description**	**Value**
T_{fv}	Filter time constant in voltage regulator (sec)	0.15
K_{PV}	Proportional gain in voltage regulator (pu)	18
K_{IV}	Integrator gain in voltage regulator (pu)	5
X_c	Line drop compensation reactance (pu)	0
T_{FP}	Filter time constant in torque regulator	5.00E-02
K_{pp}	Proportional gain in torque regulator (pu)	3
K_{IP}	Integrator gain in torque regulator (pu)	0.6
P_{MX}	Max limit in torque regulator (pu)	1.12
P_{MN}	Min limit in torque regulator (pu)	0.1
Q_{MX}	Max limit in voltage regulator (pu)	0.296
Q_{MN}	Min limit in voltage regulator (pu)	-0.436
IP_{MAX}	Max active current limit	1.1
T_{RV}	Voltage sensor time constant	5.00E-02
RP_{MX}	Max power order derivative	0.45

Table A.2: Electrical control for type 3 wind generator WT3E1

Symbol	**Description**	**Value**
RP_{MN}	Min power order derivative	-0.45
T_{Power}	Power filter time constant	5
K_{qi}	MVAR/Voltage gain	5.00E-02
V_{MINCL}	Min voltage limit	0.9
V_{MAXCL}	Max voltage limit	1.2
K_{qv}	Voltage/MVAR gain	40
XIQ_{min}		-0.5
XIQ_{max}		0.4
T_v	Lag time constant in WindVar controller	5.00E-02
T_p	Pelec filter in fast PF controller	5.00E-02
F_n	A portion of online wind turbines	1
ωP_{min}	Shaft speed at Pmin (pu)	0.69
ωP_{20}	Shaft speed at 20% rated power (pu)	0.78
ωP_{40}	Shaft speed at 40% rated power (pu)	0.98
ωP_{60}	Shaft speed at 60% rated power (pu)	1.12
P_{min}	Minimum power for operating at ωP_{100} speed (pu)	0.74
ωP_{100}	Shaft speed at 100% rated power (pu)	1.2

Table A.3: Mechanical system model for type 3 wind generator WT3T1

Symbol	Description	Value
VW	Initial wind, pu of rated wind speed	1.25
H	Total inertia constant, sec	4.95
$DAMP$	Machine damping factor, pu P/pu speed	0.0
K_{aero}	Aerodynamic gain factor	0.70000E-02
$Theta2$	Blade pitch at twice rated wind speed, deg	21.980
H_{tfrac}	Turbine inertia fraction $(Hturb/H)^1$	0.0
$Freq1$	First shaft torsional resonant frequency, Hz	1.8
D_{shaft}	Shaft damping factor (pu)	1.5

Table A.4: Pitch control model for type 3 wind generator WT3P1

Symbol	Description	Value
T_p	Blade response time constant	0.30
K_{pp}	Proportional gain of PI regulator (pu)	150
K_{ip}	Machine damping factor, pu P/pu speed	25
K_{pc}	Proportional gain of the compensator (pu)	30
K_{ic}	Integrator gain of the compensator (pu)	30
$Teta_{Min}$	Lower pitch angle limit (degrees)	0.0
$Teta_{Max}$	Upper pitch angle limit (degrees)	27.00
$RTeta_{Max}$	Upper pitch angle rate limit (degrees/sec)	10
P_{MX}	Power reference, pu on MBASE	1.0

APPENDIX B: SENSITIVITY TABLE FOR TEST SYSTEMS

This appendix contains the sensitivity data for Test Systems

B.1 IEEE 39-Bus System

The IEEE 39 bus system has 10 generators and 29 load buses, so the sensitivity table has size of 9 rows of generators and 29 columns of load buses. The transpose of the sensitivity matrix is shown in Table B.1.

Table B.1: Dataset for clustering of IEEE 39 bus

Bus	Gen 30	Gen 32	Gen 33	Gen 34	Gen 35	Gen 36	Gen 37	Gen38	Gen 39
1	0.2001	0.0256	0.0187	0.0086	0.0209	0.0119	0.1029	0.0314	0.8306
2	0.5214	0.0669	0.0487	0.0224	0.0546	0.031	0.2683	0.0818	0.171
3	0.3232	0.1618	0.1054	0.0486	0.1182	0.067	0.1808	0.096	0.1539
4	0.1688	0.3332	0.0968	0.0446	0.1085	0.0615	0.0975	0.0603	0.1858
5	0.105	0.3557	0.067	0.0309	0.0751	0.0426	0.0611	0.0391	0.2295
6	0.0949	0.3658	0.0626	0.0288	0.0702	0.0398	0.0554	0.0359	0.2166
7	0.0936	0.3439	0.061	0.0281	0.0683	0.0388	0.0545	0.0352	0.2888
8	0.092	0.3297	0.0596	0.0274	0.0667	0.0378	0.0535	0.0345	0.3221
9	0.0372	0.1333	0.0241	0.0111	0.027	0.0153	0.0217	0.0139	0.8686
10	0.0865	0.5911	0.0684	0.0315	0.0767	0.0435	0.0514	0.0355	0.1458
11	0.09	0.5159	0.0672	0.0309	0.0753	0.0427	0.0532	0.0359	0.1699
12	0.0982	0.546	0.0777	0.0358	0.0871	0.0494	0.0584	0.0403	0.1656
13	0.0991	0.5351	0.0825	0.038	0.0925	0.0524	0.0593	0.0417	0.1489
14	0.1288	0.3993	0.1164	0.0536	0.1304	0.074	0.0779	0.0564	0.1519
15	0.1245	0.2148	0.221	0.1018	0.2477	0.1405	0.0839	0.0811	0.0999
16	0.1191	0.1296	0.2594	0.1194	0.2907	0.1648	0.084	0.0893	0.0747
17	0.1859	0.1286	0.195	0.0898	0.2185	0.1239	0.1347	0.1508	0.0964
18	0.2393	0.1418	0.1613	0.0743	0.1808	0.1025	0.1527	0.1302	0.1188
19	0.044	0.048	0.6558	0.302	0.1073	0.0609	0.031	0.033	0.0276
20	0.0256	0.0281	0.3824	0.7339	0.0625	0.0355	0.0181	0.0192	0.0161
21	0.0843	0.0919	0.1836	0.0845	0.5139	0.225	0.0595	0.0632	0.0529
22	0.0448	0.0488	0.0976	0.0449	0.7203	0.2759	0.0316	0.0336	0.0281
23	0.0466	0.0508	0.1014	0.0467	0.5057	0.4873	0.0329	0.0349	0.0293
24	0.108	0.1176	0.2352	0.1083	0.3206	0.2105	0.0762	0.081	0.0678
25	0.3563	0.054	0.0461	0.0212	0.0516	0.0293	0.4857	0.1255	0.1196
26	0.2104	0.0704	0.093	0.0428	0.1042	0.0591	0.2397	0.4391	0.0837
27	0.2016	0.0981	0.1411	0.065	0.1581	0.0897	0.1943	0.3117	0.0906
28	0.1104	0.0371	0.0488	0.0225	0.0547	0.031	0.126	0.8723	0.044
29	0.0765	0.0257	0.0338	0.0156	0.0379	0.0215	0.0873	1	0.0305

B.2 IEEE 68-Bus System

The IEEE 68 bus system has 16 generators and 52 load buses, so the sensitivity table has size of 15 rows of generators and 52 columns of load buses. The transpose of the sensitivity matrix is shown in Table B.2.

Table B.2: Comparison of VCAs for 68 bus system

Bus	1	2	3	4	5	6	7	8	9	10	11	12	13	14	15
17	0.0076	0.0084	0.0067	0.0016	0.0008	0.0019	0.0011	0.0041	0.0019	0.0199	0.0356	0.1959	0.7926	0.0081	0.0018
18	0.0033	0.0021	0.0017	0.0005	0.0003	0.0006	0.0004	0.0018	0.0008	0.013	0.0166	0.0232	0.0343	0.0132	0.05
19	0.0326	0.0245	0.034	0.5252	0.2569	0.0828	0.0472	0.0229	0.0238	0.0064	0.0055	0.0082	0.0086	0.0031	0.0003
20	0.0178	0.0134	0.0186	0.2874	0.6168	0.0452	0.0258	0.0125	0.013	0.0036	0.0031	0.0046	0.005	0.002	0.0002
21	0.0659	0.0496	0.0687	0.1379	0.0675	0.4268	0.1864	0.0462	0.0481	0.0126	0.0107	0.0161	0.0169	0.0056	0.0006
22	0.034	0.0256	0.0354	0.0711	0.0348	0.5933	0.2262	0.0238	0.0248	0.0064	0.0054	0.0082	0.0085	0.0026	0.0002
23	0.0354	0.0267	0.0369	0.074	0.0362	0.4126	0.4039	0.0248	0.0258	0.0067	0.0057	0.0085	0.0088	0.0027	0.0003
24	0.0854	0.0643	0.089	0.1787	0.0874	0.2649	0.1759	0.0598	0.0623	0.0162	0.0137	0.0206	0.0215	0.0068	0.0007
25	0.284	0.0365	0.0408	0.0326	0.0159	0.0395	0.0225	0.3992	0.098	0.0326	0.0249	0.0285	0.03	0.0142	0.0012
26	0.1658	0.043	0.052	0.0664	0.0325	0.0804	0.0459	0.192	0.3517	0.0268	0.0208	0.0251	0.0263	0.0113	0.0009
27	0.1591	0.0587	0.0726	0.1018	0.0498	0.1233	0.0703	0.1533	0.2436	0.0321	0.0251	0.0312	0.0327	0.0137	0.0012
28	0.0848	0.022	0.0266	0.034	0.0166	0.0412	0.0235	0.0983	0.7075	0.0138	0.0107	0.013	0.0136	0.006	0.0005
29	0.0576	0.0149	0.0181	0.0231	0.0113	0.028	0.016	0.0669	0.8117	0.0094	0.0073	0.0089	0.0094	0.0042	0.0004
30	0.0778	0.0455	0.038	0.0122	0.006	0.0148	0.0084	0.0418	0.0177	0.2089	0.2044	0.2095	0.2186	0.0666	0.0063
31	0.0686	0.0315	0.027	0.0098	0.0048	0.0119	0.0068	0.0368	0.0153	0.3875	0.1678	0.1499	0.1597	0.063	0.007
32	0.0264	0.0164	0.0136	0.0042	0.0021	0.0051	0.0029	0.0142	0.006	0.0853	0.5915	0.1323	0.1459	0.0258	0.0039
33	0.0286	0.0186	0.0154	0.0047	0.0023	0.0057	0.0032	0.0154	0.0066	0.1069	0.4161	0.2049	0.2301	0.0313	0.006
34	0.0217	0.0186	0.0151	0.004	0.002	0.0049	0.0028	0.0118	0.0051	0.0695	0.2037	0.3325	0.3787	0.0301	0.0077
35	0.0214	0.0182	0.0147	0.0039	0.0019	0.0048	0.0027	0.0117	0.0051	0.0688	0.1905	0.3183	0.3989	0.0364	0.0113
36	0.0167	0.0186	0.0149	0.0035	0.0017	0.0043	0.0024	0.009	0.004	0.0426	0.0739	0.445	0.4497	0.0154	0.003
37	0.1488	0.0767	0.0973	0.1465	0.0717	0.1775	0.1013	0.1072	0.1178	0.0259	0.0212	0.0293	0.0306	0.0109	0.001
38	0.0574	0.0278	0.0236	0.0084	0.0041	0.0102	0.0058	0.0308	0.0129	0.3087	0.2249	0.1633	0.1795	0.0603	0.0104
39	0.0167	0.0145	0.0118	0.0031	0.0015	0.0038	0.0021	0.0091	0.004	0.0514	0.1139	0.2638	0.6219	0.0383	0.0133
40	0.0891	0.033	0.029	0.012	0.0058	0.0145	0.0083	0.0476	0.0196	0.19	0.143	0.1474	0.1628	0.5536	0.0272
41	0.0017	0.0006	0.0006	0.0002	0.0001	0.0003	0.0002	0.0009	0.0004	0.0038	0.003	0.0032	0.0037	0.9828	0.0242
42	0.0001	0.0001	0.0001	0	0	0	0	0.0001	0	0.0004	0.0005	0.0006	0.0008	0.024	0.9622
43	0.0133	0.0122	0.0099	0.0025	0.0012	0.0031	0.0018	0.0072	0.0032	0.0397	0.0846	0.2381	0.6833	0.0271	0.009
44	0.0135	0.0124	0.01	0.0026	0.0013	0.0031	0.0018	0.0074	0.0032	0.0404	0.0866	0.2398	0.679	0.0279	0.0093
45	0.0209	0.0171	0.0139	0.0038	0.0018	0.0046	0.0026	0.0114	0.005	0.0672	0.1585	0.2836	0.4484	0.0522	0.0203
46	0.054	0.026	0.0221	0.0079	0.0038	0.0095	0.0054	0.0289	0.0121	0.2837	0.2106	0.1609	0.1831	0.0739	0.0202
47	0.1069	0.0398	0.0349	0.0144	0.007	0.0174	0.0099	0.0572	0.0236	0.2247	0.166	0.1674	0.1793	0.2627	0.0154
48	0.1011	0.0375	0.0329	0.0136	0.0066	0.0164	0.0094	0.054	0.0223	0.2136	0.1589	0.1616	0.1752	0.3741	0.0203
49	0.049	0.0236	0.0201	0.0071	0.0035	0.0087	0.0049	0.0263	0.011	0.2518	0.1909	0.1533	0.1802	0.083	0.0296
50	0.018	0.0132	0.0108	0.0031	0.0015	0.0037	0.0021	0.0099	0.0042	0.0597	0.1117	0.1856	0.2869	0.0659	0.0423
51	0.0212	0.0166	0.0135	0.0037	0.0018	0.0045	0.0026	0.0116	0.005	0.0686	0.149	0.2602	0.4083	0.0627	0.0278
52	0.193	0.0899	0.1076	0.1206	0.059	0.1461	0.0834	0.1221	0.1015	0.0302	0.0247	0.0343	0.0358	0.0126	0.0011
53	0.1138	0.0424	0.0372	0.0153	0.0075	0.0185	0.0106	0.0609	0.0251	0.2375	0.1738	0.1732	0.1824	0.1	0.0079
54	0.423	0.0478	0.0523	0.0351	0.0172	0.0426	0.0243	0.2158	0.0632	0.046	0.0348	0.0391	0.0408	0.0188	0.0015
55	0.2626	0.1105	0.1233	0.0777	0.038	0.0941	0.0537	0.1455	0.0744	0.0368	0.0301	0.0419	0.0436	0.015	0.0013
56	0.137	0.2385	0.2554	0.07	0.0342	0.0847	0.0483	0.078	0.046	0.034	0.0321	0.0586	0.0607	0.0133	0.0014
57	0.0876	0.3467	0.2724	0.0471	0.023	0.0571	0.0326	0.0498	0.0298	0.0377	0.0383	0.078	0.0805	0.0139	0.0017
58	0.0788	0.3745	0.2813	0.0437	0.0214	0.0529	0.0302	0.0449	0.0271	0.0352	0.0359	0.0734	0.0757	0.0131	0.0016
59	0.0812	0.3414	0.2607	0.0425	0.0208	0.0515	0.0294	0.0458	0.0271	0.0465	0.0484	0.1017	0.1048	0.0168	0.0021
60	0.0814	0.3213	0.2476	0.0414	0.0203	0.0502	0.0286	0.0458	0.0269	0.0515	0.054	0.1146	0.118	0.0183	0.0022
61	0.0533	0.0652	0.0519	0.0119	0.0058	0.0144	0.0082	0.0287	0.0131	0.1231	0.1355	0.3081	0.3151	0.04	0.0047
62	0.0692	0.2259	0.4832	0.0486	0.0238	0.0588	0.0336	0.0404	0.0264	0.0243	0.0241	0.0473	0.049	0.0095	0.0011
63	0.073	0.2765	0.4158	0.0474	0.0232	0.0575	0.0328	0.0422	0.0269	0.0281	0.0282	0.0563	0.0582	0.0108	0.0013
64	0.0802	0.2617	0.446	0.0563	0.0275	0.0682	0.0389	0.0468	0.0306	0.0283	0.0281	0.055	0.0571	0.0114	0.0014
65	0.0798	0.2224	0.4339	0.0598	0.0292	0.0724	0.0413	0.047	0.0314	0.0255	0.025	0.0481	0.0498	0.0101	0.0012
66	0.104	0.2056	0.316	0.0863	0.0422	0.1045	0.0596	0.062	0.0432	0.0276	0.0262	0.0483	0.0501	0.011	0.0012
67	0.0995	0.1135	0.1666	0.1687	0.0825	0.2043	0.1165	0.0665	0.0628	0.0215	0.0191	0.0314	0.0328	0.0093	0.001
68	0.0947	0.0713	0.0987	0.1982	0.0969	0.24	0.1369	0.0663	0.0691	0.018	0.0153	0.0229	0.024	0.0077	0.0007